Measuring NMDA receptors using [^{18}F]GE-179 PET in health and disease.

University College London

UCL Queen Square Institute of Neurology

Department of Clinical and Experimental Epilepsy Queen Square

A thesis presented in consideration for the degree of

Doctor of Philosophy

Marian Galovic

2021

Declaration

I, Marian Galovic, confirm that the work presented in this thesis is my own. Where information has been derived from other sources, I confirm this has been indicated in the thesis.

The scientific studies presented here reflect collaborations with a team of researchers including other colleagues from the UCL Department of Clinical and Experimental Epilepsy and UCL Institute of Nuclear Medicine. However, this thesis presents only studies in which I conducted most steps of data analysis. All results and data interpretation were presented by myself and were developed based on discussions at meetings with my colleagues and my scientific supervisors. My individual contributions to the scientific studies included in this thesis are outlined below.

The first project, development and validation of a kinetic modelling pipeline independent of arterial sampling, uses data acquired at Addenbrooke's Hospital in Cambridge by our collaborators Jonathan Coles, Tim Fryer, and Young Hong. It builds on previous work of my colleague Hasan Sari in a joint project with the UCL Institute of Nuclear Medicine. I completely redeveloped the analysis pipeline with support from Kjell Erlandsson, Kris Thielemans, Benjamin A. Thomas, and Anna Barnes from the UCL Institute of Nuclear Medicine. I processed the data, performed statistical analysis, and wrote the manuscript.

For the remaining three projects (NMDA receptor activation in aging, epilepsy, and anti-NMDA-receptor encephalitis), I used PET and MR data acquired by myself at UCL Institute of Nuclear Medicine. I also used multicentre healthy volunteer data acquired using [^{18}F]GE-179 PET and MRI at Hammersmith Hospital, Imperial College London, by Colm McGinnity (n=9) and Addenbrooke's Hospital, Cambridge University, by Jonathan Coles, Tim Fryer, and Young Hong (n=10), with the permission of the collaborators. I processed all internal and external data using the same standardised methods, applied modelling software developed by Kjell Erlandsson at UCL Institute of Nuclear Medicine, performed statistical analysis, interpreted the data and wrote the manuscript.

Marian Galovic

Abstract

Background: *N*-methyl-D-aspartate receptors (NMDAR) are important glutamatergic ion channels in the brain. Studying the functional activation of NMDAR *in vivo* in humans has not been possible until recently.

Methods: We used positron emission tomography (PET) with [^{18}F]GE-179, a novel radioligand binding inside the open NMDAR channel, to assess the *in vivo* activation of NMDAR. We developed methodology for quantification of ligand binding (*Project 1*) that did not require arterial sampling and was then applied to study NMDAR activation in aging (n=29, *Project 2*), epilepsy (n=26, *Project 3*), and Anti-NMDAR encephalitis (n=5, *Project 4*).

Results: In *Project 1*, we validated a method for kinetic modelling using an image-derived input function and serial venous samples. This approach provided unbiased estimates of ligand volume of distribution (V_T) that were highly correlated (r=0.95, p<0.001) with the gold standard, an arterial input function.

In *Project 2*, we observed increased tracer uptake related to aging in healthy individuals (V_T increase of 0.6 per 10 years, p=0.04), particularly in bilateral hippocampi, temporo-parieto-occipital junctions, dorsolateral prefrontal cortex, and striata. In people with epilepsy, the age-related increase in V_T (1.4 per 10 years, p=0.006) was most pronounced in the striatum and thalamus.

In *Project 3*, we found reduced interictal ligand uptake in epilepsy that was related to longer disease duration (V_T decrease of 1.6 per 10 years, p=0.004), spatially

widespread and bihemispheric. Regional uptake was increased in those taking lacosamide and after anterior temporal lobe resection.

In *Project 4*, we observed decreased ligand uptake in Anti-NMDAR encephalitis with persisting Anti-GluN1-antibodies (mean V_T 6.2 in cases vs. 8.8 in healthy volunteers, p=0.02), particularly in bilateral anterior temporal and superior parietal lobes.

Conclusions: [^{18}F]GE-179 PET is useful to detect altered NMDAR function. We observed increased NMDAR activation in aging and decreased activation in interictal epilepsy and antibody-positive Anti-NMDAR encephalitis.

Impact statement

N-methyl-D-aspartate (NMDA) receptors are glutamatergic ion channels that are involved in a number of physiologic and pathologic processes. They play a role in synaptic plasticity, memory, excitotoxicity, and in several neurologic and psychiatric disorders. Studying NMDA receptors in humans *in vivo* has not been possible until recently.

Here, we used positron emission tomography (PET) with the novel radioligand [^{18}F]GE-179 that binds specifically to the open, i.e. activated, NMDA receptor. A wider use of this ligand has been limited by the need for arterial blood sampling to correctly quantify radiotracer binding. In *Project 1* we simplified this methodology by developing and validating a kinetic modelling approach using serial venous samples and an image-derived input function. This approach is less invasive than traditional methods relying on arterial blood sampling. It may allow the wider use of the tracer in research and, if proven useful, in clinical care.

In *Project 2* we observed increased activation of NMDA receptors related to aging in healthy volunteers and patients with focal epilepsy. These findings are particularly relevant due to the unprecedented aging of the population in high income countries. They support the hypothesis of increased neuronal network hyperexcitability during aging that may contribute to cognitive decline and neurodegeneration. If these findings are reproduced in people with mild cognitive impairment and dementia, they may open avenues for novel treatments. The NMDA receptor antagonist memantine is

currently being used as a routine treatment of Alzheimer's disease and the glutamatergic modulator riluzole is used in amyotrophic lateral sclerosis. These and other medications could be studied using [18F]GE-179 to determine their effect on NMDA receptors during healthy aging and in people with neurodegenerative disorders.

In *Project 3* we found decreased interictal NMDA receptor activation in people with refractory focal epilepsy. This observation contrasts with traditional models of neuronal hyperexcitability due to NMDA receptor overactivation in people with epilepsy. Our findings highlight the need to restore a balanced NMDA receptor activity in people with epilepsy and argue against overt blocking of NMDA receptors. We also observed the impact of anti-seizure medications on NMDA receptors that was most pronounced for lacosamide, which was not recognised previously. These results could contribute to the development of novel treatment strategies for epilepsy. [^{18}F]GE-179 PET could be useful to assess the influence of medication on the NMDA receptor.

In *Project 4* we observed decreased activation of NMDA receptors in females recovering from Anti-NMDA-receptor encephalitis. These findings confirm for the first time *in vivo* the proposed disease mechanism of this autoimmune disorder. They also highlight persisting NMDA receptor abnormalities in individuals with only mild or minimal symptoms several months after discharge from hospital. If confirmed in larger studies, [^{18}F]GE-179 PET could be used to monitor disease activity and guide treatment decisions in the subacute and chronic phases of Anti-NMDA-receptor encephalitis.

In conclusion, [^{18}F]GE-179 PET is a valuable tool to study the molecular underpinnings of healthy aging and neurological disorders and the impact of medications.

Table of contents

List of figures

Chapter 5

Chapter 6

List of tables

List of abbreviations

2c4k	2-brain-compartment 4-rate-constant
Aβ	Amyloid beta-peptide
AD	Alzheimer's disease
ADHD	Attention-deficit hyperactivity disorder
AED	Antiepileptic drug
AIF	Arterial input function
AMPA	Alpha-amino-3-hydroxy-5-methyl-4-isoxazolepropionic acid
ANCOVA	Analysis of covariance
APOE	Apolipoprotein E
APP	Amyloid precursor protein
AUC	Area under the curve
CAM	Cambridge
CAT12	Computational anatomy 12 toolbox
CoV	Coefficient of variation
CSF	Cerebrospinal fluid
CSWSS	Continuous spike and waves during slow-wave sleep syndrome

CT	Computed tomography
D2HG	D-2-hydroxyglutarate
DAPI	4',6-diamidino-2-phenylindole
DMEM	Dulbecco's Modified Eagle Medium
DMN	Default mode network
FDG	Fluorodeoxyglucose
FLE	Frontal lobe epilepsy
FWHM	Full width at half maximum
GABA	Gamma-aminobutyric acid
GIF	Geodesic Information Flows
HAM	Hammersmith
HEPES	4-(2-hydroxyethyl)-1-piperazineethanesulfonic acid
HS	Hippocampal sclerosis
$IDH1^{mut}$	Mutant isocitrate dehydrogenase 1
IDIF	Image-derived input function
LTD	Long-term depression
LTP	Long-term potentiation
mGluR	Metabotropic glutamate receptors
mRNA	Messenger ribonucleic acid
MR	magnetic resonance
MRI	Magnetic resonance imaging
MRS	Magnetic resonance spectroscopy

MTLE	Mesial temporal lobe epilepsy
NHNN	National Hospital for Neurology and Neurosurgery
NMDA	*N*-methyl-D-aspartate
NMDAR	*N*-methyl-D-aspartate receptor
PCP	Phencyclidine
PDS	Paroxysmal depolarization shifts
PET	Positron emission tomography
POB	Plasma-over-whole-blood
PVC	Partial volume correction
SPET	Single photon emission tomography
SPM12	Statistical parametric mapping 12
SUV	Standardized uptake value
TBI	Traumatic brain injury
TLE	Temporal lobe epilepsy
TOF	Time-of-flight
UCL	University College London
VBM	Voxel-based morphometry
V_T	Volume of distribution

List of publications

Original articles

Galovic M, de Tisi J, McEvoy AW, Miserocchi A, Vos SB, Borzì G, et al. Resective surgery prevents progressive cortical thinning in temporal lobe epilepsy. Brain 2020; 143: 3262–3272.

Caciagli L, Allen LA, He X, Trimmel K, Vos SB, Centeno M, **Galovic M**, Sidhu MK, Thompson PJ, Bassett DS, Winston GP, Duncan JS, Koepp MJ, Sperling MR. Thalamus and focal to bilateral seizures: A multi-scale cognitive imaging study. Neurology. 2020; 95: e2427-e2441.

Postma TS, Cury C, Baxendale S, Thompson PJ, Cano López I, de Tisi J, Burdett JL, Sidhu MK, Caciagli L, Winston GP, Vos SB, Thom M, Duncan JS, Koepp MJ*, **Galovic M***. Hippocampal Shape Is Associated with Memory Deficits in Temporal Lobe Epilepsy. Ann. Neurol. 2020; 88: 170–182.

De Blasi B, Caciagli L, Storti SF, **Galovic M**, Koepp M, Menegaz G, Barnes A, Galazzo IB. Noise removal in resting-state and task fMRI: functional connectivity and activation maps. J Neural Eng. 2020 Aug 19;17(4):046040

Brugger F, Wegener R, Walch J, **Galovic M**, Hägele-Link S, Bohlhalter S, et al. Altered activation and connectivity of the supplementary motor cortex at motor initiation in Parkinson's disease patients with freezing. Clinical Neurophysiology 2020: 1–36.

Long L*, **Galovic M***, Chen Y, Postma T, Vos SB, Xiao F, et al. Shared hippocampal abnormalities in sporadic temporal lobe epilepsy patients and their siblings. Epilepsia 2020; 61: 735–746.

Vos SB, Winston GP, Goodkin O, Pemberton HG, Barkhof F, Prados F, **Galovic M**, Koepp MJ, et al. Hippocampal profiling: Localized magnetic resonance imaging volumetry and T2 relaxometry for hippocampal sclerosis. Epilepsia 2020; 61: 297–309.

Galovic M, van Dooren VQH, Postma T, Vos SB, Caciagli L, Borzì G, et al. Progressive Cortical Thinning in Patients With Focal Epilepsy. JAMA Neurol 2019

Galovic M, Baudracco I, Wright-Goff E, Pillajo G, Nachev P, Wandschneider B, et al. Association of Piriform Cortex Resection With Surgical Outcomes in Patients With Temporal Lobe Epilepsy. JAMA Neurol 2019; 76: 690–700.

Galovic M, Stauber AJ, Leisi N, Krammer W, Brugger F, Vehoff J, et al. Development and Validation of a Prognostic Model of Swallowing Recovery and Enteral Tube Feeding After Ischemic Stroke. JAMA Neurol 2019; 76: 561–570.

Galovic M, Döhler N, Erdélyi-Canavese B, Felbecker A, Siebel P, Conrad J, et al. Prediction of late seizures after ischaemic stroke with a novel prognostic model (the SeLECT score): a multivariable prediction model development and validation study. The Lancet Neurology 2018; 17: 143–152.

Schreglmann SR, Riederer F, **Galovic M**, Ganos C, Kägi G, Waldvogel D, et al. Movement disorders in genetically confirmed mitochondrial disease and the putative role of the cerebellum. Mov. Disord. 2018; 33: 146–155.

Galovic M, Leisi N, Pastore-Wapp M, Zbinden M, Vos SB, Mueller M, et al. Diverging lesion and connectivity patterns influence early and late swallowing recovery after hemispheric stroke. Hum Brain Mapp 2017; 38: 2165–2176.

Galovic M, Leisi N, Muller M, Weber J, Tettenborn B, Brugger F, et al. Neuroanatomical correlates of tube dependency and impaired oral intake after hemispheric stroke. European Journal of Neurology 2016; 23: 926–934.

Kägi G, Leisi N, **Galovic M**, Müller-Baumberger M, Krammer W, Weder B. Prolonged impairment of deglutition in supratentorial ischaemic stroke: the predictive value of Parramatta Hospitals' Assessment of Dysphagia. Swiss Med Wkly 2016; 146: w14355.

Brugger F, **Galovic M**, Weder BJ, Kägi G. Supplementary Motor Complex and Disturbed Motor Control – a Retrospective Clinical and Lesion Analysis of Patients after Anterior Cerebral Artery Stroke. Front Neurol 2015; 6: 856–12.

Brugger F, Abela E, Hägele-Link S, Bohlhalter S, **Galovic M**, Kägi G. Do executive dysfunction and freezing of gait in Parkinson's disease share the same neuroanatomical correlates? Journal of the Neurological Sciences 2015; 356: 184–187.

Galovic M*, Leisi N*, Müller M, Weber J, Abela E, Kägi G, et al. Lesion location predicts transient and extended risk of aspiration after supratentorial ischemic stroke. Stroke 2013; 44: 2760–2767.

* authors share first or senior authorship

Reviews or commentaries

Koepp M, **Galovic M**. Functional imaging of the piriform cortex in focal epilepsy. Experimental Neurology 2020: 113305.

McGinnity CJ, Årstad E, Beck K, Brooks DJ, Coles JP, Duncan JS, **Galovic M**, Rainer H, et al. Comment on " In Vivo [18F]GE-179 Brain Signal Does Not Show NMDA-Specific Modulation with Drug Challenges in Rodents and Nonhuman Primates". ACS Chem Neurosci 2019; 10: 768–772.

Galovic M, Döhler ND, Keezer MR, Duncan JS, Sander JW, Koepp MJ, et al. The SeLECT score is useful to predict post-stroke epilepsy. The Lancet Neurology 2018: 1–2.

Galovic M. Comparing nasogastric and direct tube feeding in stroke: Enteral feeding going down the tube. Neurology 2018; 90: 305–306.

Galovic M, Koepp M. Advances of Molecular Imaging in Epilepsy. Curr Neurol Neurosci Rep 2016; 16: 58.

Galovic M, Kägi G. Wo steckt das Schlucken im Gehirn? Swiss Medical Forum 2014; 14: 830–832.

Galovic M, Tettenborn B. Fahreignung bei neurologischen Erkrankungen. InFo Neurologie & Psychiatrie 2012; 10: 4–10.

Book chapters

Koepp M, **Galovic M**, Ilayas-Feldmann M. Chapter 36: PET in Epilepsy. In: Diercks, editor. PET and SPECT in Neurology. Springer Press; 2021. P. 969-982.

Galovic M, Koepp M. Imaging Biomarkers of Acquired Epilepsies. In: Bernasconi A, Bernasconi N, Koepp MJ, editor(s). Imaging Biomarkers in Epilepsy. Cambridge University Press; 2019. p. 18–30.

Galovic M, Schmitz B, Tettenborn B. EEG in Inflammatory Disorders, Cerebrovascular Diseases, Trauma, and Migraine. In: Schomer DL, Lopes da Silva FH, editor(s). Niedermeyers Electroencephalography Basic Principles, Clinical Applicaitons, and Related Fields. Oxford University Press; 2017.

Acknowledgements

This PhD and my years of research associated with it would not have been possible and as enjoyable without the great support of a number of people to whom I would like to express my deepest gratitude.

I am very grateful to my principal supervisor, Matthias Koepp, who was always available for discussion and guidance and who I admire for his creative research approach and his ability to think translationally and beyond boundaries of different research topics and disciplines.

I would also like to thank my co-supervisor, John Duncan, for his continuous support and highly valuable advice. I admire his diligent and thorough scientific method and his ability to combine excellence in research and clinical care with a patient-centred and sociable approach.

I thank my collaborators at the UCL Institute of Nuclear Medicine, in particular Kjell Erlandsson, Kris Thielemans, Ben Thomas, Hasan Sari, and Ana Barnes, for their support with data acquisition and data modelling. It was always a huge pleasure and fun to work with the team of radiographers at the Macmillan Cancer Centre PET-MR.

I am grateful to our collaborators at Addenbrook's Hospital in Cambridge, particularly Jonathan Coles, Tim Fryer, and Young Hong, and at Hammersmith Hospital in London, particularly Colm McGinnity and Alexander Hammers, who acquired and

shared parts of the data and without whom this project would not have been possible. My thanks also goes to our collaborators at GE Healthcare.

I would also like to thank all my fellow research colleagues for all the hours of support and discussions and for sharing challenges, worries, success and friendship.

I am extremely grateful to all the patients and healthy volunteers who participated in our research. This work would not have been possible without them.

I am enormously grateful to my parents, my wife, and friends for their support, encouragement and understanding for long working hours and sparse visits back home.

1 Introduction

1.1 NMDA receptor structure and function

1.1.1 Glutamatergic receptors

Glutamate is the main excitatory neurotransmitter of the central nervous system accounting for one third of all rapid excitatory synapses (Cotman and Berchtold, 2002; Watkins and Evans, 1981). The *N*-methyl-D-aspartate (NMDA) receptor is one of three ionotropic receptor types that bind glutamate (Palmada and Centelles, 1998). Other ionotropic glutamate channels are the kainate and alpha-amino-3-hydroxy-5-methyl-4-isoxazolepropionic acid (AMPA) receptors. Eight subtypes of metabotropic glutamate receptors (mGluR) that indirectly modulate synaptic transmission have also been described (Niswender and Conn, 2010).

NMDA receptors are heteromeric ion channels consisting of four subunits that bind the agonist glutamate and the co-agonists glycine or D-serine (Wolosker, 2006). In the inactivated state, the channel pore is blocked by Mg^{2+} ions. For activation, NMDA receptors require the binding of an agonist, a co-agonist and concomitant postsynaptic depolarization to remove Mg^{2+} from the channel pore (Mori and Mishina, 1995). In this manner, the receptors are uniquely gated by both ligands and voltage.

Opening of the receptor channel leads to nonselective influx of cations, mainly Na^{+} and Ca^{2+}, and efflux of K^{+}. Compared to other glutamate receptors, NMDA receptors are the most permeable to calcium, they gate slowly, and desensitize only weakly

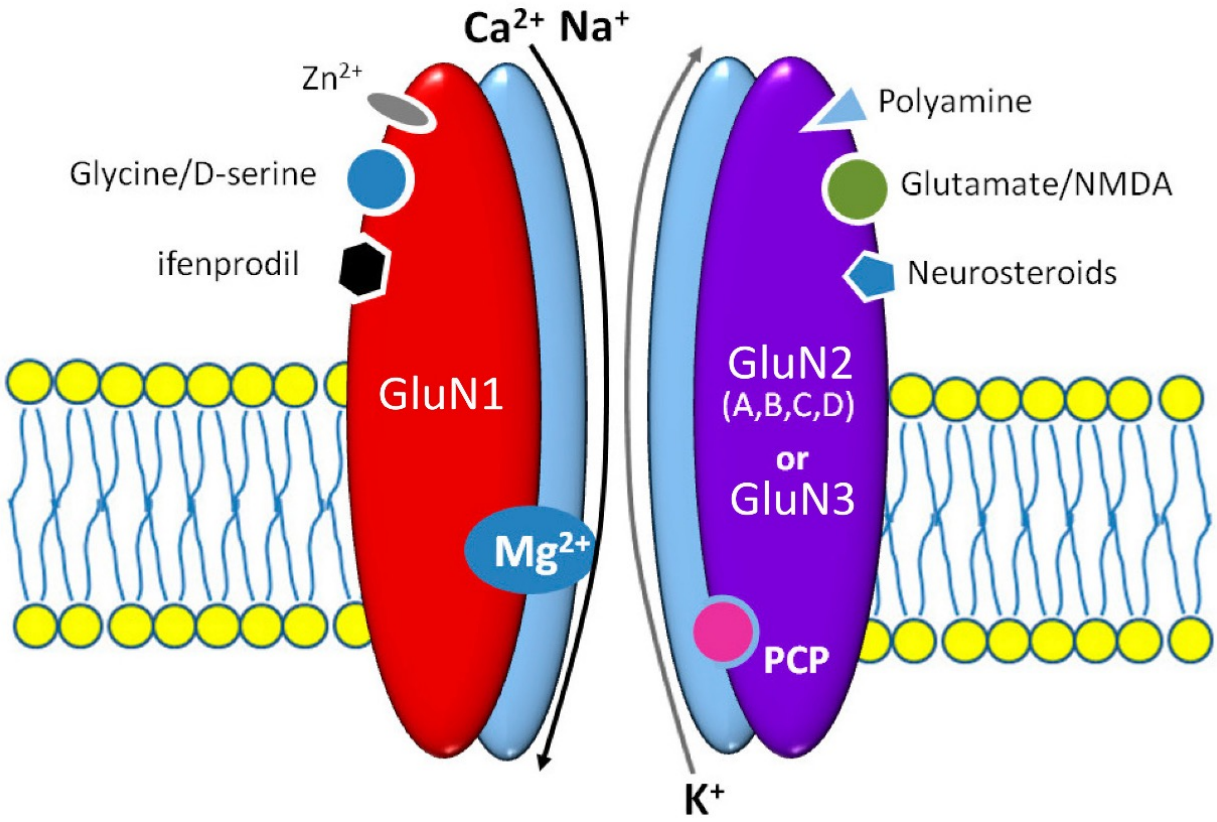

Figure 1.1: *Scheme of NMDA receptor structure*

The NMDA receptor is a heterotetramer consisting of two obligatory GluN1 subunits and a variable composition of GluN2 or GluN3 subunits. The glycine binding site is located on GluN1 subunits, the glutamate site is on GluN2/3 subunits. The channel pore is blocked by a Mg^{2+} ion at rest. Binding of Phencyclidine (PCP) requires opening of the channel pore. Reproduced with permission from Krzystanek and Palasz 2019.

(Wollmuth and Sobolevsky, 2004). These specific characteristics are important for long-term potentiation and excitotoxicity, which may play a role in several neurological disorders.

1.1.2 Subunit composition

The NMDA receptor complex consists of several subunits and this composition is variable regionally, changes throughout the lifespan, and influences the functional properties of the receptor. All receptors contain two obligatory glycine-binding GluN1

subunits (Kuryatov *et al.*, 1994) and two variable glutamate-binding GluN2 or GluN3 subunits, according to current nomenclature (Collingridge *et al.*, 2009). Different splice variants for GluN1 messenger ribonucleic acid (mRNA) have been described and they may influence the functional properties of the receptor (Magnusson *et al.*, 2010). Additionally, there is allosteric interaction between glutamate and glycine, the binding of one agonist lowering the affinity for the second (Durham *et al.*, 2020).

Four subtypes of GluN2 subunits, termed GluN2A-D, have been described. Out of these, the GluN2A and GluN2B subunits are most commonly expressed, whereas GluN2C and GluN2D are mainly present during early development (Monyer *et al.*, 1994). GluN2B-containing receptors are predominant during birth and early development, but at the onset of sexual maturity the expression of GluN2B is down-regulated (Bar-Shira *et al.*, 2015). In contrast, GluN2A expression increases during development and adulthood (Monyer *et al.*, 1994). A similar increase of the GluN2A/GluN2B ratio was observed during hippocampal development in humans (Jantzie *et al.*, 2015; Law *et al.*, 2003).

GluN2A and GluN2B subunit-containing receptors differ functionally. GluN1/GluN2A receptors have a higher opening probability and peak open probability in response to glutamate compared to GluN1/GluN2B receptors (N. Chen *et al.*, 1999; Erreger *et al.*, 2005; Gray *et al.*, 2011). In protocols of long-term potentiation (see chapter 1.2.1), GluN2A subunit-containing receptors predominantly responded to tonic stimuli, whereas GluN2B-containing receptors preferentially transferred charges of short low-frequency low-amplitude stimuli (Shipton and Paulsen, 2014). These functional differences may have differential implications for synaptic plasticity and memory. GluN2A knockout mice typically show only minor learning deficits, limited to short-term memory or the rapid acquisition of spatial information (Shipton and Paulsen, 2014). The GluN2B subunit might be relevant for novel-object recognition, spatial reference memory, and fear memory (Magnusson *et al.*, 2010).

The role of GluN3 (subtypes GluN3A und GluN3B) subunits is less well understood. Their expression has been localized to oligodendrocytes (Káradóttir *et al.*, 2005) or excitatory receptors responsive to glycine but not glutamate (Chatterton *et al.*, 2002).

The majority of receptors are either diheteromeric, i.e. containing either GluN1/GluN2A or GluN1/GluN2B subunits, or triheteromeric, i.e. containing GluN1/GluN2A/GluN2B. Most research focused on diheteromeric receptors because they can be studied selectively. Although the majority of hippocampal receptors might be triheteromeric (Rauner and Köhr, 2011), most research so far focused on diheteromeric receptors and their role remains largely unclear.

1.1.3 Synaptic and extrasynaptic sites

NMDA receptors may be localised both synaptically and extrasynaptically. Extrasynaptic sites have been implicated in neurodegenerative conditions including Alzheimer's disease (Bordji *et al.*, 2010). Both receptor populations bind glutamate, but they have different affinities towards co-agonists. Synaptic sites are mainly gated by D-serine and extrasynaptic sites by glycine (Papouin *et al.*, 2012).

It is unclear whether specific subunit compositions modulate the localisation of receptors along the synapse. Some authors observed that the organisation of NMDA receptors along synaptic and extrasynaptic sites was mobile and both GluN2A and GluN2B subunits may be located extrasynaptically (Tovar and Westbrook, 2002). Others propose that GluN2B-containing receptors are enriched extrasynaptically (Massey *et al.*, 2004; Papouin *et al.*, 2012).

The site of NMDA receptors may have an influence on their function. Activation of synaptic sites is thought to be neuroprotective, whereas activation of extrasynaptic receptors may promote cell death (Hardingham and Bading, 2010). However, conflicting findings have been reported (Papouin *et al.*, 2012).

1.2 NMDA receptor involvement in neuronal processes

1.2.1 Long-term potentiation and depression

Long-term potentiation (LTP) is a persistent strengthening of synaptic connections based on recent patterns of activity (Cooke and Bliss, 2006a). LTP provides a compelling neuronal model for synaptic plasticity, declarative learning, and memory. In contrast, long-term depression (LTD) is a persistent weakening of synaptic connections. Disturbances of LTP and LTD might play a role in chronic pain, epileptogenesis and dementia (Cooke and Bliss, 2006a).

NMDA receptors are key mediators of synaptic potentiation (LTP) and depression (LTD) that rely on their specific function of coincidence detection. Opening of NMDA receptors requires the simultaneous binding of a presynaptically released agonist, i.e. glutamate, and the depolarization of the postsynaptic membrane to remove the Mg^{2+}-block within the channel pore (Nakazawa *et al.*, 2004). The receptor remains inactivated if either one or the other is absent. In this manner, NMDA receptors detect coinciding pre- and postsynaptic activity, a process that is thought to be the molecular basis of declarative or associative learning.

Opening of NMDA receptors leads to an influx of Ca^{2+} ions that trigger a cascade of biochemical events that strengthen the postsynaptic response to glutamate by incorporating AMPA receptors into the postsynaptic membrane (Ehrlich and Malinow, 2004). An indirect mechanism might additionally facilitate presynaptic glutamate release (S. Choi *et al.*, 2003). These processes are Ca^{2+} dependent. Reduction of intracellular Ca^{2+} effectively blocks LTP (S. Williams and Johnston, 1989).

Subunit composition and synaptic localisation may modulate the functional properties of NMDA receptors. GluN2A-containing receptors may primarily subserve LTP, whereas GluN2B-containing receptors trigger LTD (L. Liu *et al.*, 2004). LTP relies on synaptic activation only, whereas LTD involves both synaptic and extrasynaptic sites (Papouin *et al.*, 2012).

Other forms of neuronal plasticity, independent of LTP or LTD, have also been described and NMDA receptors may also play a role (Becker *et al.*, 2014; Vlachos *et al.*, 2013).

1.2.2 Working memory

There is limited knowledge on the neuronal processes involved in working memory, a short-lasting form of memory that is important to transiently hold and manipulate goal-related information and to guide forthcoming actions.

Working memory is stored by the maintained firing of a memory-specific subset of neurons in the prefrontal cortex (Funahashi *et al.*, 1989). Computational modelling suggest that NMDA receptors, due to their slow kinetics, are particularly suited to sustain neuronal activity at low firing rates during working memory (Durstewitz *et al.*, 2000; Lisman *et al.*, 1998; X. J. Wang, 1999). Studies in rodents and non-human primates demonstrated that blocking NMDA receptors abolished persistent activity in prefrontal neurons during a working memory task (Jackson *et al.*, 2004; M. Wang, Yang, C.-J. Wang, Gamo, Jin, Mazer, Morrison, X.-J. Wang and Arnsten, 2013a). Significant working memory impairments were seen with local or systemic application of NMDA receptor antagonists in rodents (Jackson *et al.*, 2004; Moghaddam and Adams, 1998), non-human primates (B. M. Roberts *et al.*, 2010; M. Wang, Yang, C.-J. Wang, Gamo, Jin, Mazer, Morrison, X.-J. Wang and Arnsten, 2013a), and humans (Driesen *et al.*, 2013; Honey *et al.*, 2004).

Several neurological and psychiatric disorders are associated with both dysfunctional NMDA receptor signalling and working memory deficits. Working memory deficits are a core feature of schizophrenia (Silver *et al.*, 2003) and play an important role in attention-deficit hyperactivity disorder (ADHD) (Martinussen *et al.*, 2005). Several lines of evidence support a hypofunction of NMDA receptors in schizophrenia (Bubeníková-Valešová *et al.*, 2008). Application of NMDAR antagonists is commonly used to model

psychotic and cognitive symptoms in schizophrenia, that include deficits in working memory. Hypofunction of NMDARs has also been described in ADHD (Chang *et al.*, 2014).

Although less typical than impairments in episodic memory, working memory deficits are also commonly observed in both focal epilepsy (Stretton and Thompson, 2012; Stretton *et al.*, 2012) and Alzheimer's disease (AD) (Stopford *et al.*, 2012). NMDA receptor dysfunction has been demonstrated in these disorders.

1.2.3 Excitotoxicity

Excitotoxicity is the pathological damage to neurons after intense exposure to excitatory neurotransmitters, mainly glutamate (D. W. Choi, 1992; Olney, 1969). Excitotoxicity is predominantly, but not exclusively, mediated by prolonged opening of NMDA receptors, potentially because of their high permeability to Ca^{2+} and weak desensitization (Rothman and Olney, 1995). Prolonged opening of NMDA receptors leads to excess influx of Ca^{2+} and consequently trigger a neuronal cell-death cascade (D. W. Choi, 1995; Weiss *et al.*, 1990). Antagonising NMDA receptor activity attenuated glutamate-induced neuronal loss (D. W. Choi *et al.*, 1988; Ferrer-Montiel *et al.*, 1998; S. Liu *et al.*, 1997).

Diverging roles for different NMDA receptor subunit compositions and synaptic localisations in promoting excitotoxic damage were proposed. Activation of receptors containing GluN2B subunits resulted in cell-death, whereas GluN2A containing receptors had both neurotoxic and neuroprotective effects (Engelhardt *et al.*, 2007; Y. Liu *et al.*, 2007). Some authors proposed that synaptic receptors may be neuroprotective whereas extrasynaptic receptors may be neurotoxic (Hardingham and Bading, 2010), whereas others observed that both receptor sites are capable of mediating excitotoxicity (Y. Liu *et al.*, 2007; Sattler *et al.*, 2000; Wroge *et al.*, 2012; Zhou *et al.*, 2013).

Excitotoxicity has been observed in models of cerebral ischemia. Application of NMDA receptor antagonists reduced hypoxic neuronal injury *in vitro* (Rothman, 1984) and *in vivo* (Simon *et al.*, 1984). Excitotoxic injury has also been implicated in models of epilepsy (Meldrum, 1993), Alzheimer's disease (Olney *et al.*, 1997), Huntington's disease (DiFiglia, 1990), Parkinson's disease (Beal, 1998), and other neurodegenerative disorders.

1.2.4 Excitatory and inhibitory roles on neuronal networks

Traditionally, NMDA receptors have been linked to an activating effect on neuronal networks because they bind glutamate, the most prevalent excitatory neurotransmitter in the central nervous system. On the other hand, emerging evidence from basic and clinical science points to the potential of NMDA receptors to exhibit an inhibitory effect on neuronal networks (Fitzgerald, 2012). Although the aspect of network suppression through NMDA receptors has received only little attention, recent evidence in people with genetic forms of epilepsy provides strong support to this concept.

Typically, NMDA receptor antagonism *in vitro* and *in vivo* leads to inhibition of pyramidal neurons (Arvanov and R. Y. Wang, 1997; L. Chen *et al.*, 2003; Hirsch and Crepel, 1991). Paradoxically, NMDA receptor antagonism can, in certain situations, also produce excitatory effects (Grunze *et al.*, 1996; Homayoun and Moghaddam, 2007; Manzoni *et al.*, 1994) and lead to an activation of limbic structures (Höflich *et al.*, 2017; Kraguljac *et al.*, 2017; McMillan *et al.*, 2019). NMDA receptor antagonists may lead to network activation, detected as increased metabolism in the frontal cortex and thalamus and increased blood flow in the anterior cingulate cortex (Lahti *et al.*, 1995; Vollenweider *et al.*, 1997) and on recordings in freely moving rats (Jackson *et al.*, 2004; Suzuki *et al.*, 2002).

There are several potential explanation for the inhibitory effects of NMDA receptors. Network suppression is probably mainly mediated by NMDA receptors located on gamma-aminobutyric-acid (GABA) releasing interneurons that suppress the activity of pyramidal cells (Grunze *et al.*, 1996; Homayoun and Moghaddam, 2007; Manzoni *et al.*, 1994). Additionally, an interaction between NMDA and AMPA receptors may play a role. NMDA receptors can lead to a downregulation of excitatory AMPA receptors (Hall *et al.*, 2007). Conversely, NMDA receptor antagonism increases transmission through AMPA receptors (Moghaddam and Adams, 1998; Moghaddam *et al.*, 1997). A combination of these factors may lead to network level excitation mediated by NMDA receptor hypofunction.

Recent findings in patients with epilepsy, a disease of overt neuronal excitation and insufficient inhibition, underline these concepts. Loss-of function mutations in GRIN genes, that encode NMDA receptor subunits, can lead to a syndrome with seizures and aphasia (chapter 1.3.3) (Xu and Luo, 2018). NMDA receptor hypofunction in Anti-NMDA-receptor encephalitis (chapter 1.3.5), an autoimmune disorder, also frequently causes seizures (Hughes *et al.*, 2010; Moscato *et al.*, 2014). A therapeutic trial of the highly selective NMDA receptor antagonist D-CPP-ene caused an increase of seizures in a large proportion of cases (Sveinbjornsdottir *et al.*, 1993).

Thus, NMDA receptor activation may lead to either activation or inhibition on a network level (Fitzgerald, 2012). This consideration is important to guide the development of treatments targeting the NMDA receptor. Drugs causing overt hyper- or hypofunction of NMDA receptors were not tolerated well, because they blocked normal synaptic activity and led to intolerable side effects (Le and Lipton, 2001). A balanced tonic activation of NMDA receptors may be necessary for normal function of the brain. In this regard, uncompetitive antagonism is a promising concept. An uncompetitive antagonist is an inhibitor whose activation is contingent on prior activation of the receptor by an agonist (Lipton, 2006). In this manner, an uncompetitive antagonist would block overt hyperactivation, i.e. in the context of

excitotoxicity, but maintain normal function relatively intact to avoid side effects. Memantine is an uncompetitive NMDA receptor antagonist with a rapid off-rate and low affinity (Lipton, 2006). It has been successfully used for treatment of moderate to severe Alzheimer's disease.

1.3 NMDA receptors in health in disease

1.3.1 Aging

The worldwide population is aging at an unprecedented rate (United Nations Department of Economic and Social Population Affairs, 2019). Aging is associated with cognitive decline and a higher risk of neurodegenerative disorders (Park *et al.*, 2002).

Normal aging leads to a reduced pool of glutamate, particularly in the striatum, as measured *in vivo* with MR-spectroscopy (Kaiser *et al.*, 2005; Zahr *et al.*, 2013). On the other hand, a reduced glutamate re-uptake and decreased expression of glutamate transporters was observed in older rats (Potier *et al.*, 2010). This could lead to a facilitated activation of glutamatergic receptors, particularly located extrasynaptically, despite a lower overall glutamate pool (Potier *et al.*, 2010).

NMDA receptors may be the most vulnerable type of glutamate ion-channels to the effects of aging (Magnusson and Cotman, 1993; Magnusson *et al.*, 2010). The overall number of NMDA receptors is reduced in older animals (Castorina *et al.*, 1994; Magnusson, 2000; Magnusson and Cotman, 1993; Magnusson *et al.*, 2007; Ontl *et al.*, 2004). Particularly affected are the frontal and parieto-occipital cortex, striatum, and hippocampus.

There is limited knowledge on the effects of aging on NMDA receptors in humans. Some *post mortem* studies found a decrease of NMDA receptor numbers in older individuals that was linked to an overall loss of neurons (Kornhuber *et al.*, 1988;

Piggott *et al.*, 1992), whereas others did not find a relevant decrease (Law *et al.*, 2003).

The change in overall NMDA receptor number may be counteracted by functional changes. Several, but not all, studies found an age-related increase in sensitivity and responsiveness of the remaining receptors (Billard *et al.*, 1997; Jasek and Griffith, 1998; Kuehl-Kovarik *et al.*, 2000). There is also a well-documented shift of receptor subunit composition from GluN2B towards GluN2A-containing receptors (Brim *et al.*, 2013; Magnusson, 2000; Magnusson *et al.*, 2002; 2006; Zamzow *et al.*, 2013). NMDA receptor heteromers containg GluN2A subunits have a higher opening probability (N. Chen *et al.*, 1999; Erreger *et al.*, 2005; Gray *et al.*, 2011). Additionally, there is a shift from synaptic towards extrasynaptic NMDA receptor sites during aging (Potier *et al.*, 2010). These aspects could contribute to the neuronal hyperexcitability observed in aging (Senatorov *et al.*, 2019), mild cognitive impairment, and Alzheimer's disease (Fontana *et al.*, 2017; Haberman *et al.*, 2017; Palop *et al.*, 2007; Yassa *et al.*, 2010).

1.3.2 Epilepsy

1.3.2.1 Defining seizures and epilepsy

Epilepsy is one of the most common serious neurological disorders. There are at least 50 million people with epilepsy worldwide (World Health Organization, 2000). Epilepsy has an estimated lifetime prevalence of 5.8 per 1,000 persons in developed countries and 15.4 per 1,000 in developing countries (Ngugi *et al.*, 2010).

Epilepsy has been defined as "a disorder of the brain characterized by an enduring predisposition to generate epileptic seizures, and by the neurobiologic, cognitive, psychological, and social consequences of this condition" (Fisher et al., 2005). A more recent practical approach outlines this predisposition as any of the following (Fisher et al., 2014):

1. "At least two unprovoked (or reflex) seizures occurring >24 h apart;

2. One unprovoked (or reflex) seizure and a probability of further seizures similar to the general recurrence risk (at least 60%) after two unprovoked seizures, occurring over the next 10 years;
3. Diagnosis of an epilepsy syndrome."

This practical definition implies that a single remote symptomatic seizure after a relevant insult, e.g. ischemic stroke, qualifies as epilepsy. This is due to the high recurrence rate after stroke of > 70% (Fisher *et al.*, 2014; Hesdorffer *et al.*, 2009).

1.3.2.2 Seizures and the glutamatergic system

Glutamate is directly involved in the generation of epileptic discharges through sequences of paroxysmal depolarization shifts (PDS) (During and Spencer, 1993). An increase in extracellular glutamate can be observed before and during spontaneous seizures in humans (During and Spencer, 1993). Elevated glutamate concentrations in different epilepsy syndromes and aetiologies were demonstrated using magnetic resonance spectroscopy (MRS) (Davis *et al.*, 2015; Helms *et al.*, 2006; Simister *et al.*, 2002; 2007; Simister, McLean, Barker and Duncan, 2003a; 2003b).

PDS are mainly mediated by activation of AMPA receptors (Rogawski, 2011). Blocking of NMDA receptors does not abolish PDS (W. L. Lee and Hablitz, 1989; Neuman *et al.*, 1988). On the other hand, this initial depolarization is a necessary prerequisite for opening of NMDA channels, which consequently sustain and prolong ongoing depolarization during the later stages of epileptic activity (Baldino *et al.*, 1986; Naylor *et al.*, 2013).

NMDA receptors desensitize weakly and are, thus, likely to sustain prolonged seizures and status epilepticus. Blocking NMDA receptors interrupted status epilepticus, reduced refractoriness to benzodiazepines and enhanced survival in animal models (Ormandy *et al.*, 1989; Rice and DeLorenzo, 1999). In humans, several reports

describe successful termination of super-refractory status epilepticus with the NMDA receptor antagonist ketamine (Borris *et al.*, 2000; Prüss and Holtkamp, 2008).

These advances have been translated into antiepileptic treatment with felbamate, an NMDA receptor antagonist and sodium channel modulator (Pellock *et al.*, 2006). Cases of fatal aplastic anaemia and hepatic failure have limited the clinical use of felbamate.

On the other hand, NMDA receptor antagonists may also have proconvulsant effects (Alldredge *et al.*, 1989; Claudet and Maréchal, 2009; Modica *et al.*, 1990; Peltz *et al.*, 2005; Sveinbjornsdottir *et al.*, 1993). Treatment with the antagonist D-CPP-ene led to an increase in seizures in a large proportion of epilepsy patients (Sveinbjornsdottir *et al.*, 1993).

1.3.2.3 Mechanisms of epileptogenesis

Early epilepsy research in the twentieth century focused mainly on ictogenesis, i.e. the propensity to generate epileptic seizures (Pitkänen and Engel, 2014). Despite considerable progress and the development of over 20 anticonvulsants, approximately one third of people with epilepsy are refractory to medical treatment (Del Felice *et al.*, 2010).

Recently, scientific interest has focused on how a brain develops the enduring predisposition to generate epileptic seizures. This process is called epileptogenesis and has been defined as *"the development and extension of tissue capable of generating spontaneous seizures, resulting in a) development of an epileptic condition and/or b) progression of the epilepsy after it is established"* (Pitkänen *et al.*, 2013). By increasing our understanding of epileptogenic processes and by developing truly antiepileptogenic treatments, one could prevent and abort the development of epilepsy or modify and eventually cure the already established disease. However, after several unsuccessful antiepileptogenic treatment trials with conventional antiseizure

Possible mechanism of epileptogenesis	Selected references
Reorganisation of synaptic circuits • Loss of inhibitory interneurons leading to a decrease of GABA-mediated inhibition. • Sprouting of mossy fibres, possibly causing increased recurrent excitation.	Ribak et al. (1982) Sloviter (1987) de Lanerolle et al. (1989) Kobayashi and Buckmaster (2003) Babb et al. (1991) Sutula et al. (1989)
GABA (γ-Aminobutyric acid) • Internalisation of $GABA_A$ receptors. • Changes of $GABA_A$ subunit composition. • Disturbances of chloride homeostasis with increase of chloride influx.	Goodkin et al. (2005) Naylor et al. (2005) Brooks-Kayal et al. (1998) Loup et al. (2000) Huberfeld et al. (2007)
Growth factors • Influence of Brain Derived Neurotrophic Factor (BDNF) on $GABA_A$ subunit expression. • Antiepileptogenic effects of BDNF and erythropoietin injections.	Roberts et al. (2006) Paradiso et al. (2009) Chu et al. (2008)
Inflammation • Inflammatory mediators, reactive astrocytosis, and activated microglia found in resected human epileptic tissue. • The degree of microglia activation correlates with neuronal cell loss and spontaneous seizures. • Induction of inflammation with lipopolysaccharide lowered the seizure threshold, anti-inflammatory drugs reduced seizure frequency in animals.	Aronica et al. (2007) Crespel et al. (2002) Amhaoul et al. (2015) Bertoglio et al. (2016) Kovacs et al. (2006) Sayyah et al. (2003) Fabene et al. (2008) Polascheck et al. (2010)
mTOR (mammalian target of rapamycin) • mTOR involved in epileptogenesis in tuberous sclerosis complex (TSC). • mTOR inhibitors supress seizures in TSC and in models of acquired epilepsy.	Zeng et al. (2008) Zeng et al. (2009) Huang et al. (2010)
Tau protein • Targeting hyperphosphorylation of tau with sodium selenate prevented epileptogenesis in animal models of posttraumatic encephalopathy.	Liu et al. (2016)

Table 1.1: *Selected mechanisms of epileptogenesis*

drugs in humans (Trinka and Brigo, 2014), we are still in the beginning of understanding the mechanisms of epileptogenesis.

Epileptogenesis is best studied after a specific insult with a clear onset leading to spontaneous seizures, such as stroke or traumatic brain injury (TBI). Clinical experience

suggests a latent (seizure-free) period of several weeks to years between the initial insult and a first unprovoked seizure (Löscher *et al.*, 2015). However, it is unlikely that epileptogenesis represents a step function of time after injury. Recent data rather indicate that epileptogenesis is a continuous process beginning at the time of brain insult and extending past the first unprovoked seizure (Dudek and Staley, 2012; Kadam *et al.*, 2010; P. A. Williams *et al.*, 2009).

Seizures can develop as a relatively unspecific reaction of the brain to different insults. Hence a wide range of overlapping and parallel pathways might be involved in epileptogenesis. A summary of a few selected mechanisms of epileptogenesis is displayed in Table 1.1.

1.3.2.4 Role of NMDA receptors in epileptogenesis

Several lines of evidence support a progressive involvement of NMDA receptors during the development of epilepsy in animal models (Croucher *et al.*, 1995; Mody and Heinemann, 1987; Vezzani *et al.*, 1988; Yeh *et al.*, 1989). Antagonism of the NMDA receptor prevented epileptogenesis and seizures in the kindling and pilocarpine models of epilepsy (Croucher and Bradford, 1990; Croucher *et al.*, 1988; Gilbert, 1988; Raza *et al.*, 2004; Rice and DeLorenzo, 1998; Stasheff, Anderson, Clark and Wilson, 1989a).

Glutamate released after seizures likely has excitotoxic effects that can cause neuronal damage and could lead to an extension of the epileptic tissue (Tanaka *et al.*, 1997). These excitotoxic effects are mainly mediated through NMDA receptors. Several studies demonstrated that blocking of NMDA receptors during status epilepticus might be neuroprotective (Brandt *et al.*, 2003; Fujikawa *et al.*, 1994; Rice *et al.*, 1998).

1.3.3 Epilepsy-aphasia syndromes

Mutations of the GRIN2A gene, coding the GluN2A subunit of NMDA receptors, have been described in 8% to 20% of focal epileptic encephalopathies of childhood (Carvill *et al.*, 2013; Lemke *et al.*, 2013; Lesca *et al.*, 2013). The majority of cases presented with acquired epileptic aphasia (Landau-Kleffner syndrome) or continuous spike and waves during slow-wave sleep syndrome (CSWSS), characterised by focal motor seizures and regression of language or global cognitive skills. Mutations to other GRIN genes encoding the GluN1 and GluN2B subunits have also been associated with epilepsy (Xu and Luo, 2018).

Functional assessment of the mutated proteins revealed that the majority of these mutations caused a loss of NMDA receptor function, followed by gain-of-function mutations (Xu and Luo, 2018). In mutations affecting the GluN2A subunit, those leading to a receptor gain-of-function were associated with a more severe phenotype (Strehlow *et al.*, 2019).

1.3.4 Brain tumours

Tumour expansion of malignant gliomas inside a rigid skull is facilitated by neuronal damage of peritumoural tissue, which is mediated by glutamate excitotoxicity (Takano *et al.*, 2001). Gliomas release glutamate into the peritumoural tissue that promotes tumour growth (Takano *et al.*, 2001; Ye and Sontheimer, 1999). A potential mechanism is the overexpression of the x_c^- cystine-glutamate antiporter (Buckingham *et al.*, 2011), the increase of extracellular glutamate to toxic levels, and subsequent excitotoxicity mediated by NMDA receptors. NMDA receptor antagonism with MK801 or memantine slowed the growth of glutamate-secreting tumours (Ramaswamy *et al.*, 2014; Takano *et al.*, 2001).

Peritumoural glutamate was associated with a higher risk of seizures in animals (Buckingham *et al.*, 2011) and in humans (Yuen *et al.*, 2012). Blocking of the x_c system

and subsequent reduction of glutamate release, led to reduced frequency of epileptic events (Buckingham *et al.*, 2011). Thus, glutamate lowering agents or inhibitors of glutamate receptors may be a therapeutic option for tumour-related seizures (Campbell *et al.*, 2012). This also suggests that tumour surgery may alleviate seizures by removing the glutamate source.

In a similar manner, D-2-hydroxyglutarate (D2HG), a product of mutant isocitrate dehydrogenase 1 ($IDH1^{mut}$), is released by tumour cells into the surrounding tissue and may mimic the activity of glutamate on NMDA receptors (H. Chen *et al.*, 2017). $IDH1^{mut}$ gliomas were more likely to cause seizures that could be blocked by NMDA receptor antagonists (H. Chen *et al.*, 2017).

Considerable interest has surrounded the use of perampanel, an AMPA receptor antagonist approved for the treatment of seizures, in patients with gliomas. Perampanel slowed tumour growth and reduced extracellular glutamate levels (Lange *et al.*, 2019; Venkataramani *et al.*, 2019). Perampanel was also used to treat seizures in patients with gliomas (Maschio *et al.*, 2019; 2020). The effects of perampanel may be related to recently described *bona fide* synapses between neurons and glioma cells that produce AMPA receptor mediated postsynaptic currents and influence neuronal activity dependent brain tumour growth (Venkataramani *et al.*, 2019; Venkatesh *et al.*, 2019).

1.3.5 Anti-NMDA-receptor encephalitis

Antibodies to the GluN1 subunit of NMDA receptors cause a severe but treatable form of immune-mediated encephalitis. Anti-NMDA-receptor encephalitis is typically associated with psychiatric, cognitive, and autonomic dysfunction, seizures, speech abnormalities, movement disorders, and decreased level of consciousness (Dalmau *et al.*, 2007; Graus *et al.*, 2016). The early predominance of psychiatric symptoms, that may mimic schizophrenia, frequently leads to initial admissions on psychiatric units (Al-

Diwani *et al.*, 2019). The psychiatric spectrum is complex and involves mixed mood-psychosis symptoms (Al-Diwani *et al.*, 2019).

The disease most frequently affects young women, 95% of cases being younger than 45 years, and has a female sex predominance of 4:1 (Titulaer *et al.*, 2013). More than half of women aged between 18 and 45 affected by the encephalitis have associated tumours, most commonly ovarian teratomas (Titulaer *et al.*, 2013). Around one quarter of adults older than 45 years have associated tumours, mostly carcinomas, whereas tumours are rare in children (Titulaer *et al.*, 2013). Those with associated tumours are at lower risk of relapses if the tumour can be removed (Titulaer *et al.*, 2013).

Although 80% of cases show favourable outcome after treatment, the overall recovery may often be protracted and up to 25% suffer relapses (Gabilondo *et al.*, 2011; Titulaer *et al.*, 2013). Cognitive deficits may persist for a long time (Finke *et al.*, 2012). Long-term immunotherapy may be necessary to prevent relapses and persistent antibodies have been reported up to 15 years after disease onset (Alexopoulos *et al.*, 2011; Hansen *et al.*, 2013; Mariotto *et al.*, 2017).

The pathomechanism of Anti-NMDA-receptor encephalitis has been studied *in vitro* and in animal experiments. Anti-GluN1 antibodies first increase the clustering of NMDA receptors in both synaptic and extrasynaptic sites (Ladépêche *et al.*, 2018) and subsequently lead to a cross-linking and internalisation of receptors (Hughes *et al.*, 2010; Moscato *et al.*, 2014; Wright *et al.*, 2015). This results in a decrease of NMDA receptor surface density and NMDA receptor-mediated currents (Hughes *et al.*, 2010). *In vivo* animal experiments suggest that the magnitude of reduction in NMDA receptor density relates to antibody titres. It may be reversible, because washing out of antibodies improved synaptic receptor density and reduced disease symptoms (Hughes *et al.*, 2010; Moscato *et al.*, 2014). Data in humans is lacking but a reduced NMDA receptor density was reported *post mortem* in two autopsied patients with anti-NMDA-receptor encephalitis (Dalmau *et al.*, 2007).

1.3.6 Alzheimer's disease

Alzheimer's disease (AD) is a neurodegenerative disorder associated with progressive loss of memory and cognitive functions. It is the most common cause of dementia accounting for up to two thirds of cases. The worldwide prevalence of dementia is currently estimated at 44 million, and is expected to double by 2030 and more than triple by 2050. The global costs of dementia were estimated at $604 billion in 2010 and this number is set to rise in the coming years (Prince *et al.*, 2014).

Considerable progress has been made on the pathomechanisms of AD in the past 20 years. However, there is still a significant lack of knowledge on early diagnosis, selection of patients for prophylactic treatment and monitoring of disease progress. Studying activated NMDA receptors in living humans with advanced neuroimaging methods might provide valuable answers to some of these problems.

1.3.6.1 Basic pathomechanisms of Alzheimer's disease

The most widely accepted model for the pathomechanism of AD is the amyloid hypothesis. This is based on the observation that amyloid beta-peptide (Aβ) is the primary component of the senile plaques observed in brains of AD patients (Masters *et al.*, 1985). This peptide results from cleavage of the amyloid precursor protein (APP), coded on chromosome 21. Mutations of the APP gene can lead to early familial forms of AD (Goate *et al.*, 1991). The main genetic risk factor of AD is a polymorphism in the Apolipoprotein E (APOE) gene, a protein that was observed to bind to Aβ-peptides (Strittmatter *et al.*, 1993). The amyloid hypothesis is also supported by results of cerebrospinal fluid (CSF) and imaging studies. These show that Aβ biomarkers are the first to become abnormal even before cognitive symptoms become obvious (Jack *et al.*, 2010).

However, some concerns with the amyloid hypothesis persist. The most commonly voiced critique is that Aβ levels do not correlate well with cognitive status in affected

individuals (Giannakopoulos *et al.*, 2003). Moreover, even individuals with high Aβ levels can have normal cognition. Some studies observed that Aβ deposition was not associated with relevant neuronal loss in transgenic mice (Irizarry *et al.*, 1997). A considerable amount of controversy remains about the pathomechanism of the neurotoxic effects of Aβ, which is still mostly unknown (Hardy and Selkoe, 2002).

1.3.6.2 Role of NMDA receptors in Alzheimer's disease

Several lines of evidence link accumulation Aβ plaques with disturbances of NMDA receptors. Hence, NMDA receptors might play a major role in the pathomechanism of AD. This is not surprising, as these receptors are not only involved in learning and memory but also in neurotoxicity. The dual function of NMDA receptors and their complex relationship with Aβ leads to several well-documented interactions, including the (i) overactivation of extrasynaptic NMDA receptors, (ii) overexpression of the GluN2B subunit, (iii) reduction of synaptic NMDA receptor density, and (iv) accumulation of Aβ through NMDA receptor activation.

Aβ has been observed to cause a decreased glutamatergic transmission (Palop *et al.*, 2007; Walsh *et al.*, 2002). A reduced number of synaptic NMDA receptors was found in *post mortem* hippocampal slices of patients with AD (Jacob *et al.*, 2007; Jansen *et al.*, 1990; Kravitz *et al.*, 2013; Young, 1987) In animals, Aβ caused the internalization of synaptic NMDA receptors through dephosphorylation of the GluN2B subunit (Palop *et al.*, 2007; Snyder *et al.*, 2005). Long-term potentiation was impaired in these animals, which led to memory deficits. This mechanism was thought to explain cognitive decline in AD patients.

However, further research showed that the interaction between Aβ and NMDA receptors may be more complicated. While there was a reduction in synaptic NMDA receptors, those located extrasynaptically may be overactivated. Application of Aβ leads to increased activity of extrasynaptic NMDA receptors (Ferreira *et al.*, 2015; Hsia

et al., 1999; Kamenetz *et al.*, 2003; Shankar *et al.*, 2007; Talantova *et al.*, 2013; J. Zhang *et al.*, 2014). Subsequently, an excitotoxic cascade may cause a rise in intracellular calcium (Ferreira *et al.*, 2015) and lead to synaptic depression and dendritic spine loss (Kamenetz *et al.*, 2003; Shankar *et al.*, 2007). These effects were observed early in the course of AD and may precede the development of amyloid plaques (Hsia *et al.*, 1999).

Blocking of overactivated NMDA receptors in animal models of AD counteracted the intracellular calcium increases (Ferreira *et al.*, 2015), reduced long-term depression (J. Zhang *et al.*, 2014) and prevented synaptic damage (Kamenetz *et al.*, 2003; Shankar *et al.*, 2007; Talantova *et al.*, 2013). Despite the negative impact of NMDA antagonists on long-term potentiation, NMDA receptor antagonists improved the performance of treated animals on spatial memory tests and improved the learning process (J. Zhang *et al.*, 2014).

The uncompetitive NMDA receptor antagonist memantine demonstrated positive effects on cognition, mood, and the ability to perform daily activities in AD and was approved for the treatment of moderately to severely affected patients with AD. Memantine blocks overactivated NMDA receptors while preserving normal glutamatergic activity that may lead to a good tolerability of the drug. Additionally, memantine preferentially blocks extrasynaptic NMDA receptors which are likely to be pathologically up-regulated in AD (Lipton, 2006).

Some studies also found activated NMDA receptors to be the cause of Aβ accumulation (Bordji *et al.*, 2010; Lesné *et al.*, 2005). Such a mechanism could cause a vicious circle with increasing accumulation of Aβ, up-regulation of pathological NMDA receptors and, ultimately, neuronal degeneration. This led some authors to speculate that Aβ may not be directly causative of AD but rather represents a toxic by-product of excessive NMDA receptor activation. These complex processes need to be further elucidated in the context of other possible mechanisms including accumulation of tau protein and neuroinflammation (Hardy and Selkoe, 2002).

1.3.7 Other disorders associated with NMDA receptor dysfunction

Many neurological and psychiatric disorders may be associated with dysfunctional NMDA receptors (Kalia *et al.*, 2008). Hypofunction of NMDA receptors as a model of schizophrenia has received a lot of attention (Olney, Newcomer and Farber, 1999a). Inhibition of NMDA receptors may be a treatment strategy for major depression (Barygin *et al.*, 2017; Murrough *et al.*, 2013). Overactivation of NMDA receptors has been described in levodopa-induced dyskinesias in Parkinson's disease, that may be treated with amantadine, a noncompetitive NMDA receptor antagonist (Ahmed *et al.*, 2011). Excitotoxic damage, attributed to dysfunctional NMDA receptors, has been proposed in neurodegenerative disorders including Huntington's disease (Fan and Raymond, 2007) and amyotrophic lateral sclerosis (Shaw and Ince, 1997). Riluzole, a modulator of NMDA receptor mediated transmission, is approved for treatment of amyotrophic lateral sclerosis (Kalia *et al.*, 2008).

On the other hand, clinical trials of NMDA receptor antagonists in stroke and traumatic brain injury failed, possibly because overt blocking of NMDA mediated activity may be detrimental for neuronal survival and plasticity during rehabilitation (Ikonomidou and Turski, 2002).

1.4 Imaging NMDA receptors *in vivo*

1.4.1 Positron emission tomography of NMDA receptors

Positron emission tomography (PET) allows *in vivo* imaging of molecular targets in the brain (Galovic and Koepp, 2016) and involves the injection of a positron-emitting radioligand (tracer) and the detection of coincident gamma waves within a scanner. The resulting image represents the spatial distribution of the tracer within the brain (Gunn *et al.*, 2015).

Using PET with a receptor-specific radioligand can provide insights into the molecular functioning of a living human brain. A large number of tracers have been developed but only few demonstrated acceptable brain penetration, low-nonspecific binding, high affinity, and target selectivity to progress into clinical studies (Gunn *et al.*, 2015).

Developing radioligands targeting the NMDA receptor has proven particularly difficult. Until recently, *in vivo* imaging of NMDA receptors has not been possible due to the lack of a suitable radiotracer (Sobrio *et al.*, 2010). So far, only few tracers were tested in humans (Krämer *et al.*, 2018; McGinnity *et al.*, 2014; van der Aart *et al.*, 2018; 2019; Waterhouse, 2003). Most of these tracers bind to the phencyclidine (PCP) site inside of the NMDA receptor, requiring channel opening for the tracer to bind (McGinnity *et al.*, 2014; Waterhouse, 2003).

One study evaluated eight people with mesial temporal lobe epilepsy (MTLE) with [^{11}C]ketamine (Kumlien *et al.*, 1999). There was decreased binding in the ipsilateral temporal lobe, however the authors could not differentiate whether the changes were due to reduced NMDA-receptor density, reduced perfusion, or focal atrophy.

[^{11}C]CNS-5161 PET was used to measure binding to the PCP site on NMDA receptors in 18 patients with Parkinson's disease with (n=8) or without (n=10) levodopa-induced dyskinesias (Ahmed *et al.*, 2011). Both patient groups had similar radioligand binding in the OFF state, i.e. withdrawn from levodopa. Dyskinetic patients had higher tracer uptake in caudate, putamen, and precentral gyrus in the ON state, i.e. after levodopa administration. The results confirm abnormal glutamatergic transmission in motor areas following levodopa administration in dyskinetic patients and provide support for treatment of dyskinesias with NMDA receptor modulators, e.g. amantadine.

A structurally related tracer, [^{123}I]CNS-1261, was used in several single photon emission tomography (SPET) studies in patients with schizophrenia. The authors found reduced left hippocampal tracer uptake in medication free, but not in antipsychotic-treated, patients with schizophrenia compared to healthy controls (Pilowsky *et al.*, 2006). The authors also observed global reductions of binding in patients treated with

clozapine (Bressan *et al.*, 2005) and in healthy controls receiving ketamine (Stone *et al.*, 2008).

A limitation of studies using ^{11}C-labelled tracers is their short half-life of around 20 minutes, restricting their use to facilities with an on-site cyclotron. ^{18}F-labelled radioligands, with a half-life of around 110 minutes, are more simple to use routinely because they can be more widely distributed and offer the potential for longer acquisitions.

[^{18}F]GE-179 was developed as an ^{18}F-labelled structural analogue of [^{11}C]CNS-5161 (McGinnity *et al.*, 2014; Robins *et al.*, 2010) and was used to study eleven patients with focal epilepsy and frequent interictal epileptiform discharges (McGinnity *et al.*, 2015). A global increase in [^{18}F]GE-179 uptake was seen in eight epilepsy patients not taking antidepressants, whereas three patients taking antidepressants showed a decreased tracer uptake. Four epilepsy patients showed focal signal alterations compared to controls but the findings were difficult to interpret because of the unclear or multifocal epilepsy localisation in these cases.

In another study reported as an abstract, eight out of ten patients with refractory focal epilepsy had focal areas of increased [^{18}F]GE-179 uptake (Vibholm *et al.*, 2017). The same authors also observed increased radioligand binding after hippocampal electrical stimulation in pigs (Vibholm, Landau, Alstrup, *et al.*, 2020). A successful blocking experiment with S-ketamine was performed in rats electrically stimulated in the amygdala/hippocampus (Vibholm, Landau, Møller, *et al.*, 2020). These findings confirm that [^{18}F]GE-179 is a use-dependent radioligand of the PCP site within the open NMDA receptor ion channel (Vibholm, Landau, Møller, *et al.*, 2020).

1.4.2 [^{18}F]GE-179

The novel NMDA receptor radioligand [^{18}F]GE-179 was developed as a structural ^{18}F-labelled structural analogue of [^{11}C]CNS-5161 (Robins *et al.*, 2010). It demonstrated

affinity to the PCP site inside the open/active ion channel and is, thus, a potential use-dependent marker of NMDA receptor activation. The radioligand demonstrated high selectivity, moderate lipophilicity, high brain uptake, acceptable between-subject variability, and suitably rapid washout, making it a good candidate for further human studies (McGinnity *et al.*, 2014; Robins *et al.*, 2010).

GE-179 binding was specific to the NMDA receptor PCP site and did not demonstrate significant binding to any of the 60 other receptors, channels, and transporters assessed (McGinnity *et al.*, 2014; Robins *et al.*, 2010). The specificity of [^{18}F]GE-179 binding to the PCP site was validated *in vivo* in electrically stimulated rats (Vibholm, Landau, Møller, *et al.*, 2020). [^{18}F]GE-179 PET detected focally activated NMDA receptors following pulsed electrical stimulation in the amygdala/hippocampus that was blocked by administration of S-ketamine, confirming the use-dependent specificity of the radioligand to the open NMDA receptor ion channel.

In comparison, demonstrating binding specificity in anaesthetised animals is challenging because of the low baseline ion channel activity in sedated rodents (McGinnity *et al.*, 2019). Thus, initial blocking experiments in anaesthetised rats and rhesus monkeys were not successful (Schoenberger *et al.*, 2017), possibly due to the effects of anaesthesia. The use-dependent nature of GE-179 binding may require receptor activation/opening to demonstrate allow for blocking experiments and these may not be effective in anaesthetised specimen (McGinnity *et al.*, 2019). In the absence of ketamine or isoflurane anaesthesia, the GE-179 structural analogues CNS-5161 and GMOM showed reduced binding after administration of PCP site antagonists (Biegon *et al.*, 2007; van der Doef *et al.*, 2016).

GE-179 had no effect on any cardiovascular parameters in conscious dogs or on modified expanded acute toxicity in living rats, with a no-observed-adverse-effect-limit (NOAEL) of 316 µg/kg, equivalent to 306-times the expected maximum human clinical dose (Source: GE Healthcare plc, unpublished data, on file). CNS-5161, a structural analogue of GE-179, was administered in doses up to 2 mg to healthy volunteers

(Walters *et al.*, 2002) and up to 0.5 mg in patients with neuropathic pain (Forst *et al.*, 2007). Most commonly observed side effects were transient increases in blood pressure and heart rate, with mild headaches and mild visual disturbances also reported by some patients. No adverse effects of [^{18}F]GE-179 administered as a radiotracer were observed in a pilot study of healthy volunteers and patients with epilepsy (McGinnity *et al.*, 2014; 2015).

2 Common Methods

2.1 Participants

We included participants from four centres (National Hospital for Neurology and Neurosurgery [NHNN] London, Addenbrooke's Hospital Cambridge, John Radcliffe Hospital Oxford, and St. George's University Hospitals London). The participants were recruited as part of three studies; NMDA receptors in epilepsy, stroke, and traumatic brain injury (*UCL study*); Imaging NMDA receptor activation following head injury using positron emission tomography (*Cambridge study*); NMDA receptor binding in patients with frequent inter-ictal epileptiform discharges (McGinnity *et al.*, 2014; 2015) (*Hammersmith study*). In brief, the studies can be described as follows.

Firstly, most participants for this thesis were recruited as part of the *UCL study*, a large and ongoing multi-centre project studying NMDA receptor activation using [^{18}F]GE-179 PET in health and disease. The final study cohort involved 26 subjects with focal epilepsy and five with Anti-NMDA-receptor encephalitis. Additionally, ten healthy volunteers were recruited. The study used a Siemens Biograph mMR combined PET-MR scanner and an image-derived input function (IDIF) with venous blood sampling for quantification.

Secondly, ten healthy volunteers were recruited as part of the ongoing traumatic brain injury (TBI) study at Addenbrooke's Hospital in Cambridge. Eight of these volunteers

were later rescanned. The *Cambridge study* used a GE Discovery 690 TOF combined PET-CT scanner and an arterial input function for quantification.

Thirdly, nine healthy volunteers were recruited as part of a pilot study using [^{18}F]GE-179 PET in Hammersmith (McGinnity *et al.*, 2014; 2015). The study used a Siemens/CTI ECAT EXACT HR+ model 962 PET scanner at Hammersmith Hospital London and an arterial input function for quantification.

2.1.1 Healthy volunteers

We included 29 healthy volunteers (10 *UCL study*, 10 *Cambridge study*, 9 *Hammersmith study*) aged between 25 and 65 years without a history of neurologic or psychiatric illness and not taking regular medication. We rescanned eight healthy volunteers from the *Cambridge study*, and the remaining two participants were lost to follow-up. Out of these eight rescans, one participant was excluded because of failed metabolite analysis and another because of failure of arterial sampling during the scan, leaving a total of six rescans for analysis. An overview of demographic characteristics is given in Table 2.1.

2.1.2 Patients with epilepsy

We recruited 27 patients with unilateral focal refractory epilepsy aged between 18 and 65 years undergoing presurgical evaluation at NHNN. For each individual the diagnosis, lateralisation, and localisation of epilepsy was determined by a multidisciplinary epilepsy surgery evaluation involving neurologists, neurophysiologists, neurosurgeons, neuropsychologists, and psychiatrists specializing in epilepsy based on clinical history, neurologic examination results, seizure semiology, long-term video-electroencephalography telemetry, MRI, and

ID	Injected dose [MBq]	Age [years]	Sex	Ethnicity
HAM 01	188	26	M	European
HAM 02	173	31	M	Black
HAM 03	186	55	M	European
HAM 04	180	37	F	European
HAM 05	184	61	M	European
HAM 06	185	62	F	European
HAM 07	192	25	F	European
HAM 08	189	26	M	European
HAM 09	187	57	M	European
CAM 01	179	36	M	European
CAM 02	173	42	M	European
CAM 03	180	43	M	European
CAM 04	177	28	M	European
CAM 05	196	39	M	European
CAM 06	181	61	M	South Asian
CAM 07	165	27	M	Australian
CAM 08	177	43	M	European
CAM 09	179	47	F	European
CAM 10	171	38	M	European
UCL 01	188	26	M	Asian
UCL 02	188	58	F	European
UCL 03	187	27	M	Asian
UCL 04	195	31	M	European
UCL 05	204	46	F	European
UCL 06	190	63	M	European
UCL 07	187	32	M	European
UCL 08	199	30	M	European
UCL 09	193	46	F	Asian
UCL 10	182	47	F	European
Overview	Mean 185 ± 9	Mean 41 ± 13	72% male 28% female	79% European 21% Other

Table 2.1: *Characteristics of healthy volunteers*
HAM, Hammersmith cohort; CAM, Cambridge cohort; UCL, University College London cohort; M, male; F, female

neuropsychological and psychiatric assessments. [^{18}F]fluorodeoxyglucose(FDG)-PET was additionally performed in seven cases.

The epileptogenic zone was confirmed using intracranial electrode recordings in four subjects, and in all of these cases [^{18}F]GE-179 PET was performed before electrode implantation.

Excluded were subjects with (i) unclear or undetermined localisation of the epileptogenic zone, (ii) a history of neurologic or psychiatric conditions unrelated to epilepsy, (iii) history of traumatic brain injury leading to intracranial injuries, (iv) regular or recent (<14 days) use of antidepressants, antipsychotics, illicit substances, ketamine or felbamate. One subject was excluded after scanning because of corrupted PET images hindering reconstruction, leaving 26 participants with epilepsy in the final analysis.

All patients with epilepsy were scanned on the Siemens Biograph mMR combined PET-MR scanner and an image-derived input function with venous blood sampling was used for quantification.

2.1.3 Patients with Anti-NMDA-receptor encephalitis

We recruited five participants with clinically and laboratory-confirmed Anti-NMDA-receptor encephalitis from John Radcliffe Hospital Oxford (n=3) and St. George's University Hospitals London (n=2). Included were those who were recently discharged from hospital and able to undergo a 70-minute PET-MR scan. Excluded were subjects with a history of neurologic or psychiatric conditions unrelated to the encephalitis and those with regular or recent (<14 days) use of antidepressants, antipsychotics, illicit substances, ketamine or felbamate.

All patients with encephalitis were scanned on the Siemens Biograph mMR combined PET-MR scanner and an image-derived input function with venous blood sampling was used for quantification.

2.2 Regulatory approval

All studies were approved by the local Research Ethics Committee and the local NHS Trust research office. All studies received permission to administer [^{18}F]-GE-179 from

the Administration of Radioactive Substances Advisory Committee, U.K. All participants provided written, informed consent before participation.

2.3 Image acquisition and reconstruction

All participants underwent dynamic emission PET scans after intravenous injection of a target dose of 185 MBq of [^{18}F]GE-179.

2.3.1 Image acquisition in the UCL study

The *UCL study* used a Siemens Biograph mMR combined PET-MR scanner for acquisitions of 70-minute dynamic emission scans with a 25.8mm axial field of view. The rationale for shortening the scan duration from 90 to 70 minutes and for using an image-derived input function was to make the scanning procedure more easily applicable in clinical practice, as requested by the study funder (Medical Research Council). Our group showed that shortening the scan duration to 70 minutes provides images that correlate excellently (Spearman's rank correlation coefficient 0.99, 95% CI 0.98 - 0.99, $p<0.001$) with 90 minute scans and the results were robust for all studied subregions (7 distributed regions, Spearman's rank correlation coefficient ranging from 0.98 to 1.00) (McGinnity *et al.*, 2018). Our group also recently proposed a novel method to estimate the input function from PET images without the need for arterial sampling (Sari *et al.*, 2016). We additionally validated this method (see Project 1 in chapter 3) for use in the current study with data from 10 healthy volunteers scanned in the *Cambridge study*.

List-mode data were initially processed using an in-house motion detection algorithm (UCL Institute of Nuclear Medicine, in preparation for publication). In brief, an algorithm semi-automatically detected sudden changes in three most relevant principal components of the PET signal. These sudden changes most likely correspond

to sudden head movements. Thus, the frame timing was individually adapted to exclude these typically short (duration between seconds to max. 1 min) signal alterations and reduce the effect of interframe sudden head movement. This resulted in a variable number of 45 to 54 frames. The larger number of short frames during the first two minutes after radioligand injection was important to allow accurate estimation of the peak of an image-derived input function. Data were reconstructed with a 3-dimensional filtered backprojection to voxel sizes of 1.402 x 1.402 x 2.032 mm. A mean resolution of 6.8mm full width at half maximum (FWHM) was estimated using phantom measurements.

Each subject underwent 3T brain MRI on the Siemens Biograph mMR combined PET-MR scanner (Siemens Healthineers, Erlangen, Germany). The MR protocol included a high-resolution volumetric T1-weighted sequence (MPRAGE) with 2000 ms repetition time, 2.92 ms echo time, 256 x 256 matrix, and 1.1 x 1.1 x 1.1 mm voxels. We also performed a arterial time-of-flight magnetic resonance angiography (TOF-MRA) sequence that included the carotid arteries with 22ms repetition time, 4.17ms echo time, 256 x 256 matrix, and 0.625 x 0.625 x 2mm voxels. A T2-weighted 3D SPACE sequence was acquired with 5000 ms repetition time, 402 ms echo time, 64 x 64 matrix, and 1.1 x 1.1 x 1.1 mm voxels.

Venous samples were obtained 7, 12, 22, 42, and 62 minutes after injection. Samples were analysed for radiolabelled metabolites using high-performance liquid chromatography and for total radioactivity in whole blood and plasma.

2.3.2 Image acquisition in the Cambridge study

The *Cambridge study* used a GE Discovery 690 TOF combined PET-CT scanner for acquisitions of 90-minute dynamic emission scans with a 15.4 mm axial field of view. Data were reconstructed with a 3-dimensional filtered backprojection to 58 frames

with voxel sizes of 2.000 x 2.000 x 3.270 mm. A mean resolution of 4.98mm full width at half maximum (FWHM) was previously estimated. (Bettinardi *et al.*, 2011)

Each subject underwent 3T brain MRI on a Siemens Trio or Skyra system (Siemens Healthineers, Erlangen, Germany). The MR protocol included a high-resolution volumetric T1-weighted sequence (MPRAGE), as well as an arterial time-of-flight magnetic resonance angiography (TOF-MRA) sequence that included the carotid arteries.

Arterial blood from the radial artery was continuously sampled for the first 6.5 minutes of the scan with an Allogg ABSS on-line detector (Allogg AB, Mariefred, Sweden), with two discrete samples (30 sec and 4.5 minutes) taken beyond the on-line counter for cross-calibration against the well counter and plasma-to-whole blood ratio determination. Discrete arterial samples were also taken at 10, 15 and 20 minutes post-injection, and at 10 minute intervals thereafter. Venous samples were collected through a cannula placed in the elbow opposite the injection site at 7, 12, 22, 42, and 62 minutes following injection. The radioactivity concentration in whole blood and plasma for all discrete blood samples was determined with a Hidex Triathler well counter (Hidex, Turku, Finland) cross-calibrated to the PET/CT scanner. The fraction of parent tracer in plasma for 6 arterial plasma samples (4.5, 10, 20, 40, 60, and 90 minutes post-injection). Samples were analysed for radiolabelled metabolites using high-performance liquid chromatography and for total radioactivity in whole blood and plasma.

2.3.3 Image acquisition in the Hammersmith study

The *Hammersmith study* used a Siemens/CTI ECAT EXACT HR+ model 962 PET scanner for acquisitions of 90-minute dynamic emission scans with a 15.5 mm axial field of view. Data were reconstructed with a 2-dimensional filtered back-projection to

34 frames with voxel sizes of 2.092 x 2.092 x 2.420 mm. A mean resolution of 4.75mm FWHM was previously estimated. (Spinks *et al.*, 2000)

3D Volumetric T1-weighted coronal SPGR MRI sequences were acquired to exclude relevant intracranial structural abnormality and for co-registration with the PET images, using a GE Signa 3T HDx system (General Electric, Waukshua, WI, U.S.A.) with a voxel size of 0.938 mm x 1.100 mm x 0.938 mm. Coronal T2 and FLAIR were also acquired for each participant.

Arterial samples were obtained continuously for the first 7 minutes and at 10 discreet samples afterwards. Venous samples were obtained 7, 12, 22, 42, and 62 minutes after injection in 10 out of 18 scans. Samples were analysed for radiolabelled metabolites using high-performance liquid chromatography and for total radioactivity in whole blood and plasma.

2.4 Fitting of blood data

We used in-house software (UCL Institute of Nuclear Medicine) running in Matlab 9.2 to fit input functions, parent fractions and plasma-over-whole-blood (POB) ratios.

For each participant, the POB ratio was fitted with a function as follow:

$$f(t) = e^{-x_1 \cdot t} \cdot x_2 + x_3$$

[Where $0 < x_1$, $0 < x_2$, $0 < x_3$, t is the scan time; $x_1 \ldots x_3$ are the model parameters; f POB ratio of [^{18}F]GE-179 at scan time t].

For each participant, the fraction of plasma radioactivity attributable to the parent [^{18}F]GE-179 was fitted with a Hill type function (Gunn *et al.*, 1998) as follows:

$$f(t) = 1 + \frac{t^{x_1} \cdot (x_2 - 1)}{t^{x_1} + x_3}$$

[Where $0 < x_1$, $0 \leq x_2 < 1$, $0 < x_3$, t is the scan time; $x_1 \ldots x_4$ are the model parameters; f parent fraction of [^{18}F]GE-179 at scan time t].

The input function (arterial or image-derived) was fitted after correction for parent fraction and POB ratio with Feng's input function model (Feng *et al.*, 1993), which consists of the sum of a gamma-variate function and two exponentials.

2.5 Estimation of an image-derived input function

2.5.1 Theoretical background and rationale

We aimed to develop and validate a method for the quantification of [^{18}F]GE-179 binding that is independent of arterial blood sampling. Arterial sampling is invasive, laborious, uncomfortable, but generally safe (Zanotti-Fregonara, Chen, *et al.*, 2011). Such an invasive approach discourages participation in research studies and hinders the translation of methods into a clinical setting, where arterial sampling usually is not available.

A recent publication from our group evaluated two available options (McGinnity *et al.*, 2018), the calculation of standardized uptake value (SUV) images and the use of a population based input function. SUV images calculated over the interval of 60 to 70 minutes had a Spearman's correlation coefficient of 0.76 with arterial input function (AIF) images. A population-based input function provided a higher correlation (0.90) with AIF images, but there was a large variability of differences in volume of distribution estimates as demonstrated by Bland-Altman plots. Both proposed methods failed to replicate findings observed in a pilot project involving epilepsy patients (McGinnity *et al.*, 2015). There is no suitable reference region devoid of NMDA receptors.

Thus, we aimed to develop and validate an alternative method using an IDIF, as recently proposed by our group (Sari *et al.*, 2016). IDIFs have been used as a

noninvasive alternative for several years, but practical challenges remain regarding the identification of blood vessels, correction for partial volume effects, and determining the parent fraction of the tracer in plasma (Zanotti-Fregonara, Chen, *et al.*, 2011). Methods validated on a different tracer or scanner set-up might not be generalizable and need to be re-validated for each specific study (Zanotti-Fregonara, Liow, *et al.*, 2011).

Our method (Sari *et al.*, 2016) uses arterial time-of-flight (TOF) MRI imaging to delineate the location of carotid arteries. However, it does not account for tracer metabolism or tracer binding in plasma. Thus, we modified this method by including data from venous blood samples in the kinetic modelling. We used a robust partial volume correction (PVC) method to correct for spill-out and spill-in effects due to the small size of carotid arteries compared to the scanner resolution (Erlandsson and Hutton, 2014). The single target correction method requires the segmentation of one single volume of interest (i.e. the carotid arteries) and does not need segmentation of background areas, making it less labour-intensive than comparable methods.

PVC is particularly important to correctly detect the radioactivity peak following tracer injection. However, the method is of limited value during steady state with comparable radioactivity concentrations between soft tissues and blood vessels, as it might be susceptible to reinforce noise in images. Thus, PVC was used only for the initial 3.5 minutes after tracer injection to capture the radioactivity peak and uncorrected values were used for the remainder of the acquisition. The 3.5 minute interval was chosen as the time point when intra-carotid and tissue (background) activity started to overlap. We also adjusted the image-derived concentrations in the carotid arteries for a delay occurring when measuring arterial blood drawn from the radial artery, as described previously (Sari *et al.*, 2016).

A previous study by our group showed different tracer metabolism in epilepsy patients versus healthy controls, probably due to intake of antiepileptic drugs in the patient group (McGinnity *et al.*, 2015). Thus, we obtained 5 discrete venous samples as

described above to estimate the parent fraction and to correct for the POB ratio. This also allowed us to calibrate the IDIF with a single venous sample, as has been previously proposed (Zanotti-Fregonara, Chen, *et al.*, 2011). We used the latest venous sample obtained (i.e. 62 minutes after radioligand injection) as the correlation between arterial and venous radioactivity increases with scan duration.

2.5.2 Carotid artery segmentation

We used arterial TOF MRI scans, that provide an excellent separation of arteries from background, for segmentation of carotid arteries. We used a semi-automated region-growing algorithm with intensity constraints implemented in MRIcron (https://people.cas.sc.edu/rorden/mricron/index.html). We manually adjusted all segmentations in a slice-by-slice manner to segment the internal carotid artery and visible parts of the common carotid artery only. We did not segment other arteries, e.g. the vertebral arteries, because of their smaller size that increases the potential for partial volume effects. We segmented the internal carotid artery in the cervical, petrous, and cavernous segments. We excluded the carotid siphon and cerebral segment of the internal carotid artery, because of the sigmoid vessel shape and proximity to parts of the temporal lobe, that might make intra-vessel signal estimates less accurate and more prone to spill-in effects from brain tissue.

2.5.3 Coregistration of intra-modal images

We used the linear registration algorithm implemented in Statistical Parametric Mapping 12 (SPM12, Wellcome Centre for Human Neuroimaging) to coregister PET, T1 and TOF images. The simultaneous acquisition of PET and MR images on the combined PET-MR scanner in the *UCL study* provided am excellent starting point for coregistration between PET and MR modalities. First, we coregistered PET into the space of T1 because of the superior spatial resolution of structural MR imaging. As a

next step, we coregistered T1 to TOF and applied the transformations to the dynamic PET series.

2.5.4 Measuring and processing radioactivity concentration in the carotid arteries

We used the single target partial volume correction method with 10 iterations to correct for spill-out and spill-in effects due to the small size of carotid arteries compared to the scanner resolution (Erlandsson and Hutton, 2014). We used PVC for the initial 3.5 minutes after tracer injection to capture the radioactivity peak and obtained uncorrected values for the remainder of the acquisition to reduce the impact of noise introduced by PVC.

Next, we determined a mean delay between radioactivity arriving in the carotid arteries and detected in blood drawn from the radial artery, as described previously (Sari *et al.*, 2016). We shifted each participants curve to match the activity obtained from the radial artery and determined a mean delay of 16.4 s ± 4.5 s that was subsequently applied to all participants in a later step.

The availability of venous blood samples allowed us to calibrate each individual's image-derived measurements with blood data. We correlated late (62min) venous samples with the corresponding arterial radioactivity measurements and modelled the venous to arterial radioactivity conversion using a linear model. We then calculated the estimated arterial radioactivity per subject using this model and scaled the image-derived measurements to match this target value.

Lastly, we fit Feng's input function model (Feng *et al.*, 1993) including venous parent fraction and POB data to obtain an IDIF.

2.6 Image preprocessing and modelling

2.6.1 Smoothing

PET scans were acquired at three different sites (*UCL*, *Cambridge*, and *Hammersmith* studies) with different scanner equipment. A large proportion of between-scanner differences can be attributed to resolution. We applied a high frequency correction using smoothing, as proposed earlier (Joshi *et al.*, 2009), to correct for these differences and to adjust all data to the same target resolution.

2.6.2 Flipping

Data in people with epilepsy are influenced by the lateralisation of the epileptic focus. In our epilepsy sample, there was an equal proportion of left- and right-lateralised cases. We flipped all data of right-lateralised cases before image spatial preprocessing and used a symmetrical DARTEL normalisation template. To prevent bias introduced through flipping, we also flipped a randomly selected half of all healthy volunteer data. We used flipped volunteer data only for comparisons with epilepsy patients.

2.6.3 Rigid motion correction

Attenuation and scatter-corrected dynamic PET images were corrected for head motion using a post hoc frame-to-frame realignment method, implemented in SPM12. For each subject, an early frame with high signal-to-noise ratio and little evidence of movement was selected as the reference frame and all subsequent frames were rigidly realigned to this reference. The frames within the first 3 minutes after radioligand injection were not realigned due to low signal-to-noise ratio.

2.6.4 Inter-modal coregistration

We combined the motion-corrected dynamic PET images to a summation image that was linearly coregistered to the T1 structural MR image using SPM12. The transformations were then applied to all realigned PET frames.

2.6.5 Structural parcellation

We used an algorithm based on Geodesic Information Flows (GIF) (Cardoso *et al.*, 2015) freely available within the NiftyWeb service tool (University College London Centre for Medical Image Computing; http:// niftyweb.cs.ucl.ac.uk/) for parcellation of brain structures on T1 scans. We combined this parcellation with an image segmentation obtained using the Unified Segmentation procedure in SPM12 and added classes of cerebrospinal fluid, soft tissue, skull and air. The parcellation was simplified into 71 structures by combining smaller regions into larger areas. A second atlas was created by combining these areas into cerebral lobes, white matter, cerebellum and brainstem.

We segmented surgical resections using in-house software by comparing post- with presurgical T1 scans and iteratively extracting an empirical prior for an atypical tissue class, i.e. the resection. This procedure is based on an established lesion-segmentation algorithm (Seghier *et al.*, 2008) and has been described in detail previously (Galovic, Baudracco, *et al.*, 2019). All cavity masks were subsequently checked and, if necessary, manually refined by an investigator (MG). Lesions in epilepsy patients were manually segmented by an investigator (MG). Resections and lesions were added as a tissue class to the whole-brain parcellation.

2.6.6 Partial volume correction

The quantification of PET images is affected by the partial volume effect that is related to the limited spatial resolution of usually 5 to 6mm FWHM for modern scanners (Erlandsson *et al.*, 2016). This results in a blurring of the image and to a tissue fraction effect, occurring when a single voxel contains several tissues. These can lead to spill-in or spill-out of activity in neighbouring regions. Particularly affected are small regions in close proximity to cerebrospinal fluid or white matter, e.g. the hippocampus.

Several correction methods have been proposed that utilize structural information from high-resolution MR imaging to compensate for partial volume effects due to low resolution PET. We used the iterative Yang method (Erlandsson *et al.*, 2012) implemented in the PET-PVC toolbox developed in-house (Thomas *et al.*, 2016) for adjusting of whole brain data. The modified GIF parcellation (see above) was used for structural tissue information. As described above, data in carotid arteries for the estimation of an IDIF were corrected using single-target correction.

2.6.7 Modelling

We extracted time activity curves of the parcellated regions from partial volume corrected dynamic PET images. As described previously (McGinnity *et al.*, 2014), we used 2-brain-compartment 4-rate-constant (2c4k) full kinetic models with a variable blood volume component to quantify [^{18}F]GE-179 cerebral tissue kinetics. We calculated volume of distribution (V_T) estimates for each region.

Additionally we computed V_T for each scan on a voxel level using Logan graphical analysis (Logan *et al.*, 1990). Short frame intervals in the *NEST study* during the first 3 minutes after tracer injection were necessary to provide accurate estimates of the radioactivity peak in carotid arteries. However, these short frames might introduce additional noise that results in inaccurate V_T estimates. We implemented an additional "temporal smoothing" step that summed short PET frames and effectively reduced

noise. We also applied a median filter to effectively remove noise introduced by inaccurate V_T estimates in single voxels.

2.6.8 Spatial normalization

We used the Computational anatomy 12 toolbox (CAT12, http://www.neuro.uni-jena.de/cat/) in SPM12 to segment and nonlinearly register all T1 images to a DARTEL template. We applied the same transformations to V_T images. Lesions were cost-function masked prior to spatial processing to reduce their effect on normalisation (Brett *et al.*, 2001).

Cost-function masked postsurgical images were first nonlinearly coregistered to the participant's presurgical scan. The normalisation transformations estimated using the presurgical image were then applied to the coregistered postsurgical scan. This procedure ensured a high accuracy despite large resections, as has been described previously (Galovic, Baudracco, *et al.*, 2019).

Normalised grey matter segmentations and V_T images were masked to grey matter only, also masking any lesions or resections. An 8mm FWMH smoothing kernel was applied to both image modalities.

2.7 Statistical analysis

2.7.1 Numerical data

Categorical variables are presented as N (%), continuous variables as mean ± standard deviation. We used the general linear model implemented in SPSS (version 24.0; IBM Corp) to compute the association of global or regional V_T values with group allocation (e.g. patient vs. control) or clinical parameters. All models were corrected for age, sex,

and scanner equipment (UCL, Cambridge or Hammersmith scanner). A p-value below 0.05 was considered significant.

2.7.2 Imaging data

Voxelwise data (V_T images and grey matter segmentations) were analysed using full factorial linear models implemented in SPM12. All models were adjusted for age, sex, and scanner equipment (UCL, Cambridge or Hammersmith scanner). Results are reported at a clusterwise threshold of $p<0.05$, family-wise error corrected for multiple comparisons.

3 Project 1: Development and validation of an input function independent of arterial sampling.

3.1 Introduction

PET imaging has been used in the past 30 years to non-invasively image targets in the human brain. An ever-increasing number of radioligands have been developed (Gunn *et al.*, 2015), although only a small fraction of the more than 70 tracers tested in humans has been used routinely. Complicated methodological set-up was, besides tracer availability and costs, one of the factors hindering the translation of research findings into routine clinical scanning.

We recently described the first-in-human use of [^{18}F]GE-179, a PET radioligand selectively binding to the NMDA receptor complex (McGinnity *et al.*, 2014). NMDA receptors are not only involved in memory and synaptogenesis, but also have a proposed role in excitotoxicity and might contribute to epilepsy, Alzheimer's and Huntington's disease, and psychosis (Bordji *et al.*, 2010; Cooke and Bliss, 2006b; Fan and Raymond, 2007; McGinnity *et al.*, 2015; Olney, Newcomer and Farber, 1999a; Rothman and Olney, 1995).NMDA receptor blockers have been used to treat seizures,

Alzheimer's disease or refractory depression (Lipton, 2006; Murrough *et al.*, 2013; Pellock *et al.*, 2006). We showed increased [^{18}F]GE-179 uptake in brains of people with epilepsy, suggesting an increased activation of NMDA receptors (McGinnity *et al.*, 2015).

Several ongoing studies are using [^{18}F]GE-179 but a wide utilisation is limited by the need for arterial blood sampling for full quantification of tracer binding. Blood sampling from the radial artery is associated with local pain and bruising and carries the potential, albeit rare, risks of haemorrhage or thrombosis (Zanotti-Fregonara, Chen, *et al.*, 2011). Thus, this invasive and labour-intensive method is not favoured in routine practice. A reference region devoid of NMDA receptors is not available (McGinnity *et al.*, 2014). Standardised uptake value (SUV) images or a population-based input function did not provide accurate quantification (McGinnity *et al.*, 2018).

We have previously proposed a procedure to estimate an image-derived input function (IDIF) for molecular imaging quantification independent of arterial blood sampling (Sari *et al.*, 2016). However, this method cannot distinguish the fraction of the parent compound in plasma from total blood activity and is, thus, of limited use in tracers with relevant metabolism.

Here, we complement this method by including discrete venous samples that allow correction for parent fraction and plasma-over-blood (POB) ratios. We validate the combined procedure for the [^{18}F]GE-179 tracer showing high correlation between our approach and arterial input function.

3.2 Methods

The methods are described in detail in Chapter 2.

In brief, we studied 10 healthy volunteers at Addenbrooke's Hospital in Cambridge, UK. Dynamic PET images were acquired on a GE Discovery 690 TOF combined PET-CT scanner after injection of a target 185 MBq of [^{18}F]GE-179. We obtained arterial

blood samples continuously from the radial artery for the first 6.5 minutes and at 10 discreet intervals thereafter. Venous samples were collected through a cannula placed in the elbow opposite the injection site 7, 12, 22, 42, and 62 minutes after injection. The same procedures were used for fitting of the arterial and venous parent fraction, POB ratio, and both input functions.

We segmented the internal carotid artery (cervical, petrous, and cavernous segments) on TOF MRI scans. We linearly coregistered the dynamic PET data and T1 MRI data into TOF image space. We used single target PVC (Erlandsson and Hutton, 2014) for the initial 3.5 minutes for estimating the peak of the input function and used uncorrected data for the remainder of the scan to reduce noise. The image-derived radioactivity in the carotid arteries was then shifted by a previously estimated mean delay of 16.4 seconds to match arterial data. We calibrated the image-derived data with the 62-minute venous sample radioactivity. The rationale for this processing is described in chapter 2.5.1.

Imaging data was preprocessed and modelled as described in chapter 2.6. We used a modified GIF-atlas encompassing 11 distinct brain regions. We selected brain regions as representative for different cortical, subcortical, white matter, and infratentorial structures that might be representative for different patterns of brain tracer binding (McGinnity *et al.*, 2014). The data in these regions was modelled using a 2c4k full kinetic model and V_T was estimated for each region.

We calculated the area under the curve (AUC) for the fits of parent fraction, POB ratio, and input function. We interpolated radioactivity measurements in the radial artery to a time of 60 minutes using the fit of the Feng function (Feng *et al.*, 1993) and compared it to venous radioactivity in the sample obtained 62 minutes after injection,

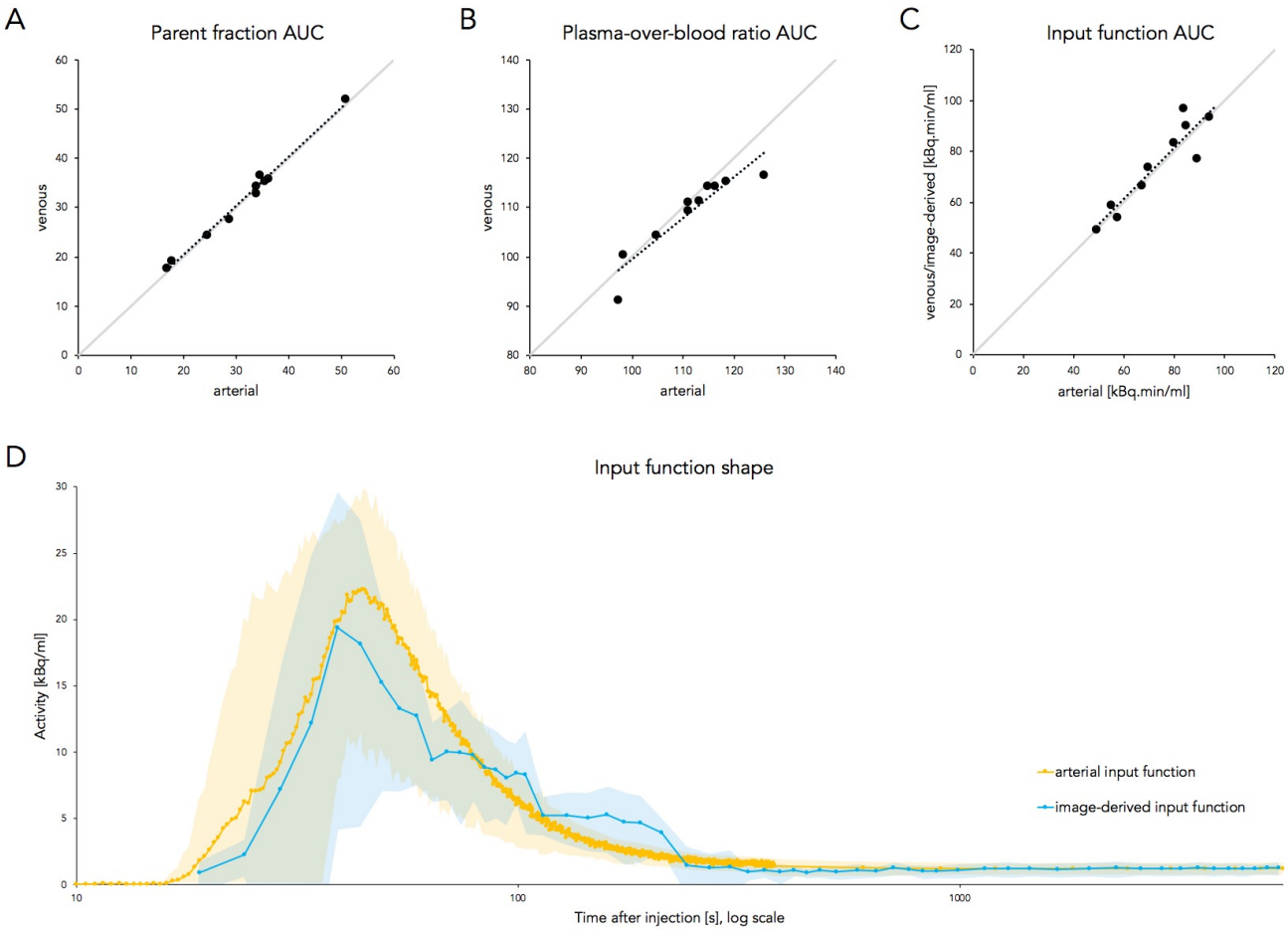

Figure 3.1: *Comparison of arterial and IDIF + venous measurements*

Comparison of the areas under the fitted curves (AUC) for arterial and venous parent fraction (**panel A**) and plasma-to-whole blood ratio (**panel B**), together with the final input function (**panel C**). On each plot the dotted line is the linear regression fit, the grey line indicates the line of unity. The comparison of the mean shapes of the arterial and IDIF + venous input functions is displayed in **panel D**. The light orange/blue areas denote the corresponding 95% confidence intervals.

assuming a 2 minute delay between arterial and venous data due to tissue diffusion. We compared AUCs, radioactivity counts, and regional V_T estimates between arterial and venous/image-derived data using Pearson's correlation coefficient (r). Additionally, Bland-Altman plots were used to compare V_T estimates. We estimated the regional and global coefficient of variation (CoV) for VT estimates modelled using the arterial (AIF) or image-derived (IDIF) input functions.

Additionally, we evaluated the effect of reducing venous sampling to only the late sample obtained 62 minutes after the injection. This approach required determination of population-based estimates of the x_1 and x_3 parameters that determine the shape of POB ratio and parent fraction curves (see chapter 2.4). The remaining x_2 parameter, determining the amplitude of the curve, was then estimated using the single venous sample. The remaining blood data processing was left unchanged.

3.3 Results

3.3.1 Standard analysis

The demographic characteristics of the studied 10 healthy volunteers are listed in Table 2.1. There was a high correlation between the areas under the curve fits of arterial (mean 31 ± 10) and venous (mean 31 ± 10) parent fraction measurements (r = 0.99, p<0.001, Figure 3.1A). There was a high correlation between AUCs of arterial (mean 111 ± 9) and venous (mean 109 ± 8) POB measurements (r = 0.93, p<0.001, Figure 3.1B).

The mean differences in measured whole blood radioactivity in arterial and venous samples declined over time (Figure 3.2A, 5 min 0.52 kBq/ml [0.25-0.80], 10 min 0.24 [0.15-0.34], 20 min 0.17 [0.11-0.23], 40 min 0.10 [0.06-0.14], 60 min 0.07 [0.04-0.10]). The highest correlation was observed between the arterial 60-minute (1.23 kBq/ml ± 0.29) and venous 62-minute (1.17 kBq/ml ± 0.29) radioactivity concentrations (r = 0.99,

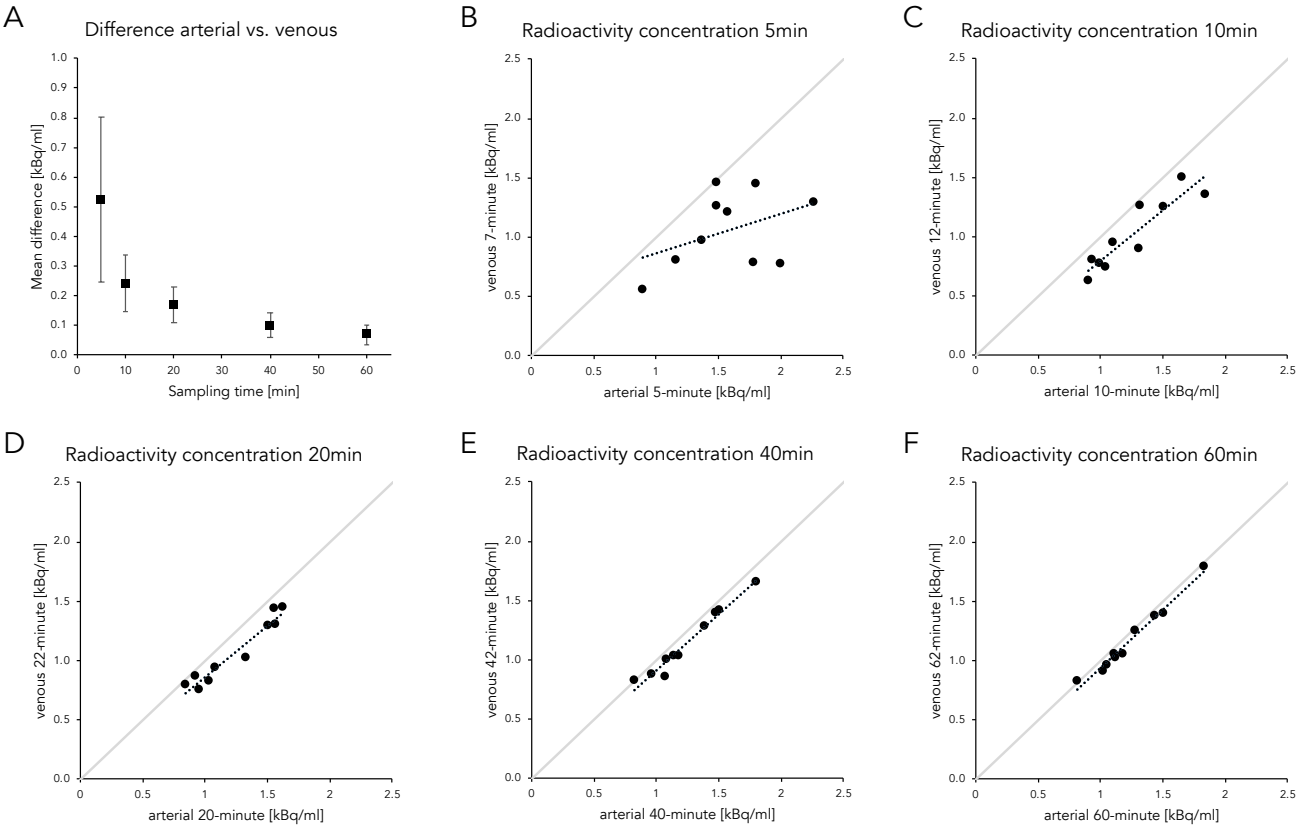

Figure 3.2: *Comparison of arterial and venous radioactivity concentrations*

The mean difference between arterial and venous radioactivity concentrations at times *t* and *t* + 2 minutes respectively is displayed in **panel A**. Vertical bars denote 95% confidence intervals. Scatter plots of arterial vs. venous radioactivity concentration for arterial sampling times of 5, 10, 20, 40, and 60 minutes post-injection are displayed in **panels B to F**. On each plot the dotted line is the linear regression fit, the grey line indicates the line of unity.

$p<0.001$, Figure 3.2F). We fitted a linear model to scale 62-minute venous to 60-minute arterial radioactivity concentrations ($Activity_{arterial} = Activity_{venous} * 0.987 + 0.082$), that was later applied to calibrate the image-derived data.

There was high correlation of AUCs of fitted AIF (73 ± 16) and IDIF+venous (74 ± 17) corrected for parent fraction and POB ratio ($r = 0.92$, $p<0.001$, Figure 3.1C). A plot of

	AIF		IDIF – all venous samples			
	V_T estimate (mean ± SD)	CoV (%)	V_T estimate (mean ± SD)	CoV (%)	r coefficient	p value
WM brain	9.2 ± 2.1	23.2	9.0 ± 2.0	21.8	0.94	<0.001
WM cerebellum	9.3 ± 2.0	21.4	9.2 ± 1.9	20.9	0.94	<0.001
GM cerebellum	8.8 ± 1.9	21.5	8.8 ± 1.9	22.1	0.96	<0.001
Brainstem	8.7 ± 1.7	19.1	8.6 ± 1.8	20.4	0.94	<0.001
Thalamus	11.9 ± 2.6	21.5	12.0 ± 2.6	21.7	0.95	<0.001
Putamen	11.3 ± 2.5	22.3	11.2 ± 2.5	22.5	0.97	<0.001
Precentral gyrus	9.2 ± 1.9	21.0	8.8 ± 1.8	20.8	0.89	0.001
Parahippocampal gyrus	8.6 ± 2.3	27.2	8.4 ± 2.2	26.5	0.93	<0.001
Occipital lobe	9.2 ± 1.7	18.2	9.0 ± 1.7	18.6	0.92	<0.001
Precuneus	10.0 ± 1.9	19.3	9.7 ± 2.0	20.6	0.92	<0.001
Insular cortex	10.1 ± 1.9	19.3	9.9 ± 2.0	20.4	0.94	<0.001
Overall	9.7 ± 2.2	21.3 ± 2.5	9.5 ± 2.2	21.5 ± 2.0	0.95	<0.001

Table 3.1: *Regional V_T estimates obtained with an arterial and venous/image-derived input function.*

AIF, arterial input function; IDIF, image-derived input function; V_T, volume of distribution; CoV, coefficient of variation; r coefficient, Pearson's correlation coefficient; SD, standard deviation; WM, white matter; GM, grey matter.

arterial and image-derived calibrated and delay-corrected radioactivity concentrations is displayed in Figure 3.1D and shows good overlap between the curve shapes.

Regional V_T estimates obtained using arterial or image-derived input functions are presented in Table 3.1. There was a high correlation of an overall 110 (11 regions in 10 subjects) V_T estimates between AIF- and IDIF-modelled data (mean V_T AIF 9.7 ± 2.2 vs. IDIF+venous 9.5 ± 2.2, r = 0.95, p<0.001). The mean correlations remained high when splitting the data per region (mean r 0.94 ± 0.02, Figure 3.3A) or per subject (mean r 0.94 ± 0.08, Figure 3.3B). A Bland Altman plot comparing V_T estimates obtained using AIF- and IDIF-modelled data is displayed in Figure 3.3C. There was a small between-method mean difference of V_T estimates of -1.7%, with a 95% confidence interval of differences ranging from -15.9% to 12.4%. The regional

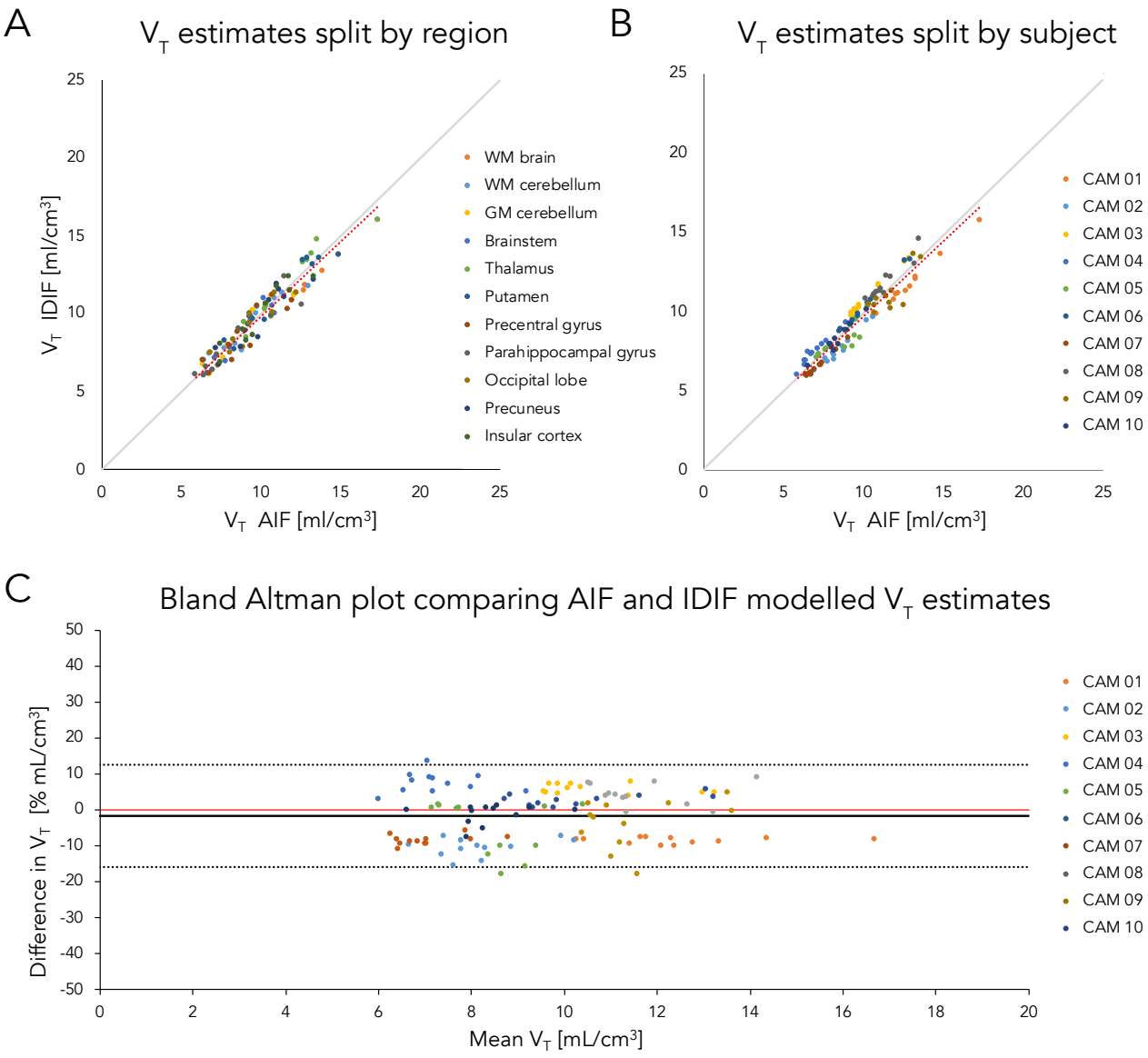

Figure 3.3: *Comparison of total volume of distribution estimates modelled with arterial or IDIF + venous input functions*

Scatter plots of total volume of distribution (V_T) estimates obtained with arterial and IDIF + venous input functions are displayed in **panel A** (split by region) and **B** (split by patient). The red dotted line is the linear regression fit, the grey line indicates the line of unity. **Panel C** displays a Bland-Altman plot comparing V_T estimates modelled with arterial and IDIF + venous input functions. The thick black line is the mean bias of the V_T estimates modelled using an IDIF + venous input function, the dotted black lines denote the 95% confidence intervals.

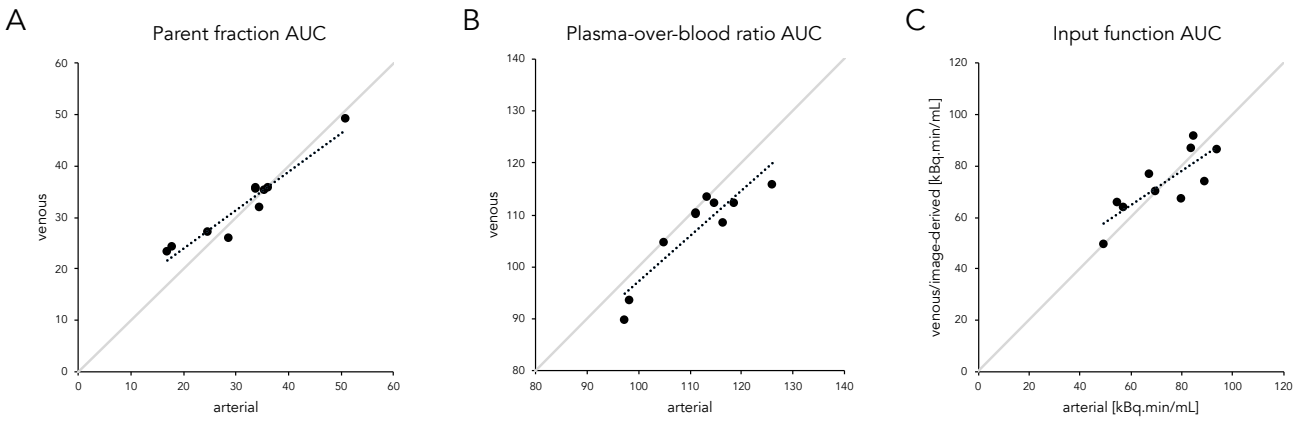

Figure 3.4: *Comparison of arterial and IDIF + single venous sample measurements*

Comparison of the areas under the fitted curves (AUC) for arterial and single venous sample parent fraction (**panel A**) and plasma-to-whole blood ratio (**panel B**), together with the final input function (**panel C**). The dotted line is the linear regression fit, the grey line indicates the line of unity.

coefficients of variation between AIF- and IDIF-modelled data were comparable (mean CoV AIF 21.3% ± 2.5% vs. IDIF 21.5% ± 2.0%, t = -0.8, p=0.46).

3.3.2 Simplification to one venous sample

We also assessed the performance of the standard venous/IDIF approach described above with a simplified procedure using only a 62-minute venous sample. Using this procedure, there was a lower correlation between the areas under the curve of parent fraction measurements (single venous sample 32 ± 8 vs. arterial 31 ± 10 min, r = 0.96, p<0.001, Figure 3.4A), POB estimates (single venous sample 107 ± 9 vs. arterial 111 ± 9 min, r = 0.91, p<0.001, Figure 3.4B) and input functions (single venous sample 73 ± 13 vs. arterial 73 ± 16 kBq.min/mL, r = 0.81, p=0.005, Figure 3.4C).

Regional V_T estimates obtained using the simplified image-derived input function are presented in Table 3.2. There was a lower correlation between arterial and IDIF + single venous sample modelled data (mean VT: arterial 9.7 ± 2.2 vs. IDIF + single

	AIF		IDIF – single venous sample			
	V_T estimate (mean ± SD)	CoV (%)	V_T estimate (mean ± SD)	CoV (%)	r coefficient	p value
WM brain	9.2 ± 2.1	23.2	9.3 ± 1.7	18.1	0.76	0.01
WM cerebellum	9.3 ± 2.0	21.4	9.6 ± 1.7	17.8	0.68	0.03
GM cerebellum	8.8 ± 1.9	21.5	9.4 ± 1.8	19.5	0.69	0.03
Brainstem	8.7 ± 1.7	19.1	9.0 ± 1.7	18.5	0.63	0.05
Thalamus	11.9 ± 2.6	21.5	13.8 ± 2.4	17.7	0.71	0.02
Putamen	11.3 ± 2.5	22.3	12.3 ± 2.5	20.5	0.72	0.02
Precentral gyrus	9.2 ± 1.9	21.0	10.8 ± 2.3	21.7	0.47	0.17
Parahippocampal gyrus	8.6 ± 2.3	27.2	9.3 ± 3.5	37.4	0.86	0.002
Occipital lobe	9.2 ± 1.7	18.2	10.7 ± 1.9	17.6	0.44	0.21
Precuneus	10.0 ± 1.9	19.3	12.0 ± 2.6	22.0	0.52	0.13
Insular cortex	10.1 ± 1.9	19.3	11.5 ± 2.4	20.9	0.52	0.12
Overall	9.7 ± 2.2	21.3 ± 2.5	10.7 ± 2.7	21.1 ± 5.7	0.71	<0.001

Table 3.2: *Regional V_T estimates obtained with an arterial input function or an input function using a single venous and image-derived measurements.*
AIF, arterial input function; IDIF, image-derived input function; V_T, volume of distribution; CoV, coefficient of variation; r coefficient, Pearson's correlation coefficient; SD, standard deviation; WM, white matter; GM, grey matter.

venous 10.7 ± 2.7, r = 0.71, p<0.001). The mean correlations were also lower when splitting the data per region (mean r 0.64 ± 0.13, Figure 3.5A) or per subject (mean r 0.89 ± 0.08, Figure 3.5B). The Bland Altman plot detected a mean difference of VT estimates of 9.9%, with a 95% confidence interval of differences ranging from -23.9% to 43.7% (Figure 3.5C). The simplified IDIF + single venous sample modelled data had similar coefficients of variation of VT compared to arterial-based data (mean VT CoV: arterial 21.3% ± 2.5% vs. IDIF + single venous 21.5% ± 5.7%, t = 0.2, p=0.87).

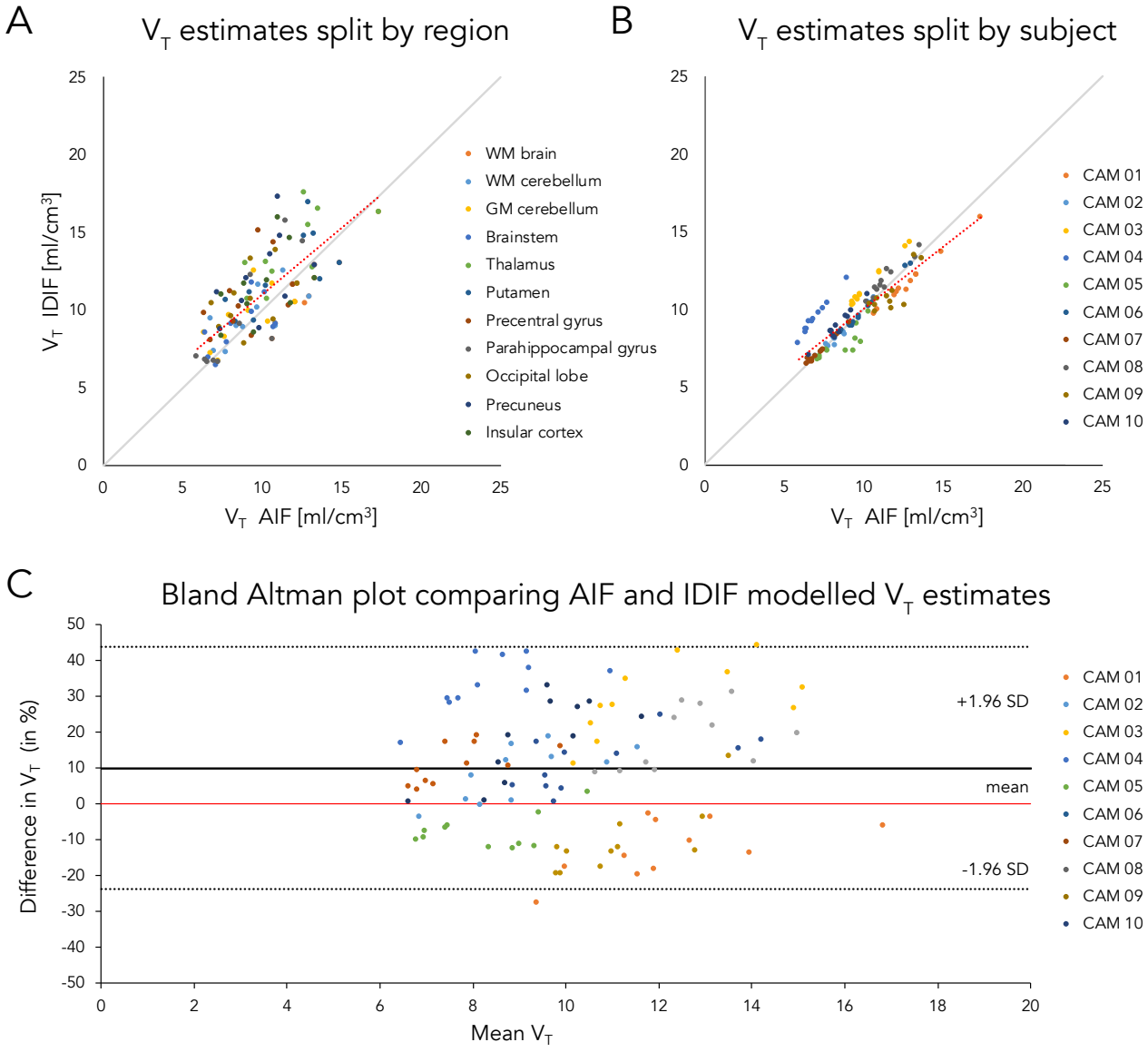

Figure 3.5: *Comparison of total volume of distribution estimates modelled with arterial or IDIF + single venous sample input functions*

Scatter plots of total volume of distribution (V_T) estimates obtained with arterial and IDIF + single venous sample input functions are displayed in **panel A** (split by region) and **B** (split by patient). The red dotted line is the linear regression fit, the grey line indicates the line of unity. **Panel C** displays a Bland-Altman plot comparing V_T estimates modelled with arterial and IDIF + single venous sample input functions. The thick black line is the mean bias of the V_T estimates modelled with an IDIF + single venous sample input function, the dotted black lines denote the 95% confidence intervals.

3.4 Discussion

We present a novel method for quantification of [^{18}F]GE-179 binding in brain that is independent of arterial sampling and might, thus, support wider use of this radiotracer for the assessment of the NMDA receptor. The input function estimated using a whole blood image-derived input function (IDIF) combined with corrections from venous data (i.e., parent fraction and plasma-to-whole blood ratio) was highly correlated with the gold standard input function determined from arterial sampling. The mean bias in V_T estimates from the IDIF + venous approach was small (< 2%) and between-method differences were within a clinically reasonable range. Furthermore, the IDIF + venous approach did not increase the variability of the V_T estimates. The performance of this procedure was better than that of previously proposed approaches aimed at obviating arterial sampling, namely the use of SUV or population-based input functions (McGinnity *et al.*, 2018). However, simplification of the IDIF + venous method to use a single venous measurement rather than data from five venous samples provided lower correlations and larger differences in V_T estimates.

Previous attempts to simplify [^{18}F]GE-179 quantification using SUV or a population-based input function did not yield convincing results and both methods failed to reproduce differences in grey-matter VT between patients with epilepsy and healthy volunteers ($p>0.05$) that were previously obtained using arterial modelled data on the same dataset (McGinnity *et al.*, 2018). A reference region devoid of NMDA receptors is not available. Thus, an alternative quantification approach is the estimation of an image-derived input function (Sari *et al.*, 2016). However, an IDIF estimates radioactivity in whole blood and cannot determine the parent fraction of the tracer in plasma or the plasma-to-whole blood ratio. Hence, a methodology completely devoid of blood sampling will not provide an accurate input function for kinetic modelling unless radiolabelled metabolites are absent and the plasma-to-whole blood ratio is close to 1. We chose a previously described approach of substituting arterial with

venous samples and used venous data to determine the tracer parent fraction in plasma, the plasma-to-whole blood ratio and to scale the IDIF.

3.4.1 Comparison of venous and arterial samples

Previous studies found that venous samples taken with a longer delay after tracer injection provided better approximations of radioactivity in arterial blood (Takagi *et al.*, 2004; Zanotti-Fregonara *et al.*, 2012). This points to an increasing equilibrium between venous and arterial blood. Previous studies reported little or no differences between venous and arterial radioactivity concentration more than 40-60 minutes after ligand injection (Meyer *et al.*, 2005; Takagi *et al.*, 2004; Wakita *et al.*, 2000; Zanotti-Fregonara *et al.*, 2012). Similarly, we found decreasing differences and increasing correlations between arterial and venous radioactivity over time. The whole blood radioactivity concentration in a venous sample drawn 62 minutes after tracer injection was highly correlated with the 60-minute arterial sample (r = 0.99). There remained a small underestimation of arterial data (mean difference -4% ± 2%) that was corrected using a linear model. Thus, we are confident that late venous whole blood radioactivity concentration provided a good estimate for calibrating the IDIF.

Greuter and colleagues performed an extensive evaluation of venous and arterial data (Greuter *et al.*, 2011), correlating arterial and venous data obtained at 3 to 7 timepoints in studies with 5 different tracers with 254 paired samples overall. They observed differences in correlation coefficients between tracers and measured parameters (radioactivity concentration, parent fraction, POB ratio) concluding that arterial samples cannot be readily substituted with venous measurements but will require validation for each tracer and measured parameter.

We provide evidence that parent fraction, POB ratio, and late radioactivity concentration can be reliably approximated using venous samples in [^{18}F]GE-179 PET. The correlations for parent fraction and late radioactivity concentration were high (r =

0.99). The correlation for POB ratio was lower (r = 0.93), but still supported the feasibility of venous measurements.

3.4.2 Combination of IDIF with venous data versus an arterial input function

The IDIF determined from the carotid arteries provided a similar shape to the input function determined from data from the radial artery. These data provide support that a previously proposed procedure correctly quantifies the radioactivity concentration in the carotid arteries (Sari *et al.*, 2016). Residual differences between the arterial sampling and IDIF-based input functions can be explained by a higher noise and lower sampling rate in the imaging data for the first 6.5 minutes over which arterial samples were continuously sampled. The slight overestimation of radioactivity between 100 and 300s after the injection could be due to spill-in effects from tracer uptake in brain or other tissue.

The combination of IDIF and venous data provided good estimates of the input function. This translated into high overall, regional, and subject-wise correlations of V_T estimates, with only minimal mean bias (-1.7%). These correlations were higher than those observed using SUV images or a population-based input function (McGinnity *et al.*, 2018). The range of relative V_T differences was not negligible but was well within a clinically reasonable 20% range. This is important and means that clinically relevant effect sizes of 20% or more are detectable with this technique. Between-method limits of agreement below 20% are less likely to be clinically relevant. In a population of patients with epilepsy not taking antidepressants scanned with [^{18}F]GE-179 PET we previously found a median whole brain V_T of 8.0 compared to a median V_T of 6.2 in healthy volunteers (McGinnity *et al.*, 2015). Thus, such a 29% between-group difference is likely to be detected by our method, providing support for its practical

applicability. There were no relevant outliers and there was no difference in overall data variability, providing further support for the robustness of the proposed method.

3.4.3 Alternative approaches

As expected, reducing the number of venous samples to only one late sample (62-minute) provided less accurate estimates. This approach requires the use of population based curves of parent fraction and POB ratio that were then scaled with the single sample. These estimates were less accurate than those obtained with a full set of venous samples. They translated into inaccuracies in input function and V_T estimates. There was relevant bias in V_T estimates (mean difference 9.9%) and the 95% confidence intervals of V_T differences exceeded the 20% range, making this approach not reliably applicable for clinically use.

Another potential approach for estimating an input function from imaging data is simultaneous estimation (SIME), that estimates the input function by fitting multiple tissue activity curves from different brain regions (Sari *et al.*, 2018). However, SIME involves the estimation of a large number of parameters, might lack precision and may need scaling with one or several discrete blood samples (Feng *et al.*, 1997). The application of SIME to [^{18}F]GE-179 PET will be the focus of future studies.

3.4.4 Limitations

This study has limitations. We studied a small number of subjects acquired at a single centre due to the limited use of this radiotracer so far. We did not include people with neuropsychiatric disorders but the large variability of tracer binding (V_T) in the included healthy subjects makes us confident that the IDIF + venous approach may be generalisable to people with brain disorders taking medication. Our procedure requires venous sampling that is invasive and labour intensive. Puncture of the cubital

vein is, nevertheless, less invasive and safer than placement of a cannula in the radial artery, and does not require such highly trained personnel. Estimation of the IDIF requires manual editing of the segmentation of the carotid arteries but this process could be automated in future (Jodas *et al.*, 2016).

3.4.5 Conclusions

We validated a reliable method to quantify [^{18}F]GE-179 binding that does not require arterial sampling. In addition, we present evidence for reliable estimation of parent fraction, POB ratio and late whole blood radioactivity concentration for this tracer using venous sampling. These approaches might widen the use of this tracer and the method could also be applied to other radiotracers, but this will require separate validation. A simplification of the method to use a single venous sample provided less accurate estimates and should not be used, unless full venous sampling is not available or not feasible.

4 Project 2: NMDA receptor activation in aging.

4.1 Introduction

A global increase in longevity has led to an unprecedented ageing of the world's population. In 2018, for the first time in human history, persons aged above 65 years outnumbered children below five years of age (United Nations Department of Economic and Social Population Affairs, 2019). The proportion of above 80-year-olds will double by 2045 and quadruple by 2095 (United Nations Department of Economic and Social Population Affairs, 2019). Ageing is associated with a decline in cognitive abilities, particularly affecting processing speed, declarative, and working memory (Park *et al.*, 2002). The risk of neurodegenerative disorders, e.g. Alzheimer's or Parkinson's disease, increases with age.

N-methyl-D-asparate (NMDA) receptors are ionotropic receptors that bind glutamate, the main excitatory neurotransmitter of the nervous system. NMDA receptors are heterotetramers assembling two GluN1 subunits with two variable units, typically GluN2A or GluN2B and less frequently GluN3. NMDA receptors are key mediators of long-term synaptic potentiation (LTP) and depression (LTD) that are believed to represent the cellular correlates of declarative learning and memory, thus gaining

considerable interest (Cooke and Bliss, 2006b; Nakazawa *et al.*, 2004). They also subserve persistent neuronal firing during working memory retention (Lisman *et al.*, 1998; M. Wang, Yang, C.-J. Wang, Gamo, Jin, Mazer, Morrison, X.-J. Wang and Arnsten, 2013b).

Activation of NMDA receptors located extrasynaptically can be neurotoxic and has been implicated in Alzheimer's disease and excitotoxicity (Hardingham and Bading, 2010; Y. Zhang *et al.*, 2016). Accumulation of amyloid-beta in Alzheimer's disease redistributes NMDA receptors from synaptic towards extrasynaptic sites (Snyder *et al.*, 2005). In turn, extrasynaptic NMDA receptor activation raises amyloid-beta production (Hoey *et al.*, 2009), overexpresses tau proteins (Sun *et al.*, 2016), and might inhibit long-term potentiation underlying memory consolidation (Li *et al.*, 2011). Suppression of overactivated, primarily extrasynaptic, receptors with the uncompetitive antagonist memantine is a routine treatment for Alzheimer's disease (Lipton, 2006).

NMDA receptors are more vulnerable to aging than other glutamate ion-channels (Magnusson and Cotman, 1993; Magnusson *et al.*, 2010). Lower overall expression of NMDA receptors was observed in older animals, particularly in the frontal and parieto-occipital cortex, striatum, and hippocampus (Castorina *et al.*, 1994; Magnusson, 2000; Magnusson and Cotman, 1993; Magnusson *et al.*, 2007; Ontl *et al.*, 2004). Despite the loss of overall receptor numbers, several, but not all, studies described an age-related increase in sensitivity and responsiveness of the remaining receptors (Billard *et al.*, 1997; Jasek and Griffith, 1998; Kuehl-Kovarik *et al.*, 2000). This might be explained by a selective decline of GluN2B subunits and shift towards a larger proportion of GluN2A-containing receptors (Brim *et al.*, 2013; Magnusson, 2000; Magnusson *et al.*, 2002; 2006; Zamzow *et al.*, 2013) that have a higher opening probability (N. Chen *et al.*, 1999; Erreger *et al.*, 2005; Gray *et al.*, 2011). In addition, aging caused a shift of receptors from the synapse to extrasynaptic sites (Potier *et al.*, 2010). A decreased expression of glutamate transporters with deficient glutamate re-uptake was observed in aged rats, leading to facilitated activation of extrasynaptic NMDA receptors (Potier

et al., 2010). A relationship between NMDA receptor abnormalities during senescence and cognitive decline has been proposed (Kumar, 2015).

Little knowledge exists on the effects of aging on NMDA receptors in humans. Several (Kornhuber *et al.*, 1988; Piggott *et al.*, 1992), but not all (Law *et al.*, 2003), studies found a decrease in NMDA receptor numbers in *post mortem* brains of older individuals, potentially linked to an overall loss of neurons. Functional aspects are, however, difficult to evaluate in post mortem tissue and can only be reliably assessed *in vivo*.

Here, we measured the *in vivo* opening probability of NMDA receptors across different age-ranges in three independent cohorts of healthy adults. We used positron emission tomography (PET) with [^{18}F]GE-179, a recently developed radiotracer that selectively binds inside the open, i.e. activated, NMDA receptor complex (McGinnity *et al.*, 2014).

4.2 Methods

Recruitment, data acquisition and imaging preprocessing were performed as described above (see Common Methods in chapter 2). In brief, we recruited 29 healthy volunteers scanned using [^{18}F]GE-179 at three sites (*UCL*, *Cambridge*, *Hammersmith*). No volunteers took regular medication or had a history of neuropsychiatric conditions.

We extracted V_T estimates in grey matter, white matter and non-brain tissue (combination of soft tissue and skull). We calculated the association of regional V_T estimates with age using the general linear model, adjusting for the effects of sex and scanner equipment. P-values below 0.05 adjusted for multiple comparisons using Bonferroni correction were considered significant. Scatter plots of age to V_T estimates are displayed for values adjusted for the effects of sex and scanner equipment.

To address the subregional distribution of findings in grey matter, we also performed a voxel-wise analysis of parametric V_T images. We calculated the association of voxelwise V_T estimates with age using a full factorial general linear model, adjusting for the effects of sex and scanner equipment. We report p-values at a threshold of $p<0.05$ on a cluster-level family-wise error corrected for multiple comparisons.

To address the contribution of age-related neurodegeneration, i.e. reductions in grey matter volume, to our findings, we performed voxel-based morphometry (VBM) using segmented and modulated parametric grey matter volume images obtained using the CAT12 toolbox on 3T T1 MRI scans. We determined the association of global [^{18}F]GE-179 V_T uptake with grey matter volume reduction and display the overlap of V_T and VBM voxelwise findings.

Lastly, we performed sensitivity analyses of age-related [^{18}F]GE-179 V_T changes in grey matter in each cohort separately. In cohorts without significant voxelwise results, we also reported exploratory findings at an uncorrected threshold of $p<0.05$ with a minimum cluster size of 100 contiguous voxels.

4.3 Results

4.3.1 Overall results

We included 29 healthy volunteers with a mean age 41 ± 13 years (range 25 to 63 years, Table 2.1). There were no between-cohort differences in distributions of age (*Hammersmith* mean 42 ± 16 years, *Cambridge* 40 ± 10, *UCL* 41 ± 13, p = 0.94) or sex (*Hammersmith* 3/9 female, *Cambridge* 1/10 female, *UCL* 4/10 female, p = 0.32).

We found a significant association of V_T in grey matter with age (F = 7.2, p = 0.04, Figure 4.1A), with an estimated V_T increase of 0.6 per 10 years (95% CI 0.1 to 1.1; corresponding to a 7% increase compared to mean V_T, 95% CI 1-12%). The linear

A Global GE-179 uptake in grey matter, association with age

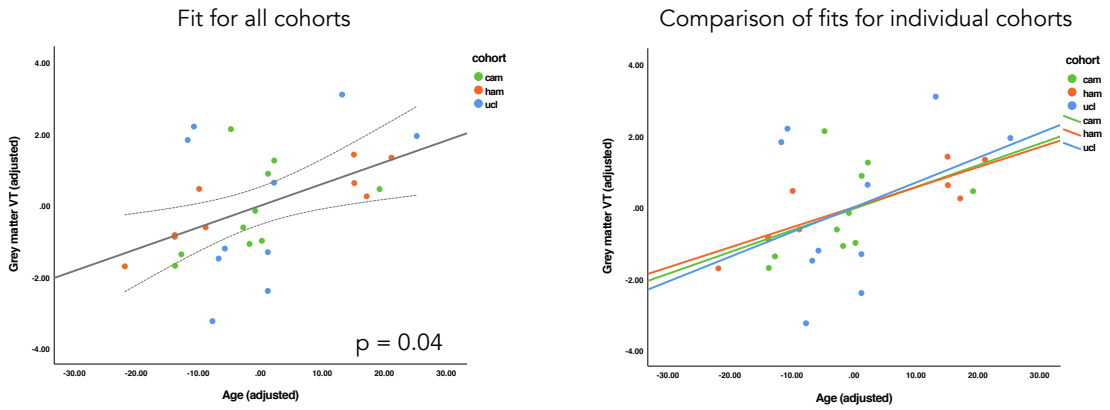

B Subregional GE-179 uptake, association with age

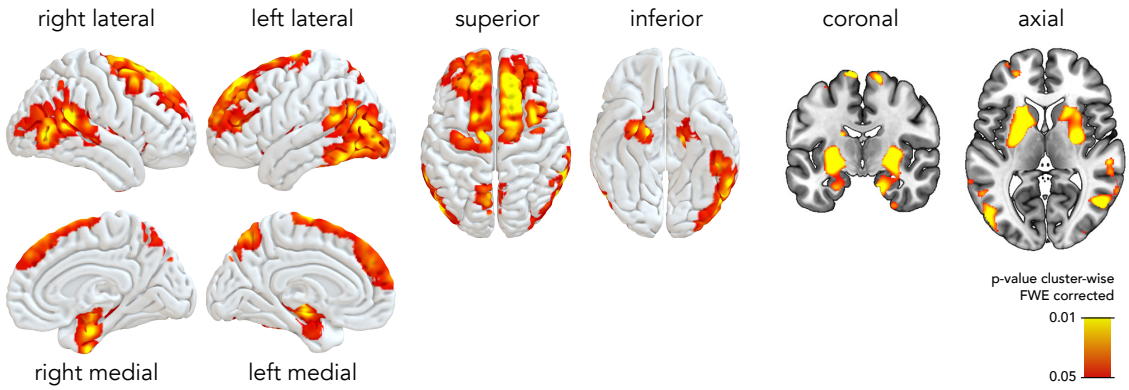

Figure 4.1: *Association of GE-179 uptake in grey matter with age in healthy volunteers*

The association of grey matter GE-179 V_T with age in healthy volunteers (n=29) is displayed in **panel A**. Grey matter V_T and age are displayed as mean centred values that were adjusted for the effects sex and scanner equipment. The regression line fit and its 95% confidence interval for the overall cohort is displayed on the left, the fits for each individual cohort are displayed on the right. The subregional distribution of grey matter V_T associated with age is shown in **panel B** ($p<0.05$ FWE corrected).

regression line fits of age over grey matter V_T were highly similar between all cohorts (Figure 4.1A right). On a subregional level (Figure 4.1B), we observed significant age-related increases in V_T in bilateral parieto-occipital junctions and posterior temporal lobes (right, T = 6.0, 4167 voxels, p<0.001; left, T = 5.1, 5295 voxels, p < 0.001), bilateral striata and hippocampal heads (right, T = 5.9, 5427 voxels, p < 0.001; left, T = 6.0, 5566 voxels, p < 0.001), and bilateral superior and middle frontal gyri (right, T = 5.8, 4854 voxels, p<0.001; left, T = 5.7, 5267 voxels, p < 0.001).

There was no association of grey matter V_T with sex (F = 1.1, p = 0.93) or scanner equipment (F = 1.2, p = 0.95). There was no association of age with V_T in white matter (F = 1.3, p = 0.78, V_T increase by 0.2 per 10 years, 95% CI -0.2 to 0.7, Figure 4.2A) or non-brain tissue (F = 1.7, p = 0.63, V_T decrease by 0.1 per 10 years, 95% CI -0.3 to 0.1, Figure 4.2B).

There was a negative association of age with grey matter volume (F = 8.4, p = 0.008, volume decrease by 19 ml per 10 years, 95% CI 5 to 32 ml, Figure 4.3A). On a voxel-wise level (Figure 4.3B), higher age correlated with lower grey matter volume in bilateral medial superior frontal gyri (T = 8.7, 7880 voxels, p < 0.001), bilateral fusiform and lingual gyri (right, F = 6.7, 1685 voxels, p = 0.001; left, F = 7.1, 2752 voxels, p < 0.001), bilateral mesial temporal lobes and insular cortices (right, F = 5.8, 5295 voxels, p < 0.001; left, F = 6.9, 8007 voxels, p < 0.001), right parietooccipital junction (F = 6.3, 781 voxels, p = 0.03), bilateral thalami (F = 5.9, 1062 voxels, p = 0.007), and bilateral posterior cingulate gyri (F = 4.8, 652 voxels, p = 0.05). Figure 4.3B shows that the majority of areas with age-related increases in [^{18}F]GE-179 uptake were different from areas that showed significantly reduced grey matter volume with age. Grey matter V_T was not associated with grey matter volume (F = 0.2, p = 0.69).

A White matter GE-179 uptake, association with age

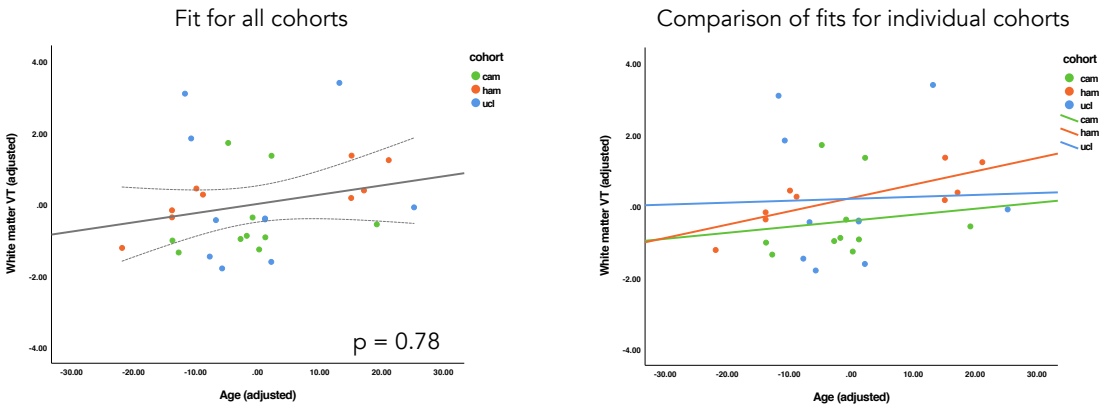

A Nonbrain tissue GE-179 uptake, association with age

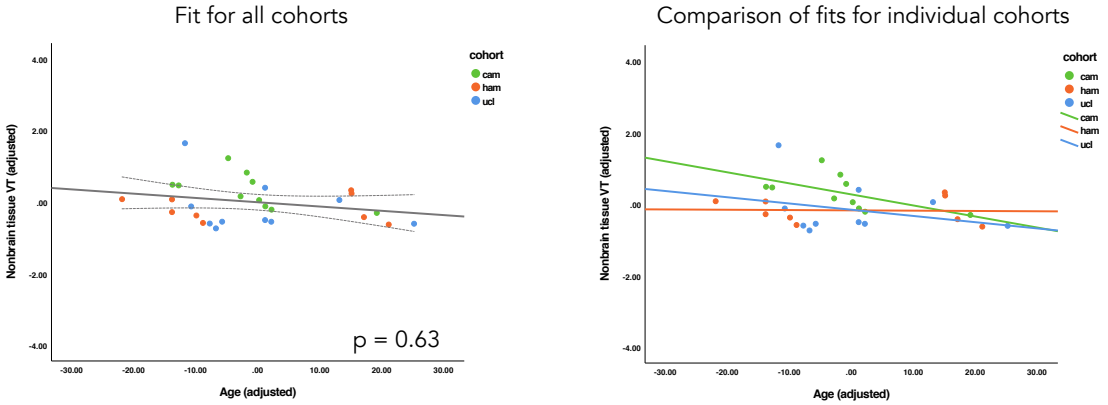

Figure 4.2: *Association of GE-179 uptake in white matter and nonbrain tissue with age in healthy volunteers*

Association of GE-179 V_T in white matter (**panel A**) and nonbrain tissue (**panel B**) with age in healthy volunteers (n=29). Grey matter V_T and age are displayed as mean centred values that were adjusted for the effects sex and scanner equipment. The regression line fit and its 95% confidence interval for the overall cohort is displayed on the left, the fits for each individual cohort are displayed on the right.

4.3.2 Sensitivity analyses

We performed sensitivity analyses in each cohort separately. The lowest coefficient of variation was observed in the *Hammersmith* cohort (13.2%) compared to the *Cambridge* (16.4%) or *UCL* (25.3%) cohorts. There was a significant association of V_T in grey matter with age in the *Hammersmith* cohort ($F = 29.6$, $p = 0.002$, V_T increase by 0.6 per 10 years, 95% CI 0.3 to 0.9, Figure 4.4A). The slope of the linear regression fit was similar but the association was non-significant in the *Cambridge* ($F = 1.7$, $p = 0.24$, V_T increase by 0.6 per 10 years, 95% CI -0.5 to 1.7, Figure 4.4B) and *UCL* ($F = 1.2$, $p = 0.30$, V_T increase by 0.8 per 10 years, 95% CI -0.9 to 2.4, Figure 4.4C) cohorts.

On a voxelwise level, there was a significant association of age with increased VT in bilateral superior frontal gyri (right, T = 5.5, 2270 voxels, p = 0.005; left, T = 5.3, 1579 voxels, p=0.02) left striatum, caudate nucleus, and hippocampus (T = 5.1, 2261 voxels, p = 0.005), and left posterior temporal lobe and temporo-occipital junction (T = 4.8, 1908 voxels, p = 0.01) in the *Hammersmith* cohort (Figure 4.4A). There were no significant clusters in the *Cambridge* or *UCL* cohorts. An exploratory analysis found non-significant ($p<0.05$ uncorrected) clusters in bilateral parieto-temporo-occipital junctions, inferior and superior frontal lobes, striata and entorhinal cortices in the *Cambridge* cohort (Figure 4.4B) and in bilateral superior and medial frontal gyri, striata, and occipital lobes in the *UCL* cohort (Figure 4.4C).

4.3.3 Epilepsy cohort

Similarly, age-related increases in [^{18}F]GE-179 V_T were observed in a group of 26 people with focal refractory epilepsy ($F = 9.9$, $p = 0.006$, V_T increase by 1.4 per 10 years, 95% CI 0.5 to 2.4; corresponding to a 14% increase per 10 years compared to mean V_T, 95% CI 5-24%) after correction for sex, duration of epilepsy, seizure frequency, number of AEDs and intake of Lamotrigine, Lacosamide, and Perampanel.

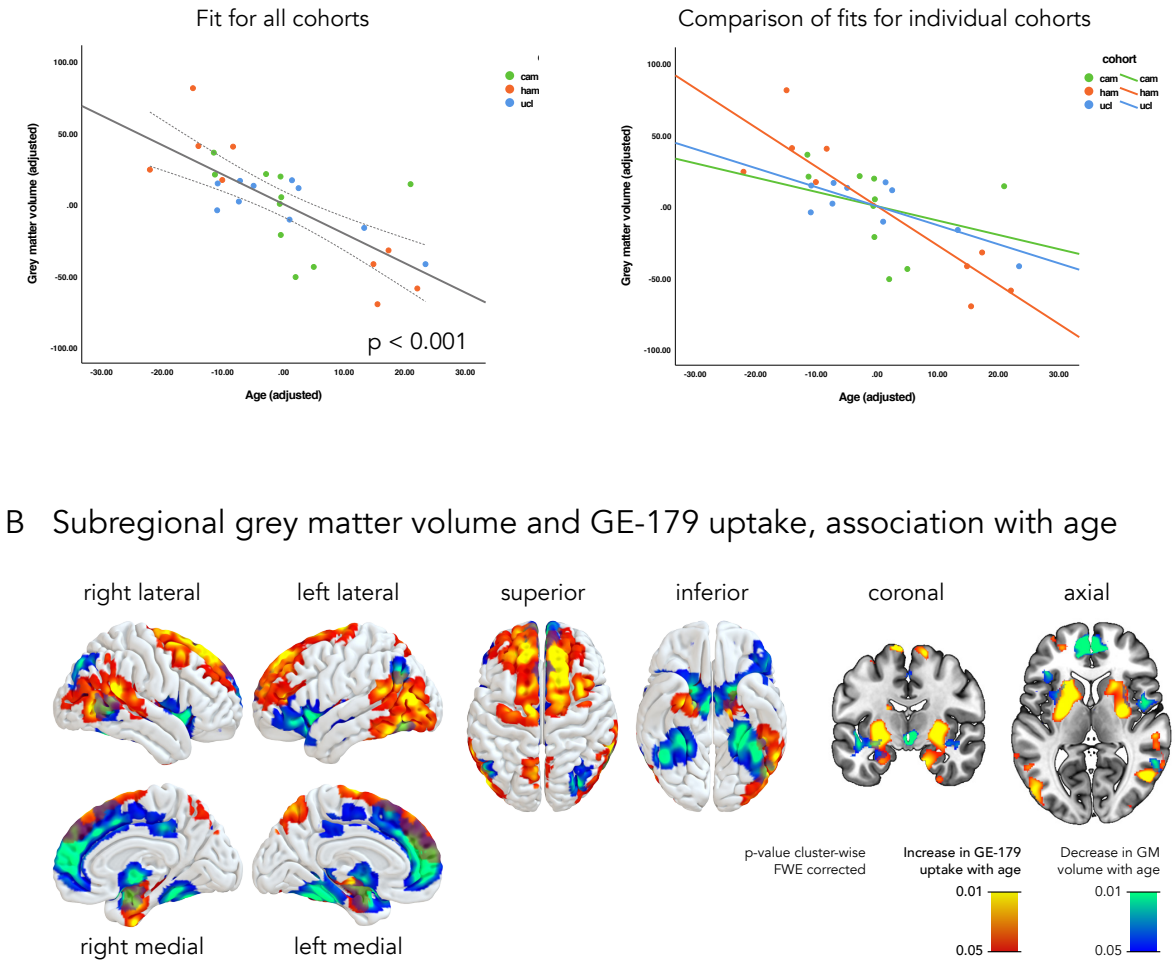

Figure 4.3: *Association of grey matter volume with age in healthy volunteers*

The association of grey matter volume with age in healthy volunteers (n=29) is displayed in **panel A**. Grey matter volume and age are displayed as mean centred values that were adjusted for the effects sex and scanner equipment. The regression line fit and its 95% confidence interval for the overall cohort is displayed on the left, the fits for each individual cohort are displayed on the right. The subregional distribution of grey matter volume (blue colours) and GE-179 V_T (yellow/red colours) associated with age is shown in **panel B** ($p<0.05$ FWE corrected).

The effects were most pronounced in the striatum and thalamus contralateral to the epileptic focus. For details please refer to chapter 5.3.2 and Figure 5.2A.

4.4 Discussion

We measured aging-related changes to the *in vivo* opening probability of NMDA receptors in humans by pooling data acquired with the novel [^{18}F]GE-179 PET radioligand. We found increased NMDA receptor opening probability in grey matter of older healthy adults and older people with focal epilepsy. These changes were specific to grey matter and were not observed in white matter or non-brain tissue. They were spatially and statistically not related to grey matter volume loss, a surrogate marker of neurodegeneration. The effects were most pronounced in bilateral superior frontal lobes, striata, temporo-parieto-occipital junctions, and, to a lesser extent, medial temporal lobes.

4.4.1 Age-related increase of NMDA receptor opening probability

There are several potential explanations for an age-related increase of NMDA receptor opening probability in humans. Firstly, it is unlikely that it reflects an increase in overall NMDA receptor availability. Most animal studies described a decrease of NMDA receptor numbers with higher age (Castorina *et al.*, 1994; Magnusson, 2000; Magnusson and Cotman, 1993; Magnusson *et al.*, 2007; Ontl *et al.*, 2004). Similarly, several (Kornhuber *et al.*, 1988; Piggott *et al.*, 1992), but not all (Law *et al.*, 2003), *post mortem* studies in humans found reduced overall NMDA receptor binding. It is unclear to what extent the reduction of NMDA receptor numbers relates to loss of neurons. The effects were, however, more pronounced for NMDA receptors compared to other glutamate ion channels (Magnusson and Cotman, 1993; Magnusson *et al.*, 2010), suggesting a higher vulnerability of NMDA receptors to aging. Thus, the higher [^{18}F]GE-179 binding observed in the current study likely relates

to a functional modification of NMDA channel opening probability, despite a probable decrease in receptor numbers. This is corroborated by several studies that found an age-related increase in sensitivity and responsiveness of the remaining receptors (Billard *et al.*, 1997; Jasek and Griffith, 1998; Kuehl-Kovarik *et al.*, 2000). It has been suggested that these adaptations could reflect functional compensation to maintain cognitive function during aging despite neuronal or ion-channel loss (Billard *et al.*, 1997; Serra *et al.*, 1994).

Secondly, an aging-related shift in NMDA receptor subunit composition and synaptic localisation could contribute to an increased opening probability. GluN2B subunits are more susceptible to aging compared to GluN2A subunits, leading to an age-related increase in the GluN2A/GluN2B ratio (Brim *et al.*, 2013; Magnusson, 2000; Magnusson *et al.*, 2002; 2006; Zamzow *et al.*, 2013). GluN2A containing NMDA receptors have a higher opening probability and peak open probability in response to glutamate (N. Chen *et al.*, 1999; Erreger *et al.*, 2005; Gray *et al.*, 2011). Additionally, aging also causes a facilitated activation of extrasynaptic compared to synaptic NMDA receptor sites (Potier *et al.*, 2010). Extrasynaptic NMDA receptors are also more likely to be activated in neurodegenerative disorders, particularly by amyloid-beta in Alzheimer's disease (Sepulcre *et al.*, 2016; Talantova *et al.*, 2013). In turn, overactivated extrasynaptic NMDA receptors are more likely to induce cell death (Hardingham and Bading, 2010) and accumulation of neurofibrillary tau tangles (Chohan and Iqbal, 2006).

Thirdly, alterations of glutamate homeostasis during aging could contribute to an increased NMDA receptor opening probability. Evidence in rodents points to a decreased expression of glutamate transporters and consequently a reduced glutamate reuptake in aged animals (Brothers *et al.*, 2013; Farrand *et al.*, 2015; Nickell *et al.*, 2007; Potier *et al.*, 2010; Vatassery *et al.*, 1998). This can lead to glutamate spillover to the extrasynaptic space and to activation of extrasynaptic NMDA receptors that might cause excitotoxicity (Farrand *et al.*, 2015; Potier *et al.*, 2010). Treating aged

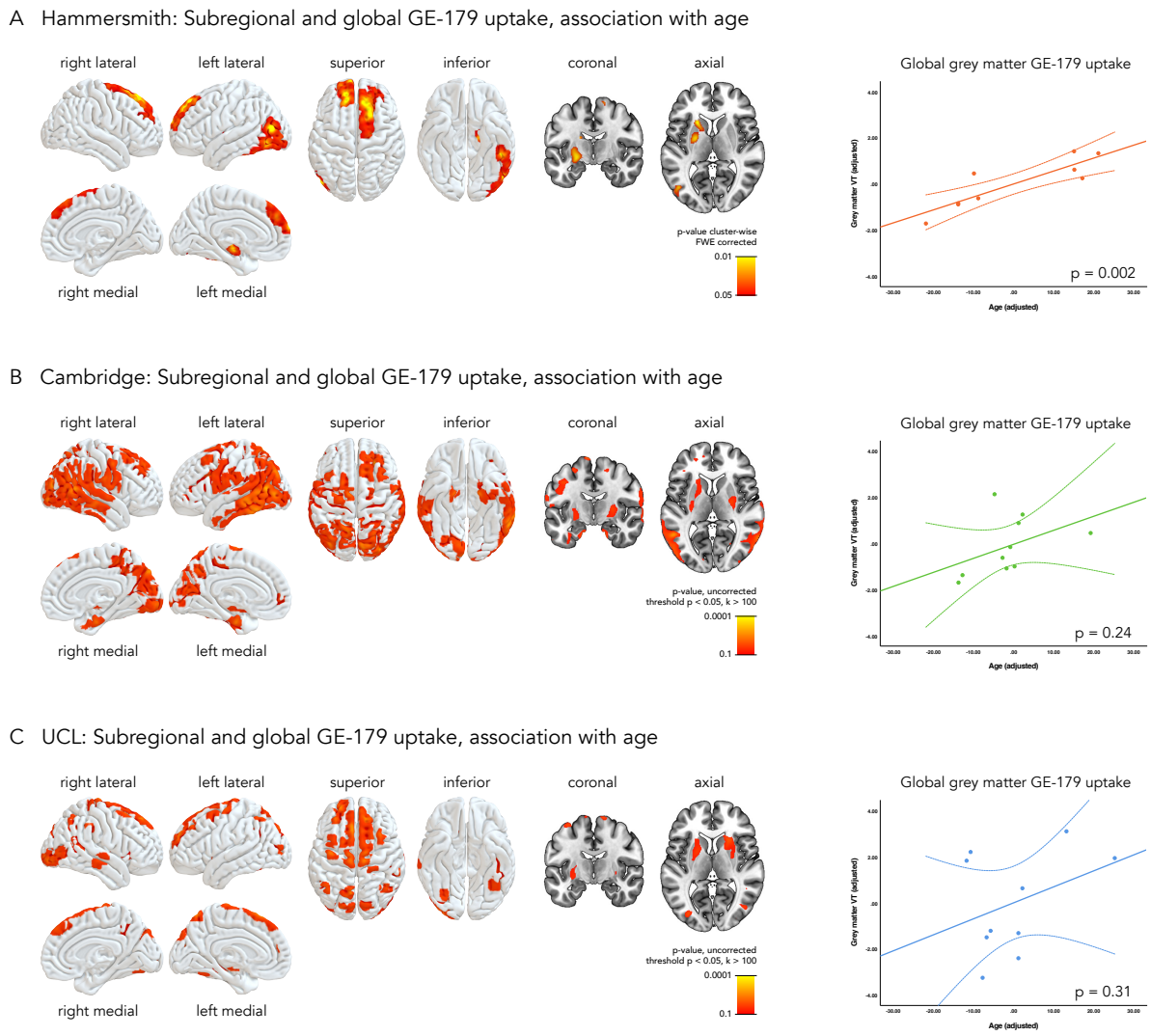

Figure 4.4: *Association of GE-179 uptake in grey matter with age in individual cohorts*

The association of grey matter GE-179 V_T with age in healthy volunteers is displayed in the Hammersmith (n=9, **panel A**), Cambridge (n=10, **panel B**), and UCL (n=10, **panel C**) cohorts. The subregional distribution of grey matter V_T associated with age is shown on the left ($p<0.05$ FWE corrected for Hammersmith, and $p<0.05$ uncorrected for Cambridge and UCL). Scatter plots with the regression line and 95% confidence intervals are shown on the right. Grey matter V_T and age are displayed as mean centred values that were adjusted for the effects sex and scanner equipment.

rodents with riluzole, a glutamate modulator, increased glutamatergic reuptake and prevented age-related cognitive deficits (Brothers *et al.*, 2013; Pereira *et al.*, 2014).

The findings observed in healthy aging were replicated in people with focal refractory epilepsy. Interestingly, the aging-related increase of tracer binding in people with epilepsy was more than double that of normal aging (V_T increase 1.4 in epilepsy vs. 0.6 in healthy volunteers per 10 years). We speculate that epilepsy and aging may have additive effects on NMDA receptor alterations. This could be due to additional release of glutamate during seizures and possible excitotoxicity (During and Spencer, 1993), oxidative stress, metabolic disturbances, and inflammation in epilepsy (Sutula *et al.*, 2003; Vezzani *et al.*, 2011). Similarly, we previously observed that the rate of ongoing neurodegeneration in epilepsy, measured with cortical thinning, was more than double that of normal aging (Galovic, van Dooren, *et al.*, 2019). Because the rate of cortical thinning was particularly accelerated in people with epilepsy aged above 55 years, we hypothesized that the brains of people with epilepsy are more vulnerable to aging-related disturbances (Galovic, van Dooren, *et al.*, 2019).

4.4.2 Spatial distribution of age-related changes to NMDA receptors

We showed that aging-related alterations of NMDA receptors were not uniform throughout the human brain but preferentially affected specific cortical and subcortical areas. Most of these regions have been suggested to play a role in cognitive processes. The superior anterior frontal cortex (D'Esposito *et al.*, 1995), the striatum (Provost *et al.*, 2015), and the temporo-parieto-occipital junction (Salmon *et al.*, 1996) play a role in working memory (Owen *et al.*, 2005). The medial temporal lobe subserves episodic memory (Nyberg *et al.*, 1996). In addition, several, but not all, of the areas with increased NMDA receptor opening probability overlap with regions of the default mode network (DMN), a brain system preferentially active when individuals

are left to think to themselves. Aging leads to increases in DMN activity that reflect a deficit in cognitive control associated with worse working memory performance (Sambataro *et al.*, 2010). Lastly, the spatial distribution of NMDA receptor alteration in our study resembles the cortical distribution of tau and amyloid-beta deposits in cognitively normal elderly individuals (Sepulcre *et al.*, 2016) and in Alzheimer's disease (Jack *et al.*, 2013; Okamura *et al.*, 2014). Early Alzheimer's disease and mild cognitive impairment are associated with network hyperexcitability (Fontana *et al.*, 2017; Haberman *et al.*, 2017; Palop *et al.*, 2007; Yassa *et al.*, 2010) that can also be observed during normal aging (Senatorov *et al.*, 2019). Taken together, the areas of greater NMDA receptor disturbances might be part of cognitive brain system that is vulnerable to aging and neurodegenerative diseases. Such functional changes may precede grey matter atrophy in these areas.

The spatial distribution of age-related effects on NMDA receptors in people with epilepsy was restricted to subcortical structures contralateral to the seizure focus. This is a more restricted pattern compared to healthy volunteers, probably because of an inverse effect of epilepsy duration on cortical structures (longer duration of epilepsy leads to lower NMDA receptor opening probability).

There is also a large overlap between the areas with age-related NMDA receptor alterations in humans and in rodents. Similarly to the current study in humans, the frontal cortex (Castorina *et al.*, 1994; Magnusson, 2000; Magnusson and Cotman, 1993; Ontl *et al.*, 2004), striatum (Castorina *et al.*, 1994; Magnusson and Cotman, 1993), parieto-occipital cortex (Magnusson, 2000; Magnusson and Cotman, 1993), and hippocampus (Castorina *et al.*, 1994; Magnusson, 2000) previously showed NMDA receptor abnormalities in older animals. This supports the notion that age-related abnormalities follow a specific spatial pattern and that some brain areas are more vulnerable than others.

4.4.3 Methodical considerations

Several methodical considerations should be noted. Firstly, [^{18}F]GE-179 is a novel radioligand that showed specific and selective binding *in vitro* and *in vivo* to the phencyclidine site inside the open NMDA channel (McGinnity *et al.*, 2014; Vibholm, Landau, Møller, *et al.*, 2020). Demonstrating specific binding *in vivo* can be challenging for use dependent tracers (McGinnity *et al.*, 2019). Recently, administration of the NMDA receptor antagonist S-ketamine successfully blocked [^{18}F]GE-179 binding in a use dependent manner *in vivo* during pulsed electrical stimulation (Vibholm, Landau, Møller, *et al.*, 2020), confirming the specificity for the phencyclidine site. Likewise, GE-179's antecedent, CNS 5161, was successfully blocked by phencyclidine site antagonists *in vivo* (Biegon *et al.*, 2007). It should be noted that the phencyclidine site is expressed on all NMDA receptors. Thus, [^{18}F]GE-179 imaging cannot distinguish between the subunit composition or synaptic/extrasynaptic localisation of receptors.

Secondly, it has been suggested that NMDA receptor abnormalities might be the consequence of neuronal loss (Billard *et al.*, 1997; Serra *et al.*, 1994). In our study, the spatial distribution of increased NMDA receptor opening probability in the brain differed from the pattern of progressive structural neurodegeneration measured with grey matter volume, suggesting that these are distinct processes. In addition, to reduce the influence of grey matter atrophy on our results we corrected the PET findings for partial volume effects, but the observed effects were comparable when using non-corrected data.

Thirdly, aging might result in differences in radioligand metabolism or cerebral blood perfusion. It is unlikely that this would influence our findings because V_T estimates are corrected for tracer metabolism and cerebral perfusion.

Fourthly, although the slope of regression fits and the subregional distribution of findings was similar between cohorts, the results were not significant in the *Cambridge*

and *UCL* cohorts. One explanation is the small sample size of cohorts. In addition, both the *Cambridge* and *UCL* cohorts showed higher PET data variability, owing to a lower PET scanner resolution and the use of image-derived input function estimates in the *UCL* cohort. This would reduce the signal-to-noise ratio and make it less likely to observe significant effects despite comparable trends. Thus, pooling of multicentre data was necessary to increase the statistical power of our study. Scanning equipment did not significantly influence the results and we adjusted all statistical models for site allocation to further minimise any residual between-cohort effects.

Lastly, we were restricted to studying a limited age range of 25 to 65 years for healthy volunteers and 18 to 65 years for people with epilepsy due to ethical considerations. Younger participants are more likely to be adversely affected by radiation and older subjects are less likely to tolerate a 70 to 90 minute scan and have a higher risk of concomitant or subclinical neurodegenerative disorders. We included few women of childbearing age due to the potential effects of radiation.

4.4.4 Conclusions

We observed *in vivo* increased NMDA receptor opening probability in older healthy adults and people with epilepsy. These functional changes were not uniform throughout the brain but particularly affected areas that may play a role in cognitive processes and preceded grey matter atrophy of these regions. The exact pathophysiology is not clear with several potential explanations for this finding. Future studies should determine the age-related expression of NMDA receptor subunits and glutamate transporters. They should examine whether increased NMDA receptor activation relates to cognitive decline or neurodegenerative disorders and whether it might be a marker of the risk to develop Alzheimer's dementia. Lastly, our findings provide support for exploratory human trials of memantine and riluzole to reduce NMDA receptor opening probability and cognitive decline in elderly individuals.

5 Project 3: NMDA receptor activation in focal epilepsy.

5.1 Introduction

Epilepsy, a disease characteristically manifesting with neuronal hyperexcitability, has been linked to dysfunction of NMDA ion-channels that bind glutamate, the main excitatory neurotransmitter in the central nervous system. Alterations of NMDA receptors played a role in animal models of epileptogenesis, the process underlying the development of epilepsy (Ghasemi and Schachter, 2011). Blocking of NMDA receptors prevented epileptogenesis and was neuroprotective (Brandt *et al.*, 2003; Raza *et al.*, 2004; Stasheff, Anderson, Clark and Wilson, 1989b).

In humans, the available evidence on the role of over- or underactivated NMDA receptors in epilepsy is conflicting. Firstly, immunohistochemistry studies of postsurgical temporal lobe specimen in people with refractory epilepsy found decreased (Bayer *et al.*, 1995; Blumcke *et al.*, 1996; Geddes *et al.*, 1990; Hosford *et al.*, 1991; Spreafico *et al.*, 1998) or increased (Brines *et al.*, 1997; Geddes *et al.*, 1990; Mathern *et al.*, 1997; McDonald *et al.*, 1991) NMDA receptor density. binding inside the open, i.e. activated, NMDA receptor channel was described (Hosford *et al.*, 1991; McDonald *et al.*, 1991). A higher proportion of GluN2B subunits has also been observed (Mathern *et al.*, 1998).

Secondly, mutations in GRIN genes coding GluN1, GluN2A, and GluN2B subunits cause a neurodevelopmental disorder with seizures. More mutations were functionally characterised as loss- than gain-of-function, but both alterations led to seizures (Xu and Luo, 2018). In mutations affecting the GluN2A subunit, those leading to a receptor gain-of-function were associated with a more severe phenotype (Strehlow *et al.*, 2019).

Thirdly, NMDA receptor antagonists have been used to treat seizures (Felbamate Study Group in Lennox-Gastaut Syndrome, 1993; Pellock, 1999) and status epilepticus (Borris *et al.*, 2000; Prüss and Holtkamp, 2008) but proconvulsant effects have also been reported (Alldredge *et al.*, 1989; Claudet and Maréchal, 2009; Modica *et al.*, 1990; Peltz *et al.*, 2005; Sveinbjornsdottir *et al.*, 1993).

Lastly, only two studies thus far analysed NMDA receptors in people with epilepsy *in vivo* using PET, but they produced contradictory results. [^{11}C]ketamine binding was reduced in the ipsilateral temporal lobe in eight people with mesial temporal lobe epilepsy (MTLE), which could either point to a reduced NMDA receptor density, reduced tissue perfusion or focal atrophy (Kumlien *et al.*, 1999). We performed a pilot study with [^{18}F]GE-179, measuring the opening probability of NMDA receptors in eleven people with focal epilepsy and frequent interictal epileptic discharges (McGinnity *et al.*, 2015). We observed globally increased binding in eight patients not taking antidepressants and decreased binding in three patients on antidepressants. Focal NMDA receptor binding alterations were detected in a subset of patients but were difficult to interpret because of the undetermined localisation of epilepsy in these cases.

Here, we measured *in vivo* NMDA receptor activation using [^{18}F]GE-179 PET in people with well-localised refractory focal epilepsy undergoing presurgical evaluation and matched healthy volunteers. We associated NMDA receptor binding with clinical characteristics and epilepsy localisation, and compared postsurgical with presurgical uptake.

Variable	Mean ± SD or N (%)	F	Beta (95% CI)	P value
Demographic characteristics				
Age *(years, unadjusted)*	38 ± 13	0.1	0.02 (-0.09, 0.13)	0.71
Female Sex *(unadjusted)*	15 (58%)	0.4	-0.8 (-3.6, 1.9)	0.53
Non-European Ethnicity	5 (20%)	0.03	-0.3 (-4.0, 3.4)	0.87
Smoking	3 (12%)	2.7	-3.3 (-7.6, 0.9)	0.12
Beck's Depression Inventory score	13 ± 9	0.003	0.004 (-0.15, 0.16)	0.95
Duration of epilepsy *(years)*	19 ± 12	4.9	-0.13 (-0.26, -0.01)	0.04
Focal lesion on MRI	17 (65%)	1.1	-1.5 (-4.4, 1.4)	0.31
Epilepsy localisation				
Mesial temporal	7 (27%)	0.1	-0.6 (-3.8, 2.7)	0.72
Temporal	18 (69%)	1.2	-1.7 (-4.9, 1.5)	0.28
Frontal	5 (19%)	0.7	1.5 (-2.4, 5.5)	0.43
Other	3 (12%)	0.3	1.2 (-3.2, 5.6)	0.57
Seizure frequency				
Overall seizure frequency *(per month)*	34 ± 40	0.7	0.02 (-0.02, 0.05)	0.40
SPS frequency *(per month)*	14 ± 27	1.5	0.03 (-0.02, 0.09)	0.24
CPS frequency *(per month)*	19 ± 31	0.03	0.004 (-0.04, 0.05)	0.87
SGS frequency *(per month)*	1 ± 3	0.9	-0.3 (-0.8, 0.3)	0.36
Last seizure *(days before scan)*	25 ± 107	0.1	-0.002 (-0.02, 0.01)	0.73
Antiepileptic drugs at scan				
Number of antiepileptic drugs	2 ± 1	4.3	1.3 (0.003, 2.5)	0.05
Levetiracetam	10 (39%)	1.5	1.7 (-1.2, 4.5)	0.24
Oxcarbazepine	10 (39%)	2.1	2.1 (-0.9, 5.0)	0.16
Lamotrigine	7 (27%)	5.7	-3.3 (-6.2, -0.4)	0.03
Zonisamide	7 (27%)	0.1	-0.6 (-3.8, 2.7)	0.73
Lacosamide	5 (19%)	6.5	3.9 (0.7, 7.1)	0.02
Clobazam	5 (19%)	0.03	-0.3 (-4.0, 3.3)	0.86
Perampanel	3 (12%)	4.2	4.1 (-0.07, 8.2)	0.05

Table 5.1: *Clinical characteristics and their association with [^{18}F]GE-179 uptake in epilepsy patients.*

SD, standard deviation; SPS, simple partial seizure; CPS, complex partial seizure; SGS, secondarily generalized seizure.

5.2 Methods

We followed the methods as described in detail in chapter 2. We included 26 people (mean age 38 ± 13 years, 11 [42%] female) with unilateral focal refractory epilepsy arising from the temporal (n=17) and frontal lobes (n=5) or other localisation (n=4) undergoing presurgical evaluation at NHNN and scanned at the *UCL* site. Seven

patients had mesial temporal lobe epilepsy with hippocampal sclerosis and half (n=13) of all patients had epilepsy lateralised to the left hemisphere. Six patients were rescanned after anterior temporal lobe resection. Twenty-nine healthy volunteers (mean age 41 ± 13 years, 8 [28%] female) were recruited and scanned at three sites (*UCL [n=10]*, *Cambridge [n=10]*, *Hammersmith [n=9]*).

The *Cambridge* and *Hammersmith* sites used PET-CT scanners with an arterial input function, whereas the *UCL* site used a PET-MR scanner with a venous/image-derived input function (see chapter 3 for method validation). Only one venous sample was obtained in 6 patients in the UCL study and we applied the simplified one-sample approach to these cases (chapter 3.3.2). Venous sampling failed in 4 scans and we used population-based parent-fraction and plasma-over-blood ratio curves in these scans (McGinnity *et al.*, 2018). Prior to preprocessing, imaging data in epilepsy patients and an equivalent proportion of randomly selected healthy volunteers were flipped to display the hemisphere ipsilateral to the epileptic focus on the left.

As a first step, we extracted V_T estimates in grey matter and calculated their association with clinical characteristics in patients with epilepsy using the general linear model adjusting for age and sex. We chose significant variables from the first set of analyses and included them in a multivariable model, additionally correcting for seizure frequency as a proxy for disease severity. To address the subregional distribution of the findings, we replicated the same multivariable general linear model on voxelwise V_T estimates in grey matter.

We determined test-retest reliability of [^{18}F]GE-179 PET scans using data from 5 healthy volunteers scanned at least 1 year apart in the *Cambridge* study using scatter plots, correlation coefficients, and Bland Altman plots. In addition to absolute V_T, we also compared relative V_T, i.e. the ratio between lobar and global grey matter V_T in a scan.

Next, we compared the overall grey matter V_T in healthy volunteers with epilepsy patients using the general linear model adjusting for sex, age, and cohort allocation

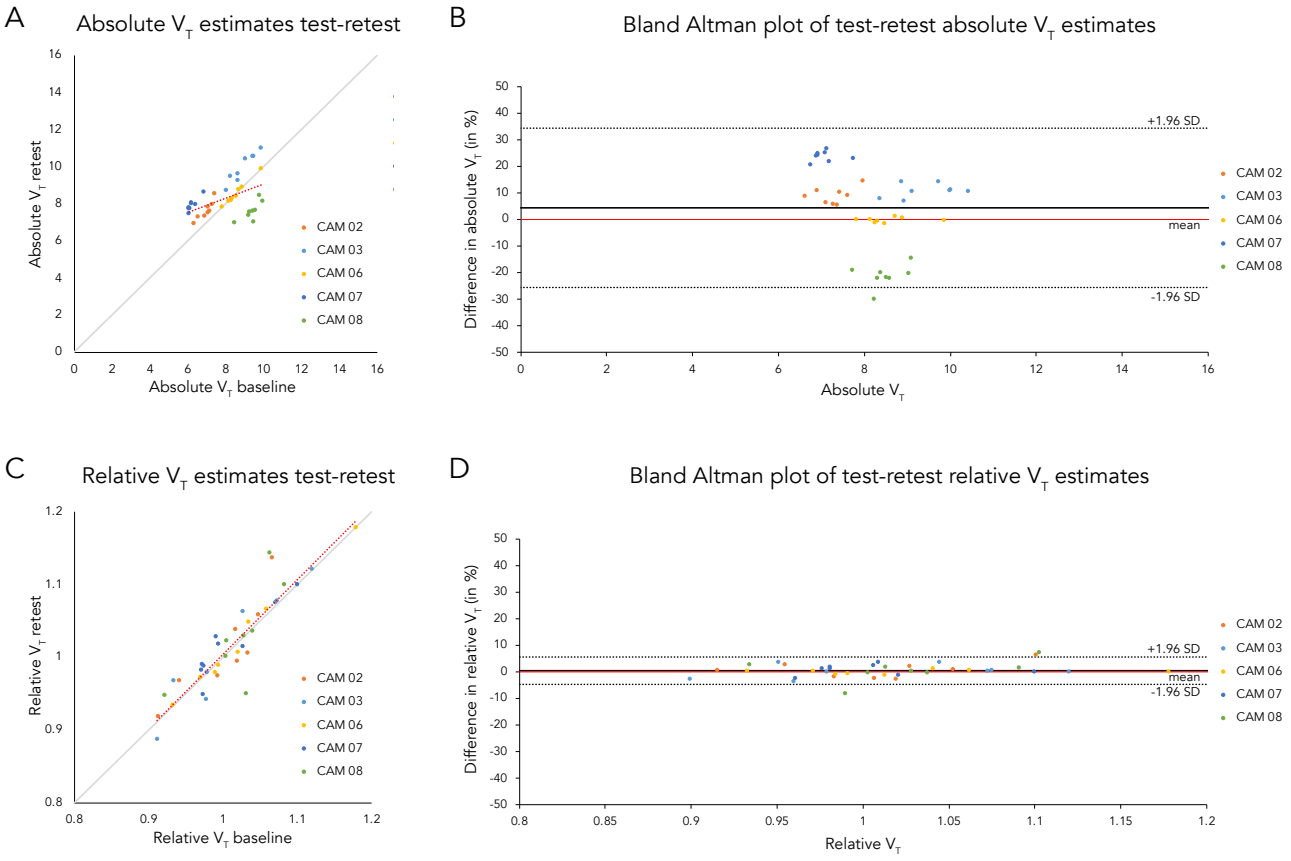

Figure 5.1: *Test-retest measurements of [^{18}F]GE-179 PET*

Test and retest regional estimates of GE-179 V_T in five healthy volunteers are displayed as absolute values (**panel A**) or relative values normalised to global grey matter V_T (**panel B**). Scatter plots on the left show the linear regression fit (red dotted line) and the optimal fit (grey line). Bland-Altman plots on the right show the bias of the mean of the V_T estimates (black line) and the 95% confidence intervals (black dotted lines).

(i.e. scanning equipment). We split patients into subgroups with mesial temporal lobe epilepsy with hippocampal sclerosis (MTLE+HS), temporal lobe epilepsy (TLE, including both neocortical or mesial localisations), and frontal lobe epilepsy (FLE). We also analysed subregional differences in voxelwise V_T estimates with a full factorial general linear model corrected for sex, age, and cohort allocation taking global V_T into account via an analysis of covariance (ANCOVA) by group (McGinnity *et al.*, 2015). To address the contribution of epilepsy-related grey matter atrophy to our findings, we performed voxel-based morphometry (VBM) using segmented and modulated

parametric grey matter volume images obtained using the CAT12 toolbox on 3T T1 MRI scans. We displayed the overlap of V_T and VBM voxelwise findings.

Lastly, we analysed changes in relative regional V_T after anterior temporal lobe resection in six patients using paired t-tests. We used relative instead of absolute V_T measurements due to their improved reproducibility (chapter 5.3.1). We compared post- with presurgical voxelwise V_T using a paired t-test and a small volume correction to regions found to be significant in the regional analysis (contralateral basal ganglia and temporal lobe).

We report voxelwise p-values at a threshold of $p<0.05$ on a cluster-level family-wise error corrected for multiple comparisons.

5.3 Results

5.3.1 Test-retest measurements of [^{18}F]GE-179 uptake

Five healthy volunteers from the Cambridge cohort were rescanned at least one year apart. Absolute grey matter V_T in cerebral lobes and subcortical structures (basal ganglia, thalamus) correlated moderately between measurements ($r = 0.48$, $p = 0.002$, Figure 5.1A). Bland Altman plots (Figure 5.1B) showed positive bias of the mean (4.4%) and large variability (95% CI -25.7 to 34.4%) of V_T differences between scans.

In contrast, relative grey matter V_T was highly correlated between measurements ($r = 0.91$, $p < 0.001$, Figure 5.1C). There was small bias of the mean (0.4%) and small variability (95% CI -4.8 to 5.7%) of relative V_T differences between scans (Figure 5.1D).

5.3.2 [^{18}F]GE-179 uptake and demographics in epilepsy patients

Detailed clinical characteristics of the included 26 patients with epilepsy and their association with global V_T in grey matter are displayed in Table 5.1. We included all

Variable	F	Beta (95% CI)	P value
Age *(per 10 years)*	9.9	1.4 (0.5, 2.4)	0.006
Duration of epilepsy *(per 10* years)	10.9	-1.6 (-2.7, -0.6)	0.004
Lacosamide intake at scan	9.8	4.5 (1.5, 7.6)	0.006
Female Sex	1.0	-1.0 (-3.2, 1.1)	0.34
Overall seizure frequency *(per month)*	0.01	0.001 (-0.03, 0.03)	0.91
Number of antiepileptic drugs	0.7	0.2 (-1.0, 1.5)	0.68
Lamotrigine intake at scan	1.5	-1.4 (-3.8, 1.0)	0.24
Perampanel intake at scans	1.2	1.9 (-1.7, 5.4)	0.28

Table 5.2: *Multivariable model of [^{18}F]GE-179 uptake in epilepsy patients.*

significant variables from Table 5.1 into a multivariable model of [^{18}F]GE-179 V_T in grey matter, additionally adjusting for age, sex, and seizure frequency (Table 5.2). We found a significant positive association of V_T in grey matter with age (F = 9.9, p = 0.006, Figure 5.2A), observing an estimated V_T increase of 1.4 (95% CI 0.5 to 2.4) per 10 years. On a subregional level (Figure 5.2A), we observed significant age-related increases in V_T in a large cluster (T = 5.1, 13465 voxels, p=0.002) involving the bilateral striata, ipsilateral orbitofrontal cortex, contralateral thalamus, and contralateral hippocampus.

We also found a significant negative association with duration of epilepsy (F = 10.9, p = 0.004, Figure 5.2B), with an estimated V_T decrease of 1.6 (95% CI 0.6 to 2.7) per 10 years. In the voxelwise analysis, duration of epilepsy was negatively associated with V_T (i.e. the longer the duration of epilepsy the lower the V_T) in the ipsilateral striatum, thalamus, temporo-frontal junction (piriform cortex, amygdala, orbitofrontal cortex), anterior temporal neocortex (T = 4.9, 7052 voxels, p = 0.03), and in the contralateral striatum, thalamus, and orbitofrontal cortex (T = 4.6, 6223 voxels, p = 0.04).

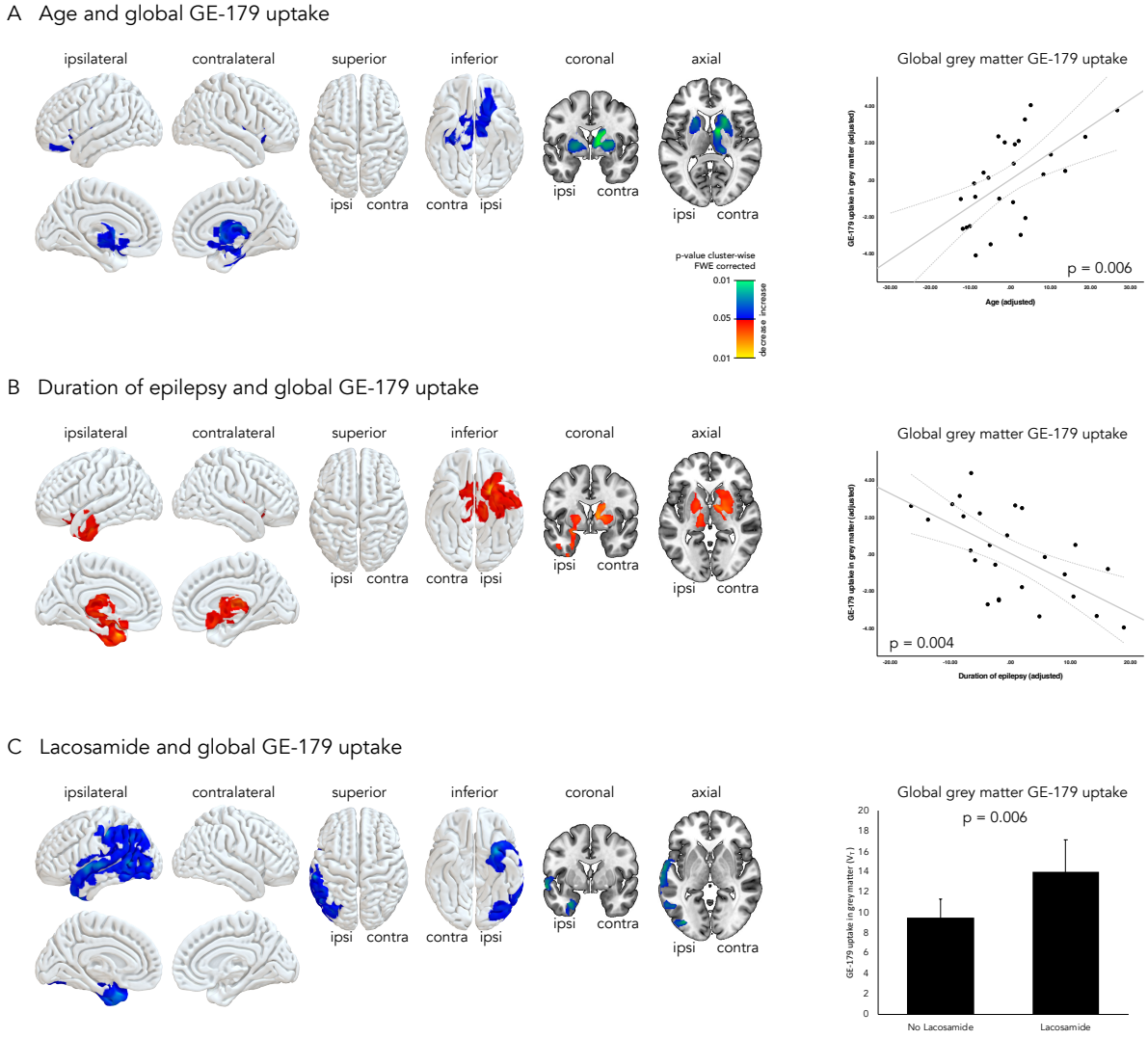

Figure 5.2: *Association of GE-179 uptake with age, disease duration, and lacosamide intake in patients with epilepsy.*

The figure shows the association of GE-179 V_T with age (**panel A**), disease duration (**panel B**), and lacosamide intake (**panel C**) in patients with epilepsy (n=26). The voxelwise distribution of results is shown on brain surfaces and slices on the left ($p<0.05$ FWE corrected; blue colours indicate increased uptake, red colour indicate decreased uptake), the global grey matter findings are shown in plots on the right. Global grey matter V_T and clinical variables are displayed as mean centred values adjusted for co-variates.

Grey matter V_T was increased in patients taking lacosamide at time of scan (F = 9.8, Beta 4.5, 95% CI 1.5 to 7.6, p = 0.006). These increases were localised to the ipsilateral temporal neocortex and temporo-parieto-occipital junction (T = 5.8, 12357 voxels, p = 0.003, Figure 5.2C). Lamotrigine intake was associated with a nonsignificant decrease in V_T (F = 1.5, Beta -1.4, 95% CI -3.8 to 1.0, p = 0.24) and perampanel intake with a nonsignificant increase in V_T (F = 1.2, Beta 1.9, 95% CI -1.7 to 5.4, p = 0.28). On voxelwise analyses, we did not detect any areas with significant changes in V_T related to lamotrigine or perampanel intake.

5.3.3 [^{18}F]GE-179 uptake in epilepsy patients compared to healthy volunteers

People with epilepsy and healthy volunteers did not significantly differ in age (F=0.4, p=0.52) and sex (F=0.1, p=0.76). Global [^{18}F]GE-179 V_T in grey matter did not differ between healthy volunteers (n = 29, mean V_T 9.2, 95% CI 8.5 to 10.0) compared with patients with mesial temporal lobe epilepsy and hippocampal sclerosis (MTLE+HS, n = 7, mean V_T 9.1, 95% CI 7.5 to 10.8, F = 0.01, p = 0.93), patients with temporal lobe epilepsy (TLE, n = 18, mean V_T 9.5, 95% CI 8.0 to 10.9, F = 0.2, p = 0.67), or patients with frontal lobe epilepsy (FLE, n = 5, mean V_T 10.4, 95% CI 7.8 to 13.0, F = 0.8, p = 0.38).

On voxelwise analysis, patients with MTLE+HS (Figure 5.3A) had focal relative decreases of V_T in bilateral precunei and cuneus (T = 8.0, 2063 voxels, p < 0.001), ipsilateral mesial temporal lobe (T = 6.4, 2166 voxels, p < 0.001), contralateral superior and middle temporal gyri (T = 6.4, 2060 voxels, p < 0.001), contralateral inferior temporal gyrus (T = 5.9, 778 voxels, p = 0.002), and bilateral opercula (ipsilateral, T= 5.3, 545 voxels, p = 0.01; contralateral, T = 6.0, 1828 voxels, p < 0.001).

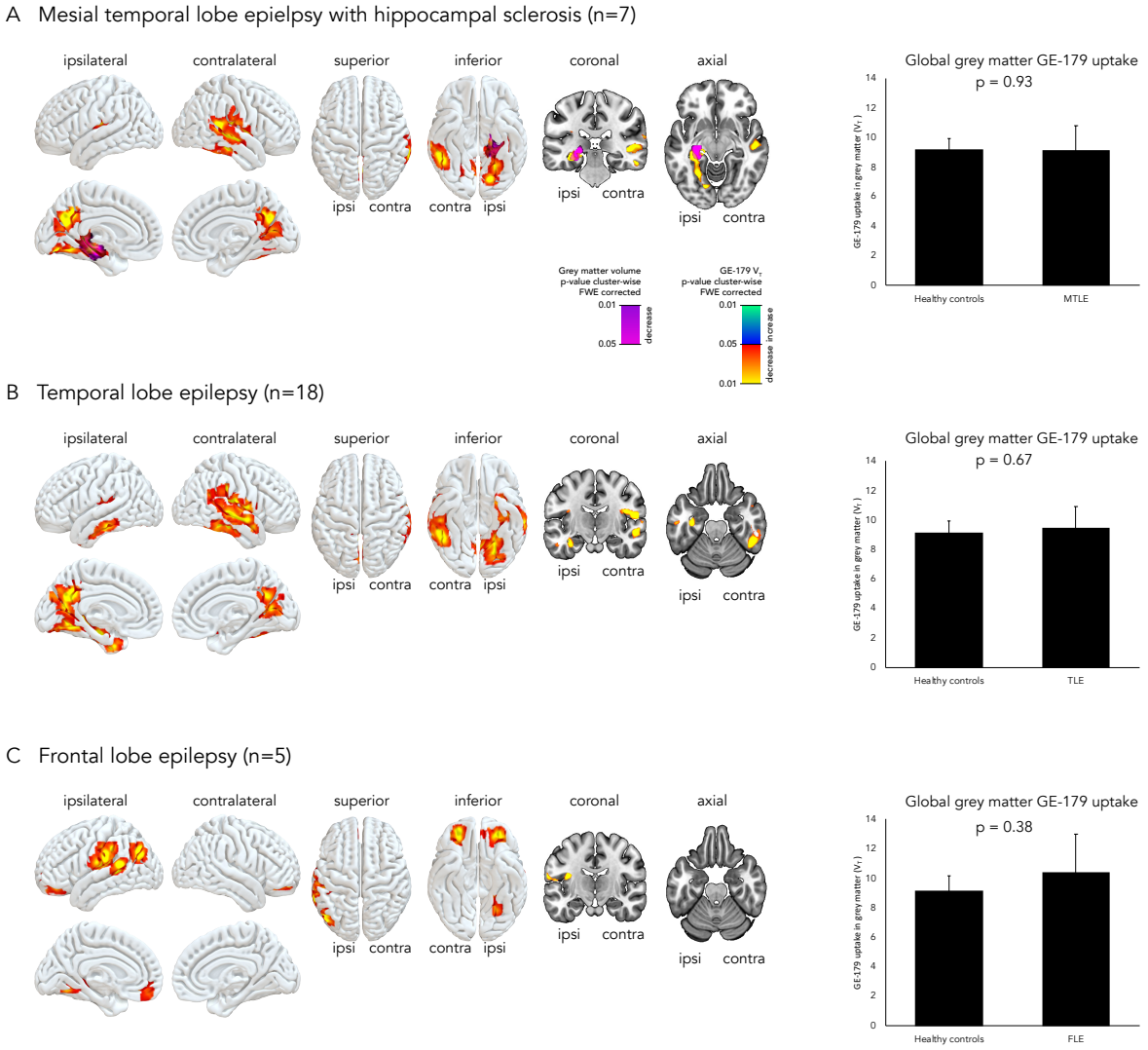

Figure 5.3: *Abnormal GE-179 uptake and epilepsy localisation.*

The figure shows abnormal GE-179 V_T in patients with mesial temporal lobe epilepsy with hippocampal sclerosis (n=7, **panel A**), temporal lobe epilepsy (n=18, **panel B**), and frontal lobe epilepsy (n=5, **panel C**) compared with healthy volunteers (n=29). The voxelwise distribution of GE-179 PET results is shown on brain surfaces and slices on the left ($p<0.05$ FWE corrected; blue colours indicate increased uptake, red colour indicate decreased uptake). Grey matter atrophy assessed with voxel-based morphometry is overlaid in purple ($p<0.05$ FWE corrected). Comparisons of estimated marginal means of global grey matter GE-179 V_T between patients and healthy volunteers are shown in plots on the right.

Patients with TLE (Figure 5.3B) had focal relative decreases of V_T in bilateral precunei (T = 6.6, 4277 voxels, p < 0.001), bilateral opercula (ipsilateral, T = 4.8, 546 voxels, p = 0.02; contralateral, T = 6.1, 2830 voxels, p < 0.001), contralateral superior and middle temporal gyri (T = 5.9, 1965 voxels, p < 0.001), contralateral inferior temporal gyrus (T = 5.7, 1401 voxels, p < 0.001), ipsilateral mesial temporal lobe (T = 5.4, 796 voxels, p = 0.002), and ipsilateral middle and inferior temporal gyri (T = 5.0, 487 voxels, p = 0.03).

Patients with FLE (Figure 5.3C) had focal relative decreases of V_T in bilateral orbitofrontal cortices (ipsilateral, T = 4.5, 650 voxels, p = 0.003; contralateral, T = 4.5, 369 voxels, p = 0.04), ipsilateral posterior superior temporal gyrus (T = 6.0, 2589 voxels, p < 0.001), ipsilateral angular gyrus (T = 5.3, 648 voxels, p = 0.003), and ipsilateral fusiform gyrus (T = 4.7, 363 voxels, p = 0.04).

We found significant grey matter atrophy measured with VBM in patients with MTLE+HS (Figure 5.3A) in the ipsilateral hippocampus (T = 7.6, 1724 voxels, p = 0.001). VBM did not detect significant grey matter atrophy in the overall group of patients with TLE (Figure 5.3B) or FLE (Figure 5.3C).

5.3.4 [^{18}F]GE-179 uptake before and after temporal lobe surgery

Due to improved reproducibility (chapter 5.3.1), we determined relative V_T ratios in cerebral lobes and subcortical structures (basal ganglia, thalamus) in six patients with temporal lobe epilepsy scanned before and after anterior temporal lobe resection. After surgery, there was a significant increase in relative V_T (Figure 5.4A) in the contralateral temporal lobe (mean relative V_T presurgical 1.00 vs. postsurgical 1.04, T = 3.2, p = 0.02) and basal ganglia (mean relative V_T presurgical 1.11 vs. postsurgical 1.15, T = 5.5 p = 0.003). In comparison, mean relative V_T in healthy volunteers was 1.05 (95% CI 0.93 to 1.17) in the temporal lobe and 1.15 (95% CI 0.97 to 1.33) in the basal ganglia. Other regions did not show significant differences. There were no

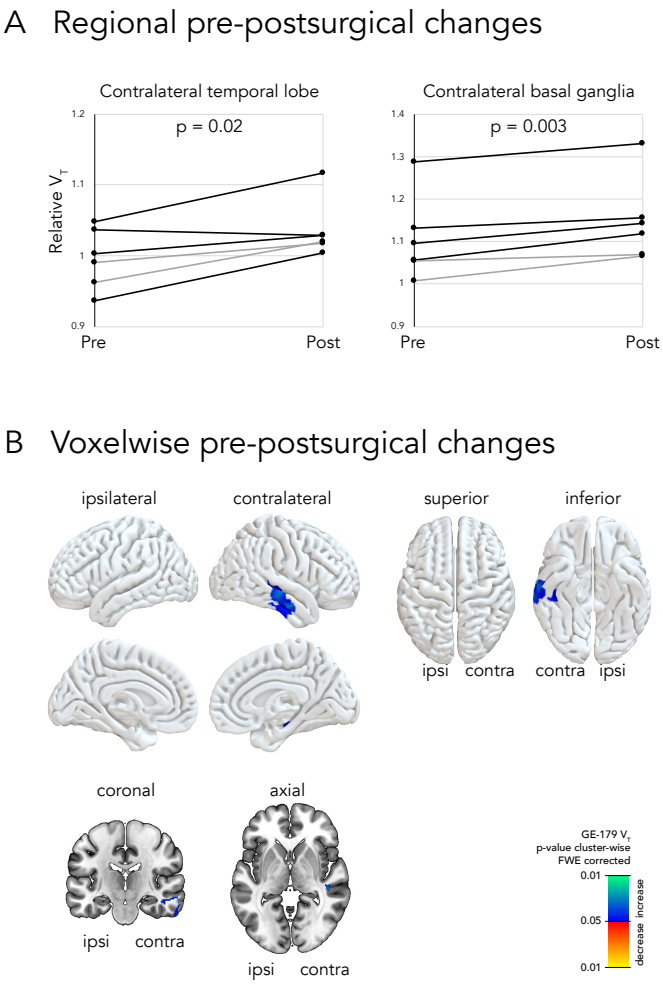

Figure 5.4: *Relative changes in GE-179 uptake after epilepsy surgery.*

Panel A shows relative changes of GE-179 V_T in the contralateral temporal lobe and basal ganglia of patients with temporal lobe epilepsy before and after anterior temporal lobe resection. **Panel B** shows the voxelwise distribution of post- vs. presurgical relative GE-179 V_T in these patients ($p<0.05$ FWE corrected; blue colours indicate increased relative uptake after surgery, red colours indicate decreased relative uptake after surgery).

differences in postsurgical relative V_T changes between patients who became seizure-free and those with ongoing seizures. On voxelwise analysis (Figure 5.4B), we confirmed postsurgical increases of relative V_T in the contralateral middle and inferior temporal gyri (T = 9.4, 546 voxels, p = 0.01).

5.4 Discussion

We report *in vivo* alterations of NMDA receptor activation in the largest cohort of patients with epilepsy studied with NMDA receptor PET to date. We found decreased interictal tracer uptake in patients with longer duration of epilepsy, whereas uptake was increased in older individuals. We observed focal reductions of tracer uptake in patients with epilepsy compared with healthy volunteers and these reductions were bilateral and spread beyond the epileptic focus. The spatial distribution of decreased uptake was related to the localisation of the epileptic focus and differed between patients with temporal or frontal lobe epilepsy. After anterior temporal lobe resection, we found relative increases in tracer binding in the contralateral temporal lobe and, less consistently, in the contralateral basal ganglia.

5.4.1 NMDA receptor hypofunction and neuronal hyperexcitability

Traditionally, activation of NMDA receptors that bind glutamate, an excitatory neurotransmitter, was thought to lead to activation of neuronal circuits. Emerging evidence from animal and human studies points to both activating and suppressing effects of NMDA receptors on neuronal networks (Fitzgerald, 2012). Network suppression could be mediated by activation of NMDA receptors on GABAergic interneurons that may in turn inhibit excitatory pyramidal cells (Grunze *et al.*, 1996; Homayoun and Moghaddam, 2007; Manzoni *et al.*, 1994). Another potential mechanism is the downregulation of excitatory AMPA receptors through NMDA receptors (Hall *et al.*, 2007). Conversely, NMDA receptor antagonism increases

glutamatergic transmission through AMPA receptors (Moghaddam and Adams, 1998; Moghaddam *et al.*, 1997). A recurrent finding is the activation of limbic structures after blocking of NMDA receptors with ketamine (Höflich *et al.*, 2017; Kraguljac *et al.*, 2017; McMillan *et al.*, 2019). Thus, NMDA receptor hypofunction may lead to hippocampal activation and subsequently to increased likelihood of seizures.

In patients with epilepsy, reduced binding inside the open, i.e. activated, NMDA ion channel and a higher proportion of GluN2B subunits, that have a lower opening probability (N. Chen *et al.*, 1999; Erreger *et al.*, 2005; Gray *et al.*, 2011), have been observed in temporal lobe specimen (Hosford *et al.*, 1991; Mathern *et al.*, 1998; McDonald *et al.*, 1991). Both gain- and loss-of-function mutations in GRIN genes encoding NMDA receptor subunits led to seizures (Xu and Luo, 2018). Seizures are frequent in anti-NMDA receptor encephalitis, an autoimmune disorder associated with internalisation and hypofunction of NMDA receptors (Hughes *et al.*, 2010; Moscato *et al.*, 2014). An increase of seizures was observed in a large proportion of patients in a trial of the competitive highly selective NMDA receptor antagonist D-CPP-ene (Sveinbjornsdottir *et al.*, 1993).

These observations allow for several interpretations of our findings. We demonstrated lower tracer uptake in epilepsy patients with longer disease duration (Figure 5.2B) and spatially distinct reductions in patients compared to controls (Figure 5.3). Lower [^{18}F]GE-179 uptake points to a reduced opening probability of NMDA receptors (McGinnity *et al.*, 2014) that could reflect a reduction in the surface expression or change of the functional properties of NMDA receptors. Our results are in line with the notion that increased NMDA receptor activation is relevant during epileptogenesis and the early stages of epilepsy whereas longer disease duration leads to progressive hypoactivation of NMDA receptors (McNamara *et al.*, 1988).

NMDA receptor hypofunction, as observed in our chronic refractory epilepsy cohort, could lead to reduced activation of inhibitory interneurons (Grunze *et al.*, 1996; Homayoun and Moghaddam, 2007; Manzoni *et al.*, 1994) and increased glutamatergic

activation of AMPA receptors (Hall *et al.*, 2007; Moghaddam and Adams, 1998; Moghaddam *et al.*, 1997), that was recently observed in patients with epilepsy (Miyazaki *et al.*, 2020). This may subsequently cause limbic hyperexcitability (Höflich *et al.*, 2017; Kraguljac *et al.*, 2017; McMillan *et al.*, 2019) and could contribute to seizures. Alternatively, NMDA receptor hypofunction could reflect a compensatory mechanism due to increased release of glutamate during seizures (During and Spencer, 1993). Glutamatergic stimulation may reduce the transcription of the obligatory GluN1 subunit, thus leading to a reduced NMDA receptor density (Gascón *et al.*, 2005). Overall, this is a less likely explanation because NMDA receptors tend to be stably expressed and are less likely to be regulated by neuronal activity than other glutamatergic ion channels (Lissin *et al.*, 1998).

Our results are in accordance with several, but not all, previous PET and immunohistochemistry studies in human epilepsy (Bayer *et al.*, 1995; Blumcke *et al.*, 1996; Geddes *et al.*, 1990; Hosford *et al.*, 1991; McDonald *et al.*, 1991; Spreafico *et al.*, 1998). A study using [^{11}C]ketamine found reduced binding in the ipsilateral temporal lobe of patients with MTLE (Kumlien *et al.*, 1999). We previously observed increased [^{18}F]GE-179 binding in eight epilepsy patients not taking antidepressants and decreased binding in three patients on antidepressants (McGinnity *et al.*, 2015). Increased binding in this previous study could reflect the selective inclusion of patients with frequent interictal epileptic discharges. Epileptic discharges during the scan could lead to glutamate release (During and Spencer, 1993) and activation of NMDA receptors. Because subjects included in the current study were less likely to have interictal epileptic discharges they may have been less prone to abnormal glutamate release during the scan.

5.4.2 Focal changes of NMDA receptor activation in epilepsy

Focally decreased NMDA receptor activation was spatially distinct between epilepsy subtypes (Figure 5.3). The ipsilateral mesial temporal lobe was more likely to show abnormal tracer uptake in MTLE+HS, whereas the ipsilateral temporal neocortex showed abnormal uptake in the overall TLE group. In contrast, patients with FLE had abnormal tracer uptake mainly in the orbitofrontal cortex and the parietal lobe. In all subgroups, reductions in NMDA receptor activation were widespread, affecting areas beyond the epileptic focus and spreading to the contralateral hemisphere. We did not observe any focal increases in NMDA receptor activation. This reinforces the concept of epilepsy as a network disorder. A similar distribution has been found in studies examining structural MRI abnormalities in epilepsy (Galovic, van Dooren, *et al.*, 2019; Whelan *et al.*, 2018). These regions may be particularly vulnerable because of their high interconnection with the epileptic focus. There is a high overlap between the areas affected in MTLE+HS (Figure 5.3A) and the regions structurally connected with the hippocampus (Figure 5.5, reproduced with permission from (Galovic, van Dooren, *et al.*, 2019).

Although we observed a different spatial distribution of NMDA receptor alterations between TLE and FLE (Figures 5.3B and 5.3C), the value of [^{18}F]GE-179 PET for presurgical evaluation may be limited because the abnormalities were bilateral and widespread. In contrast, FDG-PET shows in many cases a large area of reduced uptake that includes the epileptogenic zone and was shown to be helpful in localisation and lateralisation of the epileptic focus (Willmann *et al.*, 2007). FDG-PET was performed in 6 of our epilepsy patients and showed focal hypometabolism in the presumed epileptogenic zone in five cases and bilateral hypometabolism in one case. Further studies may be needed to directly evaluate the lateralising and localising value of [^{18}F]GE-179 PET in individual patients with epilepsy.

We found relative postsurgical increases of tracer uptake in the contralateral temporal lobe (on voxelwise and regional analysis) and basal ganglia (on regional analysis only)

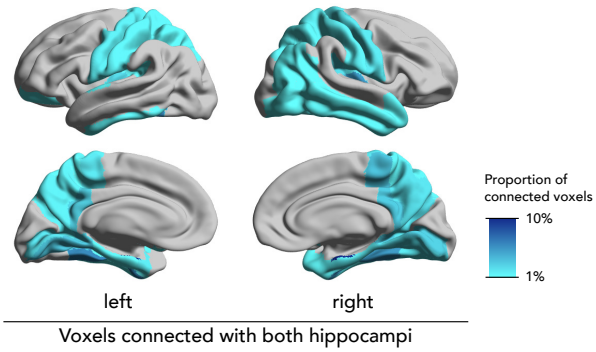

Figure 5.5: *Areas structurally connected with the hippocampus*

The structural connectivity with left and right hippocampi in 10 healthy volunteers is presented as the regional proportion of connected voxels. Reproduced with permission from (Galovic, van Dooren, *et al.*, 2019).

after anterior temporal lobe resections (Figure 5.4). These areas showed reduced tracer uptake in TLE before surgery (Figure 5.3B). Thus, postsurgically increased uptake could reflect normalisation of NMDA receptor activation in the contralateral hemisphere after removal of the ipsilateral epileptogenic zone. This is supported by the observation that postoperative relative V_T in these areas was comparable to that observed in healthy volunteers. Alternatively, it could point to neuronal compensation through increased NMDA receptor activation in the contralateral temporal cortex after removal of ipsilateral temporal lobe.

5.4.3 Effects of antiepileptic drugs

We observed increased NMDA receptor activation, particularly in the ipsilateral temporal lobe and parieto-occipital junction, in patients taking lacosamide (Figure 5.2C). Lacosamide's primary mechanism of action is thought to be the blocking of voltage-gated sodium channels. However, lacosamide is an analogue of the endogenous amino acid and NMDA-receptor modulator D-serine (European Medicines Agency Evaluation of Medicines …, 2008). *In vitro* models did not find

direct binding of lacosamide to NMDA receptors, nor did lacosamide modulate NMDA receptor currents (Errington *et al.*, 2006). On the other hand, lacosamide efficiently prevented NMDA-induced convulsions and reduced mortality in rodents (Stöhr *et al.*, 2007). Thus, lacosamide might modulate NMDA receptor function through a yet unrecognised mechanism that warrants further evaluation.

Patients taking lamotrigine showed a trend for decreased tracer binding, whereas those taking perampanel had a trend for increased tracer binding, but they were not significant in the multivariable model (Table 5.2). Lamotrigine acts as a glutamatergic modulator and attenuates cortical glutamate release and could, in accordance with our observations, cause nonsignificant reductions of NMDA receptor activation (Anand *et al.*, 2000; Farber *et al.*, 2002; C.-Y. Lee *et al.*, 2008; Ramadan *et al.*, 2012; S. J. Wang *et al.*, 1996). Lamotrigine effectively reduced glutamatergic excitotoxicity (Eisen *et al.*, 1993; Tekin *et al.*, 1998). Perampanel does not directly affect NMDA receptor currents. It might, however, lead to increased availability of unbound extracellular glutamate through AMPA receptor antagonism that could indirectly and nonsignificantly activate NMDA receptors (C.-Y. Chen *et al.*, 2014).

5.4.4 Effects of age

We confirmed in this cohort of patients with focal epilepsy that aging is associated with an increased opening probability of NMDA receptors (Figure 5.2A), as previously demonstrated in healthy individuals (detailed discussion in chapter 0). The rate of receptor overactivation per decade in epilepsy patients was more than double that of healthy volunteers, pointing to a higher vulnerability of the epileptic brain to aging. This observation supports previous findings of progressive neurodegeneration on structural neuroimaging (Galovic, van Dooren, *et al.*, 2019). The subcortical areas affected by aging in epilepsy patients (Figure 5.2A) were largely similar to those in healthy volunteers (Figure 4.1). Cortical areas were less likely to show an aging-related

increase in tracer uptake in patients with epilepsy compared to healthy individuals because epilepsy leads to decreased uptake in several cortical areas (Figure 5.3).

5.4.5 Methodical considerations

Several methodical considerations should be noted. Firstly, [^{18}F]GE-179 has demonstrated specificity for the open NMDA ion channel *in vitro* and during recent activation/blocking studies *in vivo* (discussed in more detail in chapter 0). Tracer binding is, however, not selective for any NMDA receptor subunit and, thus, cannot distinguish between heteromeric compositions or synaptic localisations of receptors. Tracer binding reflects receptor opening probability, a compound measure of receptor availability and activation.

Secondly, our findings of reduced tracer uptake in epilepsy patients are unlikely to be explained by grey matter atrophy because the PET signal changes far exceeded reductions of grey matter volume on VBM (Figure 5.3). Additionally, we corrected the PET results for partial volume effects, thus adjusting the PET signal for potential effects of brain atrophy. It is also unlikely that our findings relate to tissue hypoperfusion, because hypoperfusion is usually unilateral and restricted to the epileptogenic zone whereas our findings were bilateral and widespread (Boscolo Galazzo *et al.*, 2015). In addition, V_T estimates obtained using kinetic modelling applied to the PET signal are not dependent on tissue blood perfusion.

Thirdly, we showed large variability of test-retest [^{18}F]GE-179 measurements. Thus, PET studies might be more robust to detect relative focal differences rather than absolute global changes. This might explain why relative focal differences were consistently demonstrated in all epilepsy subgroups (Figure 5.3) and postsurgically (Figure 5.4), but global changes could not be detected compared to healthy volunteers. Additional signal variability might have been introduced by the usage of a venous/image-derived input function in the *UCL* cohort. Thus, analysing PET studies

with high signal variability requires large cohorts for group comparisons and may make comparisons on an individual level difficult and restricted to relative focal rather than absolute global changes. To increase statistical power, we pooled data from three available healthy control cohorts. Scanning equipment did not significantly influence the results (see cohort comparison in chapter 4.3.1) and we adjusted all statistical models for site allocation to further minimise any residual between-cohort effects.

Lastly, a limitation inherent to most epilepsy studies is the possible influence of AED intake in patients compared with controls. However, even when correcting for number of type of AED taken in epilepsy patients we found reduced tracer uptake in cases with longer duration of epilepsy (Figure 5.2), adding support for the finding of reduced tracer uptake in epilepsy patients compared to healthy volunteers.

5.4.6 Conclusions

We observed reduced interictal NMDA receptor activation in patients with chronic refractory focal epilepsy, particularly in those with longer disease duration. These results challenge traditional concepts of NMDA receptor overactivation in chronic epilepsy. In view of this and previous studies, achieving a balanced NMDA receptor activation might be necessary for normal neuronal function, because both increased and reduced activation of NMDA receptors can cause seizures. Such knowledge will have an impact on the development of new antiepileptic drugs targeting NMDA receptors. Further research should address the value of [^{18}F]GE-179 PET as a molecular surrogate marker for monitoring epileptic activity.

6 Project 4: NMDA receptor activation in Anti-NMDA-receptor encephalitis

6.1 Introduction

Anti-NMDA-receptor encephalitis is a recently described autoimmune disorder leading to a syndrome with psychiatric, cognitive, and autonomic dysfunction, seizures, speech abnormalities, movement disorders, and decreased level of consciousness (Dalmau *et al.*, 2007; Graus *et al.*, 2016). Around 80% of cases have a favourable outcome following immunotherapy but relapses may occur in up to a quarter of cases (Gabilondo *et al.*, 2011; Titulaer *et al.*, 2013). The majority of recovered cases report persistent cognitive deficits of variable severity affecting executive functions and memory (Finke *et al.*, 2012).

The disease is mediated by autoantibodies to the GluN1 subunit of the NMDA receptor that cause a crosslinking and internalisation of the receptors (Hughes *et al.*, 2010; Ladépêche *et al.*, 2018; Moscato *et al.*, 2014). *In vitro* and animal experiments showed that the magnitude of reduction in NMDA receptor density is related to antibody titres and the effects are reversible when the antibody titre is reduced (Hughes *et al.*, 2010; Moscato *et al.*, 2014). Similarly, a reduction of NMDA receptor

density was reported *post mortem* in two autopsied patients with anti-NMDA-receptor encephalitis (Dalmau *et al.*, 2007).

It is controversial whether antibody titres in serum and cerebrospinal fluid (CSF) correlate with clinical outcome, as persistently elevated titres were observed in some but not all patients who did not improve clinically (Dalmau *et al.*, 2008; Gresa-Arribas *et al.*, 2014). It remains unknown how to guide the intensity and duration of immunotherapy. In particular, reliable biomarkers for the risk of relapses or long-term outcome after an initial episode of Anti-NMDA-receptor encephalitis are not available and it is unclear how to monitor disease activity in the longer term.

Neuroimaging studies described several abnormalities in patients with Anti-NMDA-receptor encephalitis. Around half of cases show T2 or FLAIR hyperintensities in the hippocampi, cerebellar or cerebral cortex (Dalmau *et al.*, 2007). Volumetry may detect hippocampal atrophy that correlates with disease severity and memory performance (Finke *et al.*, 2016). Patients also show widespread white matter changes, particularly affecting the cingulum, and a reduced connectivity of both hippocampi with the default mode network (Finke *et al.*, 2013). FDG-PET shows a typical pattern of occipital hypometabolism that may be more sensitive than structural MRI (Leypoldt *et al.*, 2012; Probasco *et al.*, 2018). Nevertheless, none of the imaging methods studied so far enabled the direct measurement of NMDA receptor activity *in vivo* in patients with Anti-NMDA-receptor encephalitis.

Here, we used PET with the novel radioligand [^{18}F]GE-179 that binds inside the open, i.e. activated, NMDA ion channel to study five females after discharge from hospital following confirmed Anti-NMDA-receptor encephalitis. We aimed to determine, whether disturbances in NMDA receptor function persist even after improvement of most symptoms and whether they correlate with antibody titres in serum.

6.2 Methods

We followed the methods as described in detail in chapter 2. We screened consecutive patients with Anti-NMDA-receptor encephalitis that were hospitalised or under regular follow-up in two tertiary referral centres in the UK (John Radcliffe University Hospital Oxford and St. George's University Hospital London). We included patients with confirmed disease according to established diagnostic criteria (Graus *et al.*, 2016) who were (i) between 18 and 65 years old, (ii) had minimal or no symptoms and could thus tolerate a 70-minute PET-MR scan, and (iii) did not take any medication that could interfere with NMDA receptors, in particular antipsychotics or antidepressants, permitting immunotherapy and anticonvulsants. The included participants in the "active" group (cases #1-4) had detectable Anti-GluN1 antibodies in serum on day of scanning. We also included one "inactive" participant (case #5) with nondetectable antibodies in serum for comparison.

All patients were scanned at the *UCL* site. Clinical data were retrospectively extracted from medical records according to previously described procedures (Al-Diwani *et al.*, 2019). We calculated the CASE score, a measure of autoimmune encephalitis severity, at discharge (Lim *et al.*, 2019). Cognitive testing with Addenbrooke's Cognitive Examination III (ACE-III) and assessment with Beck's Depression Inventory (BDI) were performed shortly before the scan.

The live cell-based assays for serum Anti-GluN1 titre measurements were done as follows. HEK293T cells were cultured at 37°C in Dulbecco's Modified Eagle Medium (DMEM) supplemented with foetal calf serum and antibacterial/antimycotic solution for 30 hours on glass cover slips, then transfected with plasmid DNA containing GluN1 subunit for 15 hours. Following incubation for a further 24 hours in 1.4 µL/ml ketamine supplemented culture medium sera were tested. Serum, previously thawed to room temperature, was diluted 1:20 with DMEM supplemented with 1% bovine serum albumin and 200mM 4-(2-hydroxyethyl)-1-piperazineethanesulfonic acid (HEPES). 250µL diluted samples were testing alongside positive and negative controls. Samples

Variable	Case #1	Case #2	Case #3	Case #4	Case #5
Age, Sex, Ethnicity	22, F, Asian	36, F, Caribbean	25, F, Caribbean	30, F, European	28, F, European
Data at scan					
GE-179 uptake in GM	7.3	6.6	6.0	4.6	9.7
Serum GluN1-IgG	1:320	1:320	1:160	1:320	Not detectable
Current episode	Relapse	Relapse	First	First	First
Overall number of episodes	3	2	1	1	1
ACE-III	96	95	86	96	96
BDI	16	3	8	6	5
Timing					
Time from discharge to scan *(months)*	2	8	6	8	16
Duration of hospitalization *(months)*	1.5	1.3	10	2.5	2
Time from symptom onset to scan *(months)*	4	12	18	11	19
Time from symptom onset to admission *(days)*	14	21	64	12	25
Treatment					
Current medication	CP, Prednisone, Lorazepam, TMP/SMX, Omeprazole	Levetiracetam, Clonazepam, Ferrous fumarate	Prednisone, Lansoprazole	Levetiracetam	Oral contraceptive
Immunotherapy during hospitalisation	Steroids, PLEX, CP	Steroids, PLEX, CP	Steroids, PLEX, IVIG	Steroids, PLEX	Steroids, PLEX, IVIG, CP
Other treatments during hospitalisation	Antipsychotic, Benzodiazepine	Antipsychotic, Antiepileptic, Benzodiazepine	Antipsychotic, Antiepileptic, Benzodiazepine	Antiepileptic	Antipsychotic, Antiepileptic, Benzodiazepine
Clinical features during hospitalisation					
Hospitalised in	Oxford	Oxford	London	London	Oxford
CASE score at discharge	5	4	5	5	8
Prodrome	Y	Y	Y	Y	Y
Psychiatric	Y	Y	Y	Y	Y
Cognitive	Y	Y	Y	Y	Y
Speech dysfunction	Y	Y	N	Y	Y
Seizures	N	N	Y	Y	Y
Movement disorder	Y	Y	Y	Y	Y
Reduced consciousness	N	N	Y	Y	N
Autonomic	Y	N	N	N	Y
Central hypoventilation	N	N	N	N	N
Ovarian teratoma	N	N	Y	Y	N
Post-HSV encephalitis	N	N	N	N	N
Para-clinical features during hospitalisation					
MRI abnormal	N	N	N	N	Y
EEG abnormal	Y	Y	Y	Y	?
CSF pleocytosis	Y	Y	N	N	Y
CSF lymphocytosis	Y	Y	Y	Y	Y
CSF elevated protein	Y	Y	N	N	Y

Table 6.1: *Characteristics of patients with Anti-NMDA-receptor encephalitis*

Y, Yes/Present; N, No/Absent; ?, unknown; F, female; CM, Grey matter; ACE-III, Addenbrooke's Cognitive Examination III; BDI, Beck's Depression Inventory; CP, Cyclophosphamide, TMP/SMX, Trimethoprim/sulfamethoxazole; PLEX, Plasma exchange; IVIG, Intravenous immunoglobulins; HSV, Herpes simplex virus; MRI, Magnetic resonance imaging; EEG, Electroencephalography; CSF, Cerebrospinal fluid examination.

were incubated with transfected cells for 1 hour at room temperature. The diluted samples were then aspirated, each well was washed 3 times with DMEM-HEPES, each cover slip was then fixed with 4% formaldehyde for 5 minutes and then washed three times with DMEM-HEPES. The cells were then incubated with secondary antibody (Alexa Fluor 594-conugated donkey anti-human IgG Fc-gamma; Jackson 709-585-098) in the dark for 45 minutes. This was aspirated, and each well was washed twice in DMEM-HEPES then twice in PBS. Each coverslip was individually mounted in 4',6-diamidino-2-phenylindole (DAPI)-supplemented mounting medium on a glass slide. Following review of positive and negative control cover slips test samples were read at 40x zoom on a Leica DM2000 fluorescence microscope. Positivity was determined by the presence of a characteristic coronal cell surface deposition of fluorescent reporter antibody on multiple cells. All positive samples were repeated on an independent assay and serially diluted to establish an end-point dilution, the dilution at which the positive signal was still unambiguously present.

We compared these subjects with twenty-nine healthy volunteers from three cohorts (*UCL [n=10]*, *Cambridge [n=10]*, *Hammersmith [n=9]*). The *Cambridge* and *Hammersmith* sites used PET-CT scanners with an arterial input function, whereas the *UCL* site used a PET-MR set-up with a venous/image-derived input function (see chapter 3 for method validation). All participants gave written informed consent according to the Declaration of Helsinki.

We calculated [^{18}F]GE-179 volume of distribution (V_T) estimates in global grey and white matter and in lobar regions of interest. We compared V_T estimates between patients with encephalitis and healthy volunteers using the general linear model adjusting for age, sex, and cohort allocation (i.e. scanning equipment). We report V_T means as estimated marginal means that were adjusted for the effects of age, sex, and cohort allocation. To analyse the subregional distribution of the findings, we fitted the same general linear model on voxelwise V_T estimates. To address the contribution of grey matter atrophy to our findings, we performed voxel-based morphometry (VBM)

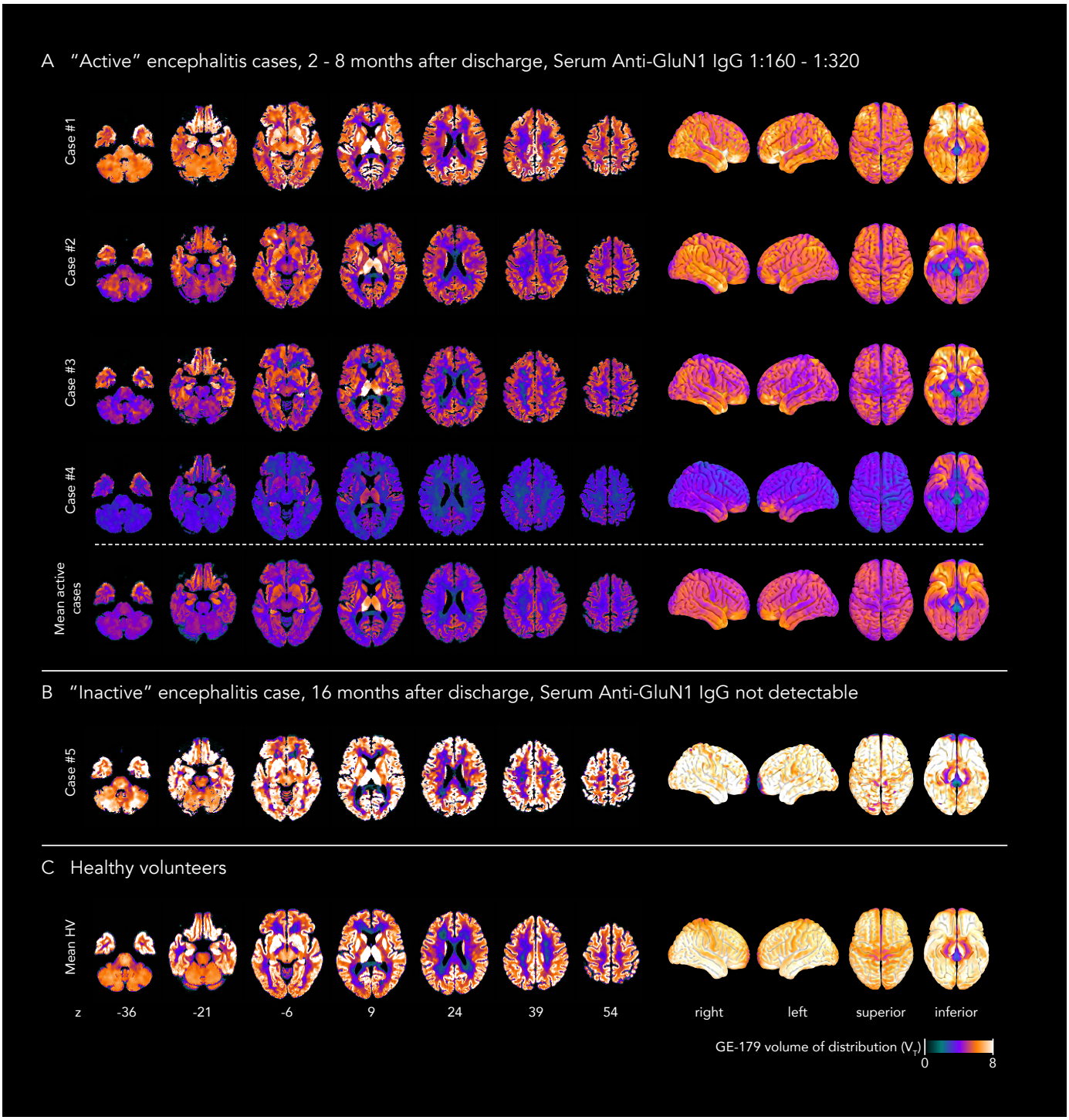

Figure 6.1: *GE-179 uptake in "active" or "nonactive" Anti-NMDA-receptor encephalitis and healthy volunteers.*

The figure shows the spatial distribution of [^{18}F]GE-179 V_T on brain slices and surface projections. **Panel A** displays individual ligand uptake in "active" Anti-NMDA-receptor encephalitis cases (n=4) that were scanned 2-8 months after discharge and had elevated serum Anti-GluN1 antibodies (1:160 – 1:320). The mean brain uptake in these cases is shown below. **Panel B** displays one "nonactive" Anti-NMDA-receptor encephalitis case scanned 16 months after discharge with undetectable Angi-GluN1 antibodies on day of scanning. **Panel C** shows mean uptake in healthy volunteers (n=29).

using segmented and modulated parametric grey matter volume images obtained using the CAT12 toolbox on 3T T1-weighted MRI scans. We report voxelwise p-values at a threshold of $p<0.05$ on a cluster-level family-wise error corrected for multiple comparisons.

6.3 Results

We included four "active" patients (cases #1-4, mean age 28 ± 6 years, all female) with Anti-NMDA-receptor encephalitis, mild or minimal symptoms, and persisting Anti-GluN1 antibodies in serum (titre range 1:160 to 1:320) that were scanned two to eight months after discharge from hospital. For comparison, we included one "inactive" patient (case #5, age 28, female) with undetectable antibodies in serum who was scanned 16 months after discharge from hospital and 29 healthy volunteers (mean age 41 ± 13 years, 8 [28%] female). Patient characteristics are displayed in Table 6.1.

Active cases #1-4 had lower [^{18}F]GE-179 brain uptake compared to the inactive case #5 and to healthy volunteers (Figure 6.1). Active cases had lower [^{18}F]GE-179 V_T in grey matter (estimated marginal mean 6.2 [95% CI 4.4 – 8.0]) compared to healthy volunteers (8.8 [95%CI 8.1 – 9.4], F=6.5, p=0.02) but not in white matter (4.3 [95% CI 2.6 – 6.0] vs. 5.6 [95% CI 5.0 – 6.2], F=2.0, p=0.17), as shown in Figure 6.2A. All female healthy volunteers younger than 40 years had V_T estimates in grey matter above 8 (mean 9.3 [95% CI 6.3-12.3]). Inactive case #5 had similar V_T estimates in grey (9.7) and white (5.8) matter compared to healthy volunteers (Figure 6.1).

The relationship between serum Anti-GluN1 IgG titres and time from discharge from hospital with grey matter V_T is displayed in Figures 6.3A-B. There was little variability in cognitive testing results at time of scanning (ACE-III, range 86 to 96, Figure 6.3C) and symptom severity at discharge (CASE score at discharge, range 4 to 8, Figure 6.3D) because all cases were only minimally affected.

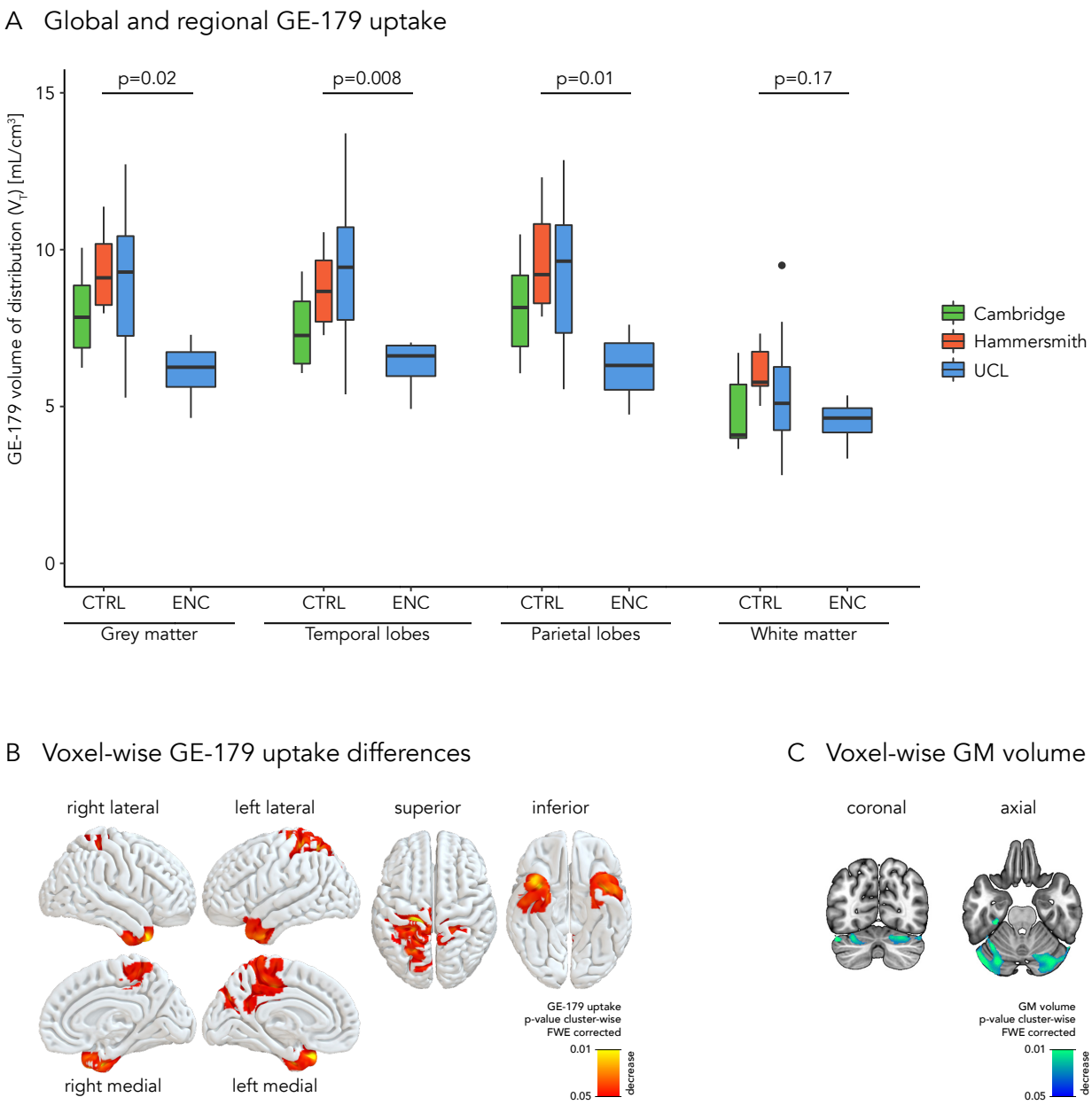

Figure 6.2: *Comparison of GE-179 uptake in antibody-positive Anti-NMDA-receptor encephalitis cases and healthy volunteers.*

Panel A shows boxplots of GE-179 V_T in global grey matter in antibody-positive "active" cases with Anti-NMDA-receptor encephalitis (ENC, n=4) and healthy volunteers (CTRL, n=29, split by cohort). **Panel B** shows voxelwise differences in GE-179 V_T between encephalitis cases and healthy volunteers ($p<0.05$ FWE corrected, red colours indicate decreased uptake in encephalitis cases). **Panel C** displays voxelwise differences in grey matter volume between encephalitis cases and healthy volunteers ($p<0.05$ FWE corrected, blue colours indicate atrophy in encephalitis cases).

On voxelwise analysis (Figure 6.2B), active cases had significantly reduced [^{18}F]GE-179 uptake in bilateral anterior temporal lobes (left, T = 4.5, 1937 voxels, p = 0.02; right, T = 4.9, 1416 voxels, p=0.05) and a large cluster involving bilateral superior parietal lobes, paracentral lobules, left posterior cingulate gyrus, and left precuneus (T = 5.8, 6593 voxels, p < 0.001). Reduced uptake in active cases compared to healthy volunteers was confirmed in the temporal (cases 5.7 [95% CI 3.9 – 7.6] vs. controls 8.6 [95% CI 8.0 – 9.2], F=8.3, p=0.008) and parietal (6.2 [95% CI 4.3 – 8.2] vs. 9.1 [95% CI 8.4 – 9.8], F=7.3, p=0.01) lobes using regional V_T estimates (Figure 6.2A). Reduced grey matter volume on VBM (Figure 6.2C) was observed in both cerebellar hemispheres (left, T = 4.6, 2189 voxels, p = 0.001; right, T = 4.3, 1337 voxels, p = 0.008) and did not overlap with the PET findings.

6.4 Discussion

We report the first use of [^{18}F]GE-179 to measure *in vivo* the activation of NMDA receptors in patients with Anti-NMDA-receptor encephalitis. We demonstrated a reduced opening probability of NMDA receptors, most prominently in the anterior temporal and superior parietal cortices, in a series of patients with detectable Anti-GluN1 antibodies in serum, despite them having only mild or minimal symptoms and being discharged from hospital several months before the scan. In contrast, a clinically recovered patient without detectable Anti-GluN1 antibodies in serum had normal NMDA receptor opening probability.

6.4.1 NMDA receptor hypofunction as a disease mechanism in Anti-NMDA-receptor encephalitis

These results confirm the proposed mechanism of Anti-GluN1 antibodies that was observed *in vitro*, in animal studies and in *post mortem* specimen. The crosslinking

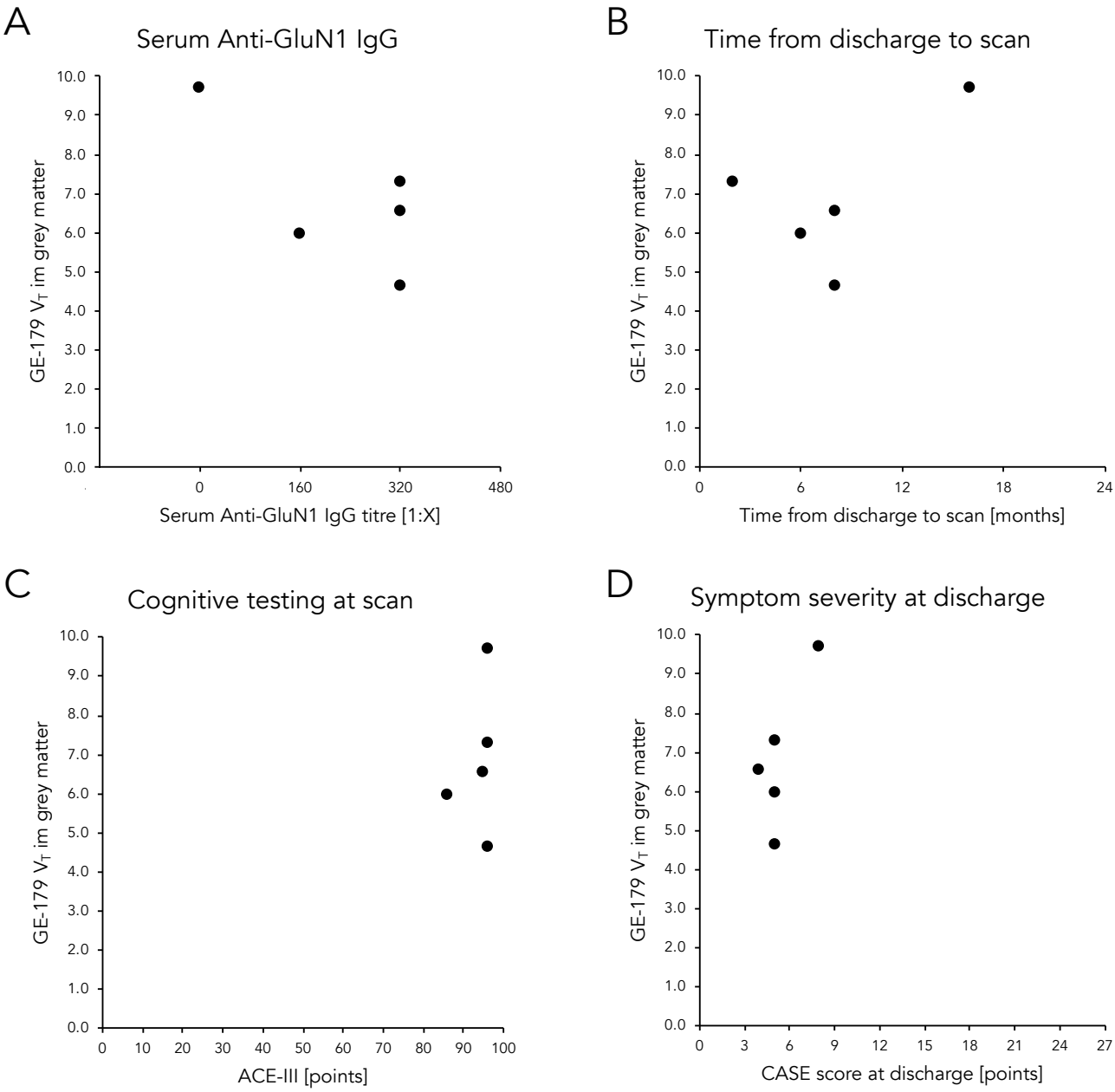

Figure 6.3: *Association of GE-179 uptake in Anti-NMDA-receptor encephalitis cases with clinical variables.*

Scatter plots show the association of GE-179 V_T in Anti-NMDA-receptor encephalitis cases (n=5, "active" and "nonactive" cases) with serum Anti-GluN1 IgG (**panel A**), time from discharge to scan (**panel B**), cognitive testing with ACE-III (**panel C**), and symptom severity at discharge measured with the CASE score (**panel D**).

and internalization of NMDA receptors mediated by these antibodies (Hughes *et al.*, 2010; Ladépêche *et al.*, 2018; Moscato *et al.*, 2014) is in accord with the reduced receptor opening probability observed in our study. The degree of this reduction (mean 30% reduction in "active" patients compared to healthy volunteers) is striking, considering the mild or minimal symptoms in the studied patients and that scanning was performed two to eight months after discharge from hospital. Our results indicate that impaired function of NMDA receptors may persist for months after discharge from hospital despite only minimal symptoms. The human brain may largely compensate for a 30% reduction of NMDA receptor opening probability at rest, thus leading only to mild symptoms.

Persistent Anti-GluN1 antibodies in CSF and serum have been previously observed up to 15 years after disease onset (Alexopoulos *et al.*, 2011; Hansen *et al.*, 2013; Mariotto *et al.*, 2017). It remains controversial whether persistent antibodies have pathogenic effects on the brain. It has been suggested that antibody synthesis might not reflect disease activity (Hansen *et al.*, 2013; Mariotto *et al.*, 2017). Our results may argue against this notion, because we observed a mean 30% reduction of NMDA receptor opening probability in cases with elevated antibody titres in contrast to normal NMDA receptor activation in a case without antibodies in serum. Our results suggest that persistent antibodies may disturb NMDA receptor function in the brain that can be compensated, leading only to minimal symptoms. It has to be noted that two out of four of the patients with antibodies in serum had relapses and three out of four were reducing their anti-inflammatory medication. Thus, it is unclear whether the studied series is representative of the typical population of Anti-NMDA-receptor encephalitis patients. Further studies with [^{18}F]GE-179 will need to assess larger groups of patients at several time points and correlate the PET findings with clinical recovery and antibody titres in CSF and serum.

We could only scan patients who tolerated a 70 minute PET scan and were not taking antipsychotics or antidepressants to prevent confounding our results with movement

artefacts or the effects of medication on NMDA receptors. We did not include cases with severe symptoms or anesthetised patients, because anaesthetics might reduce the baseline activity of NMDA receptors and could bias the results. Nevertheless, we expect that the opening probability of NMDA receptors at the peak of clinical symptoms would be substantially lower compared to the mildly affected cases studied here. Thus, future studies with [^{18}F]GE-179 should assess more severely affected cases. However, such studies would run into the risk of biasing the findings through the action of antipsychotic medication or anaesthetic agents.

6.4.2 NMDA receptor hypofunction and clinical correlates

NMDA receptor hypofunction observed in our study may explain several of the symptoms in Anti-NMDA-receptor encephalitis. NMDA receptors subserve long-term potentiation (Cooke and Bliss, 2006b), a process relevant for memory consolidation. Sustained activation of NMDA receptors is also relevant for persistent neuronal activity that is the basis for storage of working memory (Lisman *et al.*, 1998; M. Wang, Yang, C.-J. Wang, Gamo, Jin, Mazer, Morrison, X.-J. Wang and Arnsten, 2013b; X. J. Wang, 1999). Altered NMDA receptor function would, thus, explain episodic and working memory deficits. Anti-NMDA-receptor encephalitis patients typically show psychiatric features with mixed mood-psychosis symptoms, that may be initially misdiagnosed as a first episode of schizophrenia (Al-Diwani *et al.*, 2019). The administration the NMDA receptor antagonists ketamine and phencyclidine can lead to psychotic symptoms including hallucinations and dissociative experiences (Krystal *et al.*, 1994). They may also induce orofacial and limb dyskinesia, autonomic instability, and seizures (Alldredge *et al.*, 1989; Modica *et al.*, 1990; Weiner *et al.*, 2000). These observations have led to the NMDA receptor hypofunction hypothesis in schizophrenia (Olney, Newcomer and Farber, 1999b) and warrant future PET studies using [^{18}F]GE-179 in patients with psychosis.

Although we observed a global reduction of NMDA receptor activation in patients with Anti-NMDA-receptor encephalitis (Figure 6.1 and 6.2A), the effects were most pronounced in the anterior temporal, superior parietal, and posterior cingulate cortices (Figure 6.2B). The anterior temporal lobe is important for episodic memory (T. M. C. Lee *et al.*, 2002). Both parietal and posterior cingulate cortices were found to be involved in psychosis (Northoff *et al.*, 2005; Yildiz *et al.*, 2011). Electrical stimulation of the superior parietal lobule evoked visual and sensory hallucinations (Balestrini *et al.*, 2015). Thus, altered NMDA receptor function in these areas may correspond to the spectrum of symptoms observed in Anti-NMDA-receptor encephalitis.

Our findings cannot be explained by differences in grey matter volume, because VBM did not detect relevant atrophy outside of the cerebellum and the PET results were corrected for partial volume effects. The findings are also independent of brain perfusion, because V_T estimates are corrected for local and global blood perfusion effects.

It is unclear how to interpret the variability of tracer uptake in "active" cases (Figure 6.1A). This variability could reflect disease activity. Although antibody titres in serum were similar in "active" cases (range 1:160 to 1:320, Figure 6.3A), intrathecal titres might be a better marker of disease activity. However, we could not obtain CSF samples on the day of scanning because of ethical considerations. The degree of cognitive deficits at time of scan (Figure 6.3C), disease severity at discharge (Figure 6.3D) and other clinical parameters (Table 1) were not related to tracer uptake. ACE-III might not be sufficiently sensitive to detect mild deficits that were reported by the patients at time of scanning. Another explanation for the variability observed between "active" patients is the 21.3% coefficient of variation for [^{18}F]GE-179 PET.

6.4.3 Limitations

This study has limitations. Firstly, the sample size in this pilot study was small. However, despite including only four active patients, we found marked and significant reductions of tracer binding compared to healthy volunteers.

Secondly, the age and sex distribution of heathy volunteers differed from patients. The healthy control group was obtained by pooling the majority of data obtained with [^{18}F]GE-179 PET worldwide in order to maximise statistical power. These healthy volunteers were acquired for studies of patients with epilepsy and traumatic brain injury and they infrequently included young female individuals to reduce the potential effects of radiation. Future studies of Anti-NMDA-receptor encephalitis cases will require a dedicated control group. Nevertheless, no healthy females below age 40 in our study had tracer uptake in grey matter below 8, thus making it unlikely that our results can be explained by difference in age or gender alone. Additionally, all analyses were statistically corrected for age, gender, and cohort effects to reduce confounding to a minimum.

Thirdly, data of healthy controls was acquired in several cohorts with different scanner equipment and data acquisition protocols. Small between-cohort differences remained (i.e. lower signal across all regions in the *Cambridge* cohort, Figure 6.2A) and we statistically corrected for these factors in all models. Additionally, Figure 6.2A indicates a lower grey matter V_T in patients vs. controls at the *UCL* site, making it unlikely that the results can be explained by between-cohort differences alone.

Lastly, we could not completely eliminate the effect of medication on scanning but, because substances with potential effects on NMDA receptors were not permitted, the effects are likely to be minor.

6.4.4 Conclusions

To conclude, we observed *in vivo* the reduced activation of NMDA receptors in a series of patients with Anti-NMDA-receptor encephalitis using a novel and minimally invasive imaging approach. If validated in larger and longitudinal studies, this method might be used to track disease activity and response to treatment in Anti-NMDA receptor encephalitis and might generate novel insights into disease mechanisms.

7 Conclusions and outlook

In this thesis, I describe the use of [^{18}F]GE-179 PET to characterize NMDA receptor activation in aging, focal epilepsy, and Anti-NMDA-receptor encephalitis.

NMDA receptors are involved in several physiological neuronal processes and in the disease mechanisms of several neurological and psychiatric disorders (Bordji *et al.*, 2010; Cooke and Bliss, 2006b; Fan and Raymond, 2007; McGinnity *et al.*, 2015; Olney, Newcomer and Farber, 1999a; Rothman and Olney, 1995). The recent development of [^{18}F]GE-179, a radioligand specific to the open, i.e. activated, NMDA receptor is an important step towards understanding of their role in physiological and pathological processes in the human brain. So far, a small number of studies have been reported with this tracer (McGinnity *et al.*, 2014; 2015; Vibholm *et al.*, 2017; Vibholm, Landau, Alstrup, *et al.*, 2020).

I present data from the largest cohort assessed with [^{18}F]GE-179 PET so far. We developed and validated a methodology for kinetic modelling independent of arterial sampling, that may allow a more widespread adoption of this radioligand. We found increased opening probability of NMDA receptors during aging in healthy volunteers and patients with focal epilepsy. Conversely, we observed a reduced NMDA receptor opening probability in adults with focal epilepsy and women with Anti-NMDA-receptor encephalitis. These findings increase our understanding of NMDA receptor function in health and disease and may guide the development of future treatment strategies.

7.1 Methodological considerations

[^{18}F]GE-179 binds specifically to the phencyclidine site inside the NMDA receptor channel (McGinnity *et al.*, 2014). Tracer binding requires the opening of the receptor channel complex. NMDA receptor opening is a complicated process that usually involves binding of an agonist and co-agonist as well as the removal of the Mg^{2+} ion blocking the channel pore (Mori and Mishina, 1995). This typically occurs during simultaneous pre- and postsynaptic activation. In other words, there may far less opening of NMDA receptors at rest than during activation, e.g. during a memory task. NMDA receptor opening may also be subject to the modulatory effects of co-agonists and other receptor types.

Successful blocking experiments were performed *in vivo* for GE-179 in rats following activation of NMDA receptors using electrical stimulation (Vibholm, Landau, Møller, *et al.*, 2020) and for the structural analogues CNS-5161 and GMOM in non-anaesthetised rodents (Biegon *et al.*, 2007; van der Doef *et al.*, 2016), confirming the specificity of the tracer to the phencyclidine site within the open NMDA receptor ion channel. Because anaesthesia is expected to reduce the baseline opening probability of NMDA receptors, blocking experiments in anaesthetized rodents were not successful (Schoenberger *et al.*, 2017). We found reduced [^{18}F]GE-179 uptake in our study of people with Anti-NMDA-receptor antibodies (Project 4). This supports the current hypothesis of receptor internalisation caused by Anti-NMDA-receptor antibodies, as described in animal studies (Hughes *et al.*, 2010; Moscato *et al.*, 2014; Wright *et al.*, 2015), and provides further *in vivo* evidence that GE-179 binding reflects the number of activated NMDA receptors.

These observations are important for the interpretation of [^{18}F]GE-179 binding. Firstly, tracer binding does not reflect the number or overall density of NMDA receptors. It is a use-dependent measure of receptor opening probability, i.e. the number of

activated NMDA receptors. This reflects a compound measure of receptor availability on the cell surface and their opening/activation. Secondly, the phencyclidine site is present on all types of NMDA receptors. Thus, tracer binding is not specific to any receptor subunit composition. The tracer cannot distinguish between synaptic and extrasynaptic receptor localisation. Thirdly, our findings were obtained in subjects while resting inside the scanner and reflect the baseline opening probability of NMDA receptors at rest. Future studies may explore task-specific binding, e.g. during a memory task or during electrographic seizures. NMDA receptor opening probability in these conditions may differ from activation observed during rest.

The adoption of [^{18}F]GE-179 PET in a larger number of studies and in clinical routine depends not only on tracer availability but also on the methodological set up. We simplified kinetic modelling of [^{18}F]GE-179 PET by validating an approach independent of arterial sampling. The method still requires the acquisition and analysis of serial venous samples. Future refinement might involve the use of a simultaneous estimation (SIME) approach that may determine the parent fraction of tracer bound in plasma without the need for blood data (Sari et al., 2018). Widespread clinical use will also require the development of an automated pipeline that does not require manual input, which is currently not feasible due to the requirement to analyse blood data.

Although [^{18}F]GE-179 has relevant shortcomings, particularly considering the high test-retest variability of absolute binding (whereas relative binding had a favourable test-retest performance), there are few viable alternatives. An evaluation of [^{18}F]PK-209, a radioligand for the ion channel binding site of NMDA receptors, did not demonstrate sufficient reliability or specificity (van der Aart *et al.*, 2018). [^{11}C]HACH242 has been evaluated as a radioligand for the GluN2B subunit of NMDA receptor in non-human primates but an evaluation in humans has not yet been performed (van der Aart *et al.*, 2019).

7.2 NMDA receptor activation in aging

We found a higher opening probability of NMDA receptors in grey matter of older individuals. This effect was demonstrated both in a multicentre cohort of healthy volunteers and in a single-centre cohort of patients with refractory focal epilepsy. The annualised rate of increased NMDA receptor activation in people with epilepsy (V_T increase by 1.4 per 10 years) was almost double that of healthy volunteers (V_T increase by 0.8 per 10 years), suggesting that epilepsy may lead to accelerated brain aging (Galovic, van Dooren, *et al.*, 2019). Aging-related NMDA receptor alterations particularly affected areas that may be involved in cognitive processes (Sambataro *et al.*, 2010) and those that are susceptible to tau and amyloid-beta deposits in elderly individuals (Sepulcre *et al.*, 2016).

There are several potential explanations for an increased activation of NMDA receptors in older individuals. It could be related to an altered NMDA receptor subunit composition (Brim *et al.*, 2013; Magnusson, 2000; Magnusson *et al.*, 2002; 2006; Zamzow *et al.*, 2013) or disturbed glutamate homeostasis (Brothers *et al.*, 2013; Farrand *et al.*, 2015; Nickell *et al.*, 2007; Potier *et al.*, 2010; Vatassery *et al.*, 1998). Alternatively, it may reflect functional compensation to maintain cognitive function during aging despite neuronal or ion-channel loss (Billard *et al.*, 1997; Serra *et al.*, 1994).

Further experiments will be required to distinguish between these potential explanations. Gene expression patterns of NMDA receptor subunits and glutamate transporters during aging could address their differential contribution to altered NMDA receptor function. Alternatively, immunohistochemistry in surgical specimen from people with epilepsy or post mortem brain samples could be used to address the expression of NMDA receptor subunits and glutamate transporters. However, these methods cannot directly assess functional alterations of receptors *in vivo*.

A further step in understanding the functional relevance of NMDA receptor alterations is to assess their impact on cognition by acquiring [^{18}F]GE-179 PET data in healthy aging and in neurodegenerative disorders together with cognitive testing. Alzheimer's disease (Bordji *et al.*, 2010) and other neurodegenerative conditions may be related to NMDA receptor dysfunction. Studying people with dementia using [^{18}F]GE-179 PET before and after the administration of memantine, an uncompetitive NMDA receptor antagonist, will be of interest in future.

Lastly, our studies were so far restricted to tracer uptake at rest. Activity of NMDA receptors may, however, be highly susceptible to stimulation during specific tasks. We performed a pilot study of 5 healthy volunteers using a working memory task with simultaneous [^{18}F]GE-179 PET and functional MRI. The results of this project are currently being analysed.

7.3 NMDA receptor activation in epilepsy

We found a lower interictal NMDA receptor opening probability in patients with longer duration of epilepsy. The spatial distribution of decreased tracer uptake formed distinct patterns and differed between temporal and frontal lobe epilepsy. Surgical removal of the epileptic focus in the ipsilateral temporal lobe caused a relative increase in postsurgical tracer uptake in the contralateral temporal lobe and basal ganglia. We also found effects of certain AEDs, lacosamide in particular, on NMDA receptors that merit further study.

Our results argue against traditional models that postulate an increased activation of NMDA receptors in people with epilepsy. Our findings rather support more recent models that suggest that both an increase or decrease in NMDA receptor function may lead to network hyperexcitability. Thus, AEDs should restore the balance of NMDA receptor activity. Use-dependent or uncompetitive antagonists may be particularly promising in this regard. Excessive blocking of NMDA receptors may in

turn exacerbate seizures and cause a number of neuropsychiatric side effects (Sveinbjornsdottir *et al.*, 1993). These observations will be relevant for the development of treatment strategies for epileptic seizures.

In contrast, a previous study from our group in patients with epilepsy and frequent epileptic discharges on EEG showed an increase of tracer binding in a subset of patients. This may relate to an increased release of glutamate during epileptic discharges that may, in turn, activate NMDA receptors.

Future research should focus on the process of epileptogenesis which has been related to NMDA receptor abnormalities in animal studies (McNamara *et al.*, 1988). We will study people at risk of developing epilepsy after ischemic stroke or traumatic brain injury as part of this ongoing project. They will receive a [^{18}F]GE-179 PET scan shortly after the insult and a follow up scan after two years. These ongoing studies may be a first step to develop biomarkers of epileptogenesis and may inform the investigation of antiepileptogenic or disease-modifying treatments.

We also found previously unrecognised effects of certain AEDs on NMDA receptor function. These findings provide support for future Pharmaco-PET studies, that could measure NMDA receptor activation before and after treatment with specific AEDs. Such studies could reveal direct or indirect effects *in vivo* that may be difficult to assess *in vitro*.

The increase of contralateral tracer uptake after unilateral removal of the epileptic focus in the temporal lobe should be studied in a larger cohort. This effect could relate either to compensation, restitution of normal contralateral function, or both. In our small cohort, we did not see a clear effect of post-surgical outcome on tracer binding. A larger study should determine whether postsurgical [^{18}F]GE-179 is a predictor of surgical outcome. In this regard, it also remains to be determined whether [^{18}F]GE-179 PET may qualify as a biomarker of ongoing epileptogenesis or ictogenesis. This would require a properly powered longitudinal study that may be difficult to perform. Nevertheless. such a biomarker would be helpful for treatment

decisions, i.e. starting people on AEDs after a first seizure or withdrawal of AEDs after successful surgery.

7.4 NMDA receptor activation in Anti-NMDA-receptor encephalitis

We found a reduced opening probability of NMDA receptors in patients with detectable Anti-GluN1 antibodies after hospitalisation for Anti-NMDA-receptor encephalitis. The findings were most prominent in anatomical areas associated with cognitive processes and psychosis. One recovered case without detectable antibodies in serum had normal brain tracer uptake.

Our results provide a first *in vivo* human confirmation of the proposed receptor phenomena induced by Anti-GluN1 antibodies. We also observed that a mean 30% reduction of NMDA receptor activation at rest can persist for months after discharge from hospital and may be well compensated, causing only minimal symptoms.

Future studies will need to expand on these findings in larger cohorts of patients with Anti-NMDA-receptor encephalitis by including serum and CSF antibody titres and detailed cognitive testing. Longitudinal scanning may also be helpful to characterise receptor phenomena during the course of the disease and to relate them with response to treatment and the risk of relapses.

It will be of interest to scan patients during their peak clinical symptoms. However, this may prove difficult because more severely affected patients are unlikely to tolerate a long PET scan and the results may be confounded by concomitant medication, e.g. antipsychotics or anaesthetics.

7.5 Overall conclusion

[^{18}F]GE-179 PET provides unprecedented insights into *in vivo* functional alterations of NMDA receptors. It may increase our knowledge on receptor phenomena in health and disease and may generate novel hypothesis for the development of treatment strategies. It could also be used to assess direct or indirect effects of medication on NMDA receptors or to non-invasively monitor disease activity.

Several questions were raised in this thesis that merit further evaluation. The development of entirely computational fully automated and non-invasive methods for the quantification of radioligand binding will be helpful to adopt novel tracers in clinical routine. It should be determined whether the effects of aging on NMDA receptors relate to cognitive decline or promote neurodegeneration and whether they can be mitigated by pharmaceuticals targeting of glutamate transporters or NMDA receptors. The bi-directional role of NMDA receptors in epilepsy may need to be re-evaluated and could lead to novel therapeutic strategies. Lastly, the development of uncompetitive agonists could represent a well-tolerated treatment for a number of disorders with disturbed NMDA receptor function.

8 References

Ahmed I, Bose SK, Pavese N, Ramlackhansingh A, Turkheimer F, Hotton G, et al. Glutamate NMDA receptor dysregulation in Parkinson's disease with dyskinesias. Brain 2011; 134: 979–986.

Al-Diwani A, Handel A, Townsend L, Pollak T, Leite MI, Harrison PJ, et al. The psychopathology of NMDAR-antibody encephalitis in adults: a systematic review and phenotypic analysis of individual patient data. Lancet Psychiatry 2019; 6: 235–246.

Alexopoulos H, Kosmidis ML, Dalmau J, Dalakas MC. Paraneoplastic anti-NMDAR encephalitis: long term follow-up reveals persistent serum antibodies. J Neurol 2011; 258: 1568–1570.

Alldredge BK, Lowenstein DH, Simon RP. Seizures associated with recreational drug abuse. Neurology 1989; 39: 1037–1039.

Amhaoul H, Hamaide J, Bertoglio D, Reichel SN, Verhaeghe J, Geerts E, et al. Brain inflammation in a chronic epilepsy model: Evolving pattern of the translocator protein during epileptogenesis. Neurobiol. Dis. 2015; 82: 526–539.

Anand A, Charney DS, Oren DA, Berman RM, Hu XS, Cappiello A, et al. Attenuation of the neuropsychiatric effects of ketamine with lamotrigine: support for hyperglutamatergic effects of N-methyl-D-aspartate receptor antagonists. Arch. Gen. Psychiatry 2000; 57: 270–276.

Aronica E, Boer K, van Vliet EA, Redeker S, Baayen JC, Spliet WGM, et al. Complement activation in experimental and human temporal lobe epilepsy. Neurobiol. Dis. 2007; 26: 497–511.

Arvanov VL, Wang RY. NMDA-induced response in pyramidal neurons of the rat medial prefrontal cortex slices consists of NMDA and non-NMDA components. Brain Res. 1997; 768: 361–364.

Babb TL, Kupfer WR, Pretorius JK, Crandall PH, Levesque MF. Synaptic reorganization by mossy fibers in human epileptic fascia dentata. Neuroscience 1991; 42: 351–363.

Baldino F, Wolfson B, Heinemann U, Gutnick MJ. An N-methyl-D-aspartate (NMDA) receptor antagonist reduces bicuculline-induced depolarization shifts in neocortical explant cultures. Neurosci Lett 1986; 70: 101–105.

Balestrini S, Francione S, Mai R, Castana L, Casaceli G, Marino D, et al. Multimodal responses induced by cortical stimulation of the parietal lobe: a stereo-electroencephalography study. Brain 2015; 138: 2596–2607.

Bar-Shira O, Maor R, Chechik G. Gene Expression Switching of Receptor Subunits in Human Brain Development. PLoS Comput. Biol. 2015; 11: e1004559.

Barygin OI, Nagaeva EI, Tikhonov DB, Belinskaya DA, Vanchakova NP, Shestakova NN. Inhibition of the NMDA and AMPA receptor channels by antidepressants and antipsychotics. Brain Res. 2017; 1660: 58–66.

Bayer TA, Wiestler OD, Wolf HK. Hippocampal loss of N-methyl-D-aspartate receptor subunit 1 mRNA in chronic temporal lobe epilepsy. Acta Neuropathologica 1995; 89: 446–450.

Beal MF. Excitotoxicity and nitric oxide in Parkinson's disease pathogenesis. Ann. Neurol. 1998; 44: S110–4.

Becker D, Ikenberg B, Schiener S, Maggio N, Vlachos A. NMDA-receptor inhibition restores Protease-Activated Receptor 1 (PAR1) mediated alterations in homeostatic synaptic plasticity of denervated mouse dentate granule cells. Neuropharmacology 2014; 86: 212–218.

Bertoglio D, Verhaeghe J, Santermans E, Amhaoul H, Jonckers E, Wyffels L, et al. Non-invasive PET imaging of brain inflammation at disease onset predicts spontaneous recurrent seizures and reflects comorbidities. Brain Behav. Immun. 2016

Bettinardi V, Presotto L, Rapisarda E, Picchio M, Gianolli L, Gilardi MC. Physical performance of the new hybrid PET/CT Discovery-690. Med Phys 2011; 38: 5394–5411.

Biegon A, Gibbs A, Alvarado M, Ono M, Taylor S. In vitro and in vivo characterization of [3H]CNS-5161--a use-dependent ligand for the N-methyl-D-aspartate receptor in rat brain. Synapse 2007; 61: 577–586.

Billard JM, Jouvenceau A, Lamour Y, Dutar P. NMDA receptor activation in the aged rat: electrophysiological investigations in the CA1 area of the hippocampal slice ex vivo. Neurobiol. Aging 1997; 18: 535–542.

Blumcke I, Beck H, Scheffler B, Hof PR, Morrison JH, Wolf HK, et al. Altered distribution of the alpha-amino-3-hydroxy-5-methyl-4-isoxazole propionate receptor subunit GluR2(4) and the N-methyl-D-aspartate receptor subunit NMDAR1 in the hippocampus of patients with temporal lobe epilepsy. Acta Neuropathologica 1996; 92: 576–587.

Bordji K, Becerril-Ortega J, Nicole O, Buisson A. Activation of extrasynaptic, but not synaptic, NMDA receptors modifies amyloid precursor protein expression pattern and increases amyloid-ß production. J. Neurosci. 2010; 30: 15927–15942.

Borris DJ, Bertram EH, Kapur J. Ketamine controls prolonged status epilepticus. Epilepsy Res 2000; 42: 117–122.

Boscolo Galazzo I, Storti SF, Del Felice A, Pizzini FB, Arcaro C, Formaggio E, et al. Patient-specific detection of cerebral blood flow alterations as assessed by arterial spin labeling in drug-resistant epileptic patients. PLoS ONE 2015; 10: e0123975.

Brandt C, Potschka H, Loscher W, Ebert U. N-methyl-D-aspartate receptor blockade after status epilepticus protects against limbic brain damage but not against epilepsy in the kainate model of temporal lobe epilepsy. Neuroscience 2003; 118: 727–740.

Bressan RA, Erlandsson K, Stone JM, Mulligan RS, Krystal JH, Ell PJ, et al. Impact of schizophrenia and chronic antipsychotic treatment on [123I]CNS-1261 binding to N-methyl-D-aspartate receptors in vivo. BPS 2005; 58: 41–46.

Brett M, Leff AP, Rorden C, Ashburner J. Spatial normalization of brain images with focal lesions using cost function masking. Neuroimage 2001; 14: 486–500.

Brim BL, Haskell R, Awedikian R, Ellinwood NM, Jin L, Kumar A, et al. Memory in aged mice is rescued by enhanced expression of the GluN2B subunit of the NMDA receptor. Behav. Brain Res. 2013; 238: 211–226.

Brines ML, Sundaresan S, Spencer DD, de Lanerolle NC. Quantitative autoradiographic analysis of ionotropic glutamate receptor subtypes in human temporal lobe epilepsy: up-regulation in reorganized epileptogenic hippocampus. Eur. J. Neurosci. 1997; 9: 2035–2044.

Brooks-Kayal AR, Shumate MD, Jin H, Rikhter TY, Coulter DA. Selective changes in single cell GABA(A) receptor subunit expression and function in temporal lobe epilepsy. Nat. Med. 1998; 4: 1166–1172.

Brothers HM, Bardou I, Hopp SC, Kaercher RM, Corona AW, Fenn AM, et al. Riluzole partially rescues age-associated, but not LPS-induced, loss of glutamate transporters and spatial memory. J Neuroimmune Pharmacol 2013; 8: 1098–1105.

Bubeníková-Valešová V, Horáček J, Vrajová M, Höschl C. Models of schizophrenia in humans and animals based on inhibition of NMDA receptors. Neurosci Biobehav Rev 2008; 32: 1014–1023.

Buckingham SC, Campbell SL, Haas BR, Montana V, Robel S, Ogunrinu T, et al. Glutamate release by primary brain tumors induces epileptic activity. Nat. Med. 2011; 17: 1269–1274.

Campbell SL, Buckingham SC, Sontheimer H. Human glioma cells induce hyperexcitability in cortical networks. Epilepsia 2012; 53: 1360–1370.

Cardoso MJ, Modat M, Wolz R, Melbourne A, Cash D, Rueckert D, et al. Geodesic Information Flows: Spatially-Variant Graphs and Their Application to Segmentation and Fusion. IEEE Trans Med Imaging 2015; 34: 1976–1988.

Carvill GL, Regan BM, Yendle SC, O'Roak BJ, Lozovaya N, Bruneau N, et al. GRIN2A mutations cause epilepsy-aphasia spectrum disorders. Nat. Genet. 2013; 45: 1073–1076.

Castorina M, Ambrosini AM, Pacific L, Ramacci MT, Angelucci L. Age-dependent loss of NMDA receptors in hippocampus, striatum, and frontal cortex of the rat: prevention by acetyl-L-carnitine. Neurochem Res 1994; 19: 795–798.

Chang JP-C, Lane H-Y, Tsai GE. Attention deficit hyperactivity disorder and N-methyl-D-aspartate (NMDA) dysregulation. Curr. Pharm. Des. 2014; 20: 5180–5185.

Chatterton JE, Awobuluyi M, Premkumar LS, Takahashi H, Talantova M, Shin Y, et al. Excitatory glycine receptors containing the NR3 family of NMDA receptor subunits. Nature 2002; 415: 793–798.

Chen C-Y, Matt L, Hell JW, Rogawski MA. Perampanel inhibition of AMPA receptor currents in cultured hippocampal neurons. PLoS ONE 2014; 9: e108021.

Chen H, Judkins J, Thomas C, Wu M, Khoury L, Benjamin CG, et al. Mutant IDH1 and seizures in patients with glioma. Neurology 2017; 88: 1805–1813.

Chen L, Muhlhauser M, Yang CR. Glycine tranporter-1 blockade potentiates NMDA-mediated responses in rat prefrontal cortical neurons in vitro and in vivo. J. Neurophysiol. 2003; 89: 691–703.

Chen N, Luo T, Raymond LA. Subtype-dependence of NMDA receptor channel open probability. J. Neurosci. 1999; 19: 6844–6854.

Chohan MO, Iqbal K. From tau to toxicity: emerging roles of NMDA receptor in Alzheimer's disease. J. Alzheimers Dis. 2006; 10: 81–87.

Choi DW, Koh JY, Peters S. Pharmacology of glutamate neurotoxicity in cortical cell culture: attenuation by NMDA antagonists. Journal of Neuroscience 1988; 8: 185–196.

Choi DW. Excitotoxic cell death. J. Neurobiol. 1992; 23: 1261–1276.

Choi DW. Calcium: still center-stage in hypoxic-ischemic neuronal death. Trends Neurosci. 1995; 18: 58–60.

Choi S, Klingauf J, Tsien RW. Fusion pore modulation as a presynaptic mechanism contributing to expression of long-term potentiation. Philos. Trans. R. Soc. Lond., B, Biol. Sci. 2003; 358: 695–705.

Chu K, Jung K-H, Lee S-T, Kim J-H, Kang K-M, Kim H-K, et al. Erythropoietin reduces epileptogenic processes following status epilepticus. Epilepsia 2008; 49: 1723–1732.

Claudet I, Maréchal C. Status epilepticus in a pediatric patient with amantadine overdose. Pediatr. Neurol. 2009; 40: 120–122.

Collingridge GL, Olsen RW, Peters J, Spedding M. A nomenclature for ligand-gated ion channels. Neuropharmacology 2009; 56: 2–5.

Cooke SF, Bliss TVP. Plasticity in the human central nervous system. Brain 2006; 129: 1659–1673.

Cotman CW, Berchtold NC. Exercise: a behavioral intervention to enhance brain health and plasticity. Trends Neurosci. 2002; 25: 295–301.

Crespel A, Coubes P, Rousset M-C, Brana C, Rougier A, Rondouin G, et al. Inflammatory reactions in human medial temporal lobe epilepsy with hippocampal sclerosis. Brain Res. 2002; 952: 159–169.

Croucher MJ, Bradford HF, Sunter DC, Watkins JC. Inhibition of the development of electrical kindling of the prepyriform cortex by daily focal injections of excitatory amino acid antagonists. Eur. J. Pharmacol. 1988; 152: 29–38.

Croucher MJ, Bradford HF. NMDA receptor blockade inhibits glutamate-induced kindling of the rat amygdala. Brain Res. 1990; 506: 349–352.

Croucher MJ, Cotterell KL, Bradford HF. Amygdaloid kindling by repeated focal N-methyl-D-aspartate administration: comparison with electrical kindling. Eur. J. Pharmacol. 1995; 286: 265–271.

D'Esposito M, Detre JA, Alsop DC, Shin RK, Atlas S, Grossman M. The neural basis of the central executive system of working memory. Nature 1995; 378: 279–281.

Dalmau J, Gleichman AJ, Hughes EG, Rossi JE, Peng X, Lai M, et al. Anti-NMDA-receptor encephalitis: case series and analysis of the effects of antibodies. The Lancet Neurology 2008; 7: 1091–1098.

Dalmau J, Tuzun E, Wu H-Y, Masjuan J, Rossi JE, Voloschin A, et al. Paraneoplastic anti-N-methyl-D-aspartate receptor encephalitis associated with ovarian teratoma. Ann. Neurol. 2007; 61: 25–36.

Davis KA, Nanga RPR, Das S, Chen SH, Hadar PN, Pollard JR, et al. Glutamate imaging (GluCEST) lateralizes epileptic foci in nonlesional temporal lobe epilepsy. Sci Transl Med 2015; 7: 309ra161–309ra161.

de Lanerolle NC, Kim JH, Robbins RJ, Spencer DD. Hippocampal interneuron loss and plasticity in human temporal lobe epilepsy. Brain Res. 1989; 495: 387–395.

Del Felice A, Beghi E, Boero G, La Neve A, Bogliun G, De Palo A, et al. Early versus late remission in a cohort of patients with newly diagnosed epilepsy. Epilepsia 2010; 51: 37–42.

DiFiglia M. Excitotoxic injury of the neostriatum: a model for Huntington's disease. Trends Neurosci. 1990; 13: 286–289.

Driesen NR, McCarthy G, Bhagwagar Z, Bloch MH, Calhoun VD, D'Souza DC, et al. The impact of NMDA receptor blockade on human working memory-related prefrontal function and connectivity. Neuropsychopharmacology 2013; 38: 2613–2622.

Dudek FE, Staley KJ. The Time Course and Circuit Mechanisms of Acquired Epileptogenesis. In: Noebels J, Avoli M, Rogawski MA, Olsen RW, Delgado-Escueta AV, editor(s). Jaspers Basic Mechanisms of the Epilepsies. Bethesda (MD): National Center for Biotechnology Information (US); 2012.

Durham RJ, Paudyal N, Carrillo E, Bhatia NK, Maclean DM, Berka V, et al. Conformational spread and dynamics in allostery of NMDA receptors. Proc. Natl. Acad. Sci. U.S.A. 2020; 117: 3839–3847.

During MJ, Spencer DD. Extracellular hippocampal glutamate and spontaneous seizure in the conscious human brain. The Lancet 1993; 341: 1607–1610.

Durstewitz D, Seamans JK, Sejnowski TJ. Neurocomputational models of working memory. Nat. Neurosci. 2000; 3 Suppl: 1184–1191.

Ehrlich I, Malinow R. Postsynaptic density 95 controls AMPA receptor incorporation during long-term potentiation and experience-driven synaptic plasticity. J. Neurosci. 2004; 24: 916–927.

Eisen A, Stewart H, Schulzer M, Cameron D. Anti-glutamate therapy in amyotrophic lateral sclerosis: a trial using lamotrigine. Can J Neurol Sci 1993; 20: 297–301.

Engelhardt von J, Coserea I, Pawlak V, Fuchs EC, Köhr G, Seeburg PH, et al. Excitotoxicity in vitro by NR2A- and NR2B-containing NMDA receptors. Neuropharmacology 2007; 53: 10–17.

Erlandsson K, Buvat I, Pretorius PH, Thomas BA, Hutton BF. A review of partial volume correction techniques for emission tomography and their applications in neurology, cardiology and oncology. Phys Med Biol 2012; 57: R119–59.

Erlandsson K, Dickson J, Arridge S, Atkinson D, Ourselin S, Hutton BF. MR Imaging-Guided Partial Volume Correction of PET Data in PET/MR Imaging. PET Clin 2016; 11: 161–177.

Erlandsson K, Hutton B. A novel voxel-based partial volume correction method for single regions of interest. J Nucl Med 2014; 55: 2123–2123.

Erreger K, Dravid SM, Banke TG, Wyllie DJA, Traynelis SF. Subunit-specific gating controls rat NR1/NR2A and NR1/NR2B NMDA channel kinetics and synaptic signalling profiles. J. Physiol. (Lond.) 2005; 563: 345–358.

Errington AC, Coyne L, Stöhr T, Selve N, Lees G. Seeking a mechanism of action for the novel anticonvulsant lacosamide. Neuropharmacology 2006; 50: 1016–1029.

European Medicines Agency Evaluation of Medicines …. Assessment report for Vimpat. Doc. Ref.: EMEA/460925/2008. 2008.

Fabene PF, Navarro Mora G, Martinello M, Rossi B, Merigo F, Ottoboni L, et al. A role for leukocyte-endothelial adhesion mechanisms in epilepsy. Nat. Med. 2008; 14: 1377–1383.

Fan MMY, Raymond LA. N-methyl-D-aspartate (NMDA) receptor function and excitotoxicity in Huntington's disease. Progress in Neurobiology 2007; 81: 272–293.

Farber NB, Jiang X-P, Heinkel C, Nemmers B. Antiepileptic drugs and agents that inhibit voltage-gated sodium channels prevent NMDA antagonist neurotoxicity. Mol. Psychiatry 2002; 7: 726–733.

Farrand AQ, Gregory RA, Scofield MD, Helke KL, Boger HA. Effects of aging on glutamate neurotransmission in the substantia nigra of Gdnf heterozygous mice. Neurobiol. Aging 2015; 36: 1569–1576.

Felbamate Study Group in Lennox-Gastaut Syndrome. Efficacy of felbamate in childhood epileptic encephalopathy (Lennox-Gastaut syndrome). N Engl J Med 1993; 328: 29–33.

Feng D, Huang SC, Wang X. Models for computer simulation studies of input functions for tracer kinetic modeling with positron emission tomography. Int. J. Biomed. Comput. 1993; 32: 95–110.

Feng D, Wong KP, Wu CM, Siu WC. A technique for extracting physiological parameters and the required input function simultaneously from PET image measurements: theory and simulation study. IEEE Trans Inf Technol Biomed 1997; 1: 243–254.

Ferreira IL, Ferreiro E, Schmidt J, Cardoso JM, Pereira CMF, Carvalho AL, et al. Aβ and NMDAR activation cause mitochondrial dysfunction involving ER calcium release. Neurobiol. Aging 2015; 36: 680–692.

Ferrer-Montiel AV, Merino JM, Blondelle SE, Perez-Payà E, Houghten RA, Montal M. Selected peptides targeted to the NMDA receptor channel protect neurons from excitotoxic death. Nat. Biotechnol. 1998; 16: 286–291.

Finke C, Kopp UA, Pajkert A, Behrens JR, Leypoldt F, Wuerfel JT, et al. Structural Hippocampal Damage Following Anti-N-Methyl-D-Aspartate Receptor Encephalitis. Biol. Psychiatry 2016; 79: 727–734.

Finke C, Kopp UA, Prüss H, Dalmau J, Wandinger K-P, Ploner CJ. Cognitive deficits following anti-NMDA receptor encephalitis. J Neurol Neurosurg Psychiatr 2012; 83: 195–198.

Finke C, Kopp UA, Scheel M, Pech L-M, Soemmer C, Schlichting J, et al. Functional and structural brain changes in anti-N-methyl-D-aspartate receptor encephalitis. Ann. Neurol. 2013; 74: 284–296.

Fisher RS, Acevedo C, Arzimanoglou A, Bogacz A, Cross JH, Elger CE, et al. ILAE official report: a practical clinical definition of epilepsy. Epilepsia 2014; 55: 475–482.

Fisher RS, Van Emde Boas W, Blume W, Elger C, Genton P, Lee P, et al. Epileptic seizures and epilepsy: definitions proposed by the International League Against Epilepsy (ILAE) and the International Bureau for Epilepsy (IBE). Epilepsia 2005; 46: 470–472.

Fitzgerald PJ. The NMDA receptor may participate in widespread suppression of circuit level neural activity, in addition to a similarly prominent role in circuit level activation. Behav. Brain Res. 2012; 230: 291–298.

Fontana R, Agostini M, Murana E, Mahmud M, Scremin E, Rubega M, et al. Early hippocampal hyperexcitability in PS2APP mice: role of mutant PS2 and APP. Neurobiol. Aging 2017; 50: 64–76.

Forst T, Smith T, Schütte K, Marcus P, Pfützner A, CNS 5161 Study Group. Dose escalating safety study of CNS 5161 HCl, a new neuronal glutamate receptor antagonist (NMDA) for the treatment of neuropathic pain. Br J Clin Pharmacol 2007; 64: 75–82.

Fujikawa DG, Daniels AH, Kim JS. The competitive NMDA receptor antagonist CGP 40116 protects against status epilepticus-induced neuronal damage. Epilepsy Res 1994; 17: 207–219.

Funahashi S, Bruce CJ, Goldman-Rakic PS. Mnemonic coding of visual space in the monkey's dorsolateral prefrontal cortex. J. Neurophysiol. 1989; 61: 331–349.

Gabilondo I, Saiz A, Galán L, González V, Jadraque R, Sabater L, et al. Analysis of relapses in anti-NMDAR encephalitis. Neurology 2011; 77: 996–999.

Galovic M, Baudracco I, Wright-Goff E, Pillajo G, Nachev P, Wandschneider B, et al. Association of Piriform Cortex Resection With Surgical Outcomes in Patients With Temporal Lobe Epilepsy. JAMA Neurol 2019; 76: 690–700.

Galovic M, Koepp M. Advances of Molecular Imaging in Epilepsy. Curr Neurol Neurosci Rep 2016; 16: 58.

Galovic M, van Dooren VQH, Postma T, Vos SB, Caciagli L, Borzì G, et al. Progressive Cortical Thinning in Patients With Focal Epilepsy. JAMA Neurol 2019; 76: 1230-1239.

Gascón S, Deogracias R, Sobrado M, Roda JM, Renart J, Rodríguez-Peña A, et al. Transcription of the NR1 subunit of the N-methyl-D-aspartate receptor is down-regulated by excitotoxic stimulation and cerebral ischemia. J. Biol. Chem. 2005; 280: 35018–35027.

Geddes JW, Cahan LD, Cooper SM, Kim RC, Choi BH, Cotman CW. Altered distribution of excitatory amino acid receptors in temporal lobe epilepsy. Experimental Neurology 1990; 108: 214–220.

Ghasemi M, Schachter SC. The NMDA receptor complex as a therapeutic target in epilepsy: a review. Epilepsy & Behavior 2011; 22: 617–640.

Giannakopoulos P, Herrmann FR, Bussière T, Bouras C, Kövari E, Perl DP, et al. Tangle and neuron numbers, but not amyloid load, predict cognitive status in Alzheimer's disease. Neurology 2003; 60: 1495–1500.

Gilbert ME. The NMDA-receptor antagonist, MK-801, suppresses limbic kindling and kindled seizures. Brain Res. 1988; 463: 90–99.

Goate A, Chartier-Harlin MC, Mullan M, Brown J, Crawford F, Fidani L, et al. Segregation of a missense mutation in the amyloid precursor protein gene with familial Alzheimer's disease. Nature 1991; 349: 704–706.

Goodkin HP, Yeh J-L, Kapur J. Status epilepticus increases the intracellular accumulation of GABAA receptors. J. Neurosci. 2005; 25: 5511–5520.

Graus F, Titulaer MJ, Balu R, Benseler S, Bien CG, Cellucci T, et al. A clinical approach to diagnosis of autoimmune encephalitis. The Lancet Neurology 2016; 15: 391–404.

Gray JA, Shi Y, Usui H, During MJ, Sakimura K, Nicoll RA. Distinct modes of AMPA receptor suppression at developing synapses by GluN2A and GluN2B: single-cell NMDA receptor subunit deletion in vivo. Neuron 2011; 71: 1085–1101.

Gresa-Arribas N, Titulaer MJ, Torrents A, Aguilar E, McCracken L, Leypoldt F, et al. Antibody titres at diagnosis and during follow-up of anti-NMDA receptor encephalitis: a retrospective study. The Lancet Neurology 2014; 13: 167–177.

Greuter H, Lubberink M, Hendrikse NH, van der Veldt A, Wong Y, Schuit R, et al. Venous versus arterial blood samples for plasma input pharmacokinetic analysis of different radiotracer PET studies. J Nucl Med 2011; 52: 1974–1974.

Grunze HC, Rainnie DG, Hasselmo ME, Barkai E, Hearn EF, McCarley RW, et al. NMDA-dependent modulation of CA1 local circuit inhibition. Journal of Neuroscience 1996; 16: 2034–2043.

Gunn RN, Sargent PA, Bench CJ, Rabiner EA, Osman S, Pike VW, et al. Tracer kinetic modeling of the 5-HT1A receptor ligand [carbonyl-11C]WAY-100635 for PET. Neuroimage 1998; 8: 426–440.

Gunn RN, Slifstein M, Searle GE, Price JC. Quantitative imaging of protein targets in the human brain with PET. Phys Med Biol 2015; 60: R363–411.

Haberman RP, Branch A, Gallagher M. Targeting Neural Hyperactivity as a Treatment to Stem Progression of Late-Onset Alzheimer's Disease. Neurotherapeutics 2017; 14: 662–676.

Hall BJ, Ripley B, Ghosh A. NR2B Signaling Regulates the Development of Synaptic AMPA Receptor Current. Journal of Neuroscience 2007; 27: 13446–13456.

Hansen H-C, Klingbeil C, Dalmau J, Li W, Weißbrich B, Wandinger K-P. Persistent intrathecal antibody synthesis 15 years after recovering from anti-N-methyl-D-aspartate receptor encephalitis. JAMA Neurol 2013; 70: 117–119.

Hardingham GE, Bading H. Synaptic versus extrasynaptic NMDA receptor signalling: implications for neurodegenerative disorders. Nat. Rev. Neurosci. 2010; 11: 682–696.

Hardy J, Selkoe DJ. The amyloid hypothesis of Alzheimer's disease: progress and problems on the road to therapeutics. Science 2002; 297: 353–356.

Helms G, Ciumas C, Kyaga S, Savic I. Increased thalamus levels of glutamate and glutamine (Glx) in patients with idiopathic generalised epilepsy. J Neurol Neurosurg Psychiatr 2006; 77: 489–494.

Hesdorffer DC, Benn EKT, Cascino GD, Hauser WA. Is a first acute symptomatic seizure epilepsy? Mortality and risk for recurrent seizure. Epilepsia 2009; 50: 1102–1108.

Hirsch JC, Crepel F. Blockade of NMDA receptors unmasks a long-term depression in synaptic efficacy in rat prefrontal neurons in vitro. Exp Brain Res 1991; 85: 621–624.

Hoey SE, Williams RJ, Perkinton MS. Synaptic NMDA receptor activation stimulates alpha-secretase amyloid precursor protein processing and inhibits amyloid-beta production. J. Neurosci. 2009; 29: 4442–4460.

Homayoun H, Moghaddam B. NMDA receptor hypofunction produces opposite effects on prefrontal cortex interneurons and pyramidal neurons. J. Neurosci. 2007; 27: 11496–11500.

Honey RAE, Honey GD, O'Loughlin C, Sharar SR, Kumaran D, Bullmore ET, et al. Acute ketamine administration alters the brain responses to executive demands in a verbal working memory task: an FMRI study. Neuropsychopharmacology 2004; 29: 1203–1214.

Hosford DA, Crain BJ, Cao Z, Bonhaus DW, Friedman AH, Okazaki MM, et al. Increased AMPA-sensitive quisqualate receptor binding and reduced NMDA receptor binding in epileptic human hippocampus. Journal of Neuroscience 1991; 11: 428–434.

Höflich A, Hahn A, Küblböck M, Kranz GS, Vanicek T, Ganger S, et al. Ketamine-dependent neuronal activation in healthy volunteers. Brain Struct Funct 2017; 222: 1533–1542.

Hsia AY, Masliah E, McConlogue L, Yu GQ, Tatsuno G, Hu K, et al. Plaque-independent disruption of neural circuits in Alzheimer's disease mouse models. Proc. Natl. Acad. Sci. U.S.A. 1999; 96: 3228–3233.

Huang X, Zhang H, Yang J, Wu J, McMahon J, Lin Y, et al. Pharmacological inhibition of the mammalian target of rapamycin pathway suppresses acquired epilepsy. Neurobiol. Dis. 2010; 40: 193–199.

Huberfeld G, Wittner L, Clemenceau S, Baulac M, Kaila K, Miles R, et al. Perturbed chloride homeostasis and GABAergic signaling in human temporal lobe epilepsy. J. Neurosci. 2007; 27: 9866–9873.

Hughes EG, Peng X, Gleichman AJ, Lai M, Zhou L, Tsou R, et al. Cellular and synaptic mechanisms of anti-NMDA receptor encephalitis. J. Neurosci. 2010; 30: 5866–5875.

Ikonomidou C, Turski L. Why did NMDA receptor antagonists fail clinical trials for stroke and traumatic brain injury? The Lancet Neurology 2002; 1: 383–386.

Irizarry MC, Soriano F, McNamara M, Page KJ, Schenk D, Games D, et al. Abeta deposition is associated with neuropil changes, but not with overt neuronal loss in the human amyloid precursor protein V717F (PDAPP) transgenic mouse. Journal of Neuroscience 1997; 17: 7053–7059.

Jack CR, Barrio JR, Kepe V. Cerebral amyloid PET imaging in Alzheimer's disease. Acta Neuropathologica 2013; 126: 643–657.

Jack CR, Knopman DS, Jagust WJ, Shaw LM, Aisen PS, Weiner MW, et al. Hypothetical model of dynamic biomarkers of the Alzheimer's pathological cascade. The Lancet Neurology 2010; 9: 119–128.

Jackson ME, Homayoun H, Moghaddam B. NMDA receptor hypofunction produces concomitant firing rate potentiation and burst activity reduction in the prefrontal cortex. Proc Natl Acad Sci USA 2004; 101: 8467–8472.

Jacob CP, Koutsilieri E, Bartl J, Neuen-Jacob E, Arzberger T, Zander N, et al. Alterations in expression of glutamatergic transporters and receptors in sporadic Alzheimer's disease. J. Alzheimers Dis. 2007; 11: 97–116.

Jansen KL, Faull RL, Dragunow M, Synek BL. Alzheimer's disease: changes in hippocampal N-methyl-D-aspartate, quisqualate, neurotensin, adenosine, benzodiazepine, serotonin and opioid receptors--an autoradiographic study. Neuroscience 1990; 39: 613–627.

Jantzie LL, Talos DM, Jackson MC, Park H-K, Graham DA, Lechpammer M, et al. Developmental expression of N-methyl-D-aspartate (NMDA) receptor subunits in human white and gray matter: potential mechanism of increased vulnerability in the immature brain. Cereb. Cortex 2015; 25: 482–495.

Jasek MC, Griffith WH. Pharmacological characterization of ionotropic excitatory amino acid receptors in young and aged rat basal forebrain. Neuroscience 1998; 82: 1179–1194.

Jodas DS, Pereira AS, R S Tavares JM. Lumen segmentation in magnetic resonance images of the carotid artery. Comput. Biol. Med. 2016; 79: 233–242.

Joshi A, Koeppe RA, Fessler JA. Reducing between scanner differences in multi-center PET studies. Neuroimage 2009; 46: 154–159.

Kadam SD, White AM, Staley KJ, Dudek FE. Continuous electroencephalographic monitoring with radio-telemetry in a rat model of perinatal hypoxia-ischemia reveals progressive post-stroke epilepsy. J. Neurosci. 2010; 30: 404–415.

Kaiser LG, Schuff N, Cashdollar N, Weiner MW. Age-related glutamate and glutamine concentration changes in normal human brain: 1H MR spectroscopy study at 4 T. Neurobiol. Aging 2005; 26: 665–672.

Kalia LV, Kalia SK, Salter MW. NMDA receptors in clinical neurology: excitatory times ahead. The Lancet Neurology 2008; 7: 742–755.

Kamenetz F, Tomita T, Hsieh H, Seabrook G, Borchelt D, Iwatsubo T, et al. APP processing and synaptic function. Neuron 2003; 37: 925–937.

Káradóttir R, Cavelier P, Bergersen LH, Attwell D. NMDA receptors are expressed in oligodendrocytes and activated in ischaemia. Nature 2005; 438: 1162–1166.

Kobayashi M, Buckmaster PS. Reduced inhibition of dentate granule cells in a model of temporal lobe epilepsy. J. Neurosci. 2003; 23: 2440–2452.

Kornhuber J, Retz W, Riederer P, Heinsen H, Fritze J. Effect of antemortem and postmortem factors on [3H]glutamate binding in the human brain. Neurosci Lett 1988; 93: 312–317.

Kovács Z, Kékesi KA, Szilágyi N, Ábrahám I, Székács D, Király N, et al. Facilitation of spike-wave discharge activity by lipopolysaccharides in Wistar Albino Glaxo/Rijswijk rats. Neuroscience 2006; 140: 731–742.

Kraguljac NV, Frölich MA, Tran S, White DM, Nichols N, Barton-McArdle A, et al. Ketamine modulates hippocampal neurochemistry and functional connectivity: a combined magnetic resonance spectroscopy and resting-state fMRI study in healthy volunteers. Mol. Psychiatry 2017; 22: 562–569.

Kravitz E, Gaisler-Salomon I, Biegon A. Hippocampal glutamate NMDA receptor loss tracks progression in Alzheimer's disease: quantitative autoradiography in postmortem human brain. PLoS ONE 2013; 8: e81244.

Krämer SD, Betzel T, Mu L, Haider A, Herde AM, Boninsegni AK, et al. Evaluation of 11C-Me-NB1 as a Potential PET Radioligand for Measuring GluN2B-Containing NMDA Receptors, Drug Occupancy, and Receptor Cross Talk. J Nucl Med 2018; 59: 698–703.

Krystal JH, Karper LP, Seibyl JP, Freeman GK, Delaney R, Bremner JD, et al. Subanesthetic effects of the noncompetitive NMDA antagonist, ketamine, in humans. Psychotomimetic, perceptual, cognitive, and neuroendocrine responses. Arch. Gen. Psychiatry 1994; 51: 199–214.

Krzystanek M, Pałasz A. NMDA Receptor Model of Antipsychotic Drug-Induced Hypofrontality. Int J Mol Sci 2019; 20: 1442.

Kuehl-Kovarik MC, Magnusson KR, Premkumar LS, Partin KM. Electrophysiological analysis of NMDA receptor subunit changes in the aging mouse cortex. Mech. Ageing Dev. 2000; 115: 39–59.

Kumar A. NMDA Receptor Function During Senescence: Implication on Cognitive Performance. Front Neurosci 2015; 9: 473.

Kumlien E, Hartvig P, Valind S, Oye I, Tedroff J, Långström B. NMDA-receptor activity visualized with (S)-[N-methyl-11C]ketamine and positron emission tomography in patients with medial temporal lobe epilepsy. Epilepsia 1999; 40: 30–37.

Kuryatov A, Laube B, Betz H, Kuhse J. Mutational analysis of the glycine-binding site of the NMDA receptor: structural similarity with bacterial amino acid-binding proteins. Neuron 1994; 12: 1291–1300.

Ladépêche L, Planagumà J, Thakur S, Suárez I, Hara M, Borbely JS, et al. NMDA Receptor Autoantibodies in Autoimmune Encephalitis Cause a Subunit-Specific Nanoscale Redistribution of NMDA Receptors. Cell Rep 2018; 23: 3759–3768.

Lahti AC, Holcomb HH, Medoff DR, Tamminga CA. Ketamine activates psychosis and alters limbic blood flow in schizophrenia. Neuroreport 1995; 6: 869–872.

Lange F, Weßlau K, Porath K, Hörnschemeyer J, Bergner C, Krause BJ, et al. AMPA receptor antagonist perampanel affects glioblastoma cell growth and glutamate release in vitro. PLoS ONE 2019; 14: e0211644.

Law AJ, Weickert CS, Webster MJ, Herman MM, Kleinman JE, Harrison PJ. Expression of NMDA receptor NR1, NR2A and NR2B subunit mRNAs during development of the human hippocampal formation. Eur. J. Neurosci. 2003; 18: 1197–1205.

Le DA, Lipton SA. Potential and current use of N-methyl-D-aspartate (NMDA) receptor antagonists in diseases of aging. Drugs Aging 2001; 18: 717–724.

Lee C-Y, Fu W-M, Chen C-C, Su M-J, Liou H-H. Lamotrigine inhibits postsynaptic AMPA receptor and glutamate release in the dentate gyrus. Epilepsia 2008; 49: 888–897.

Lee TMC, Yip JTH, Jones-Gotman M. Memory deficits after resection from left or right anterior temporal lobe in humans: a meta-analytic review. Epilepsia 2002; 43: 283–291.

Lee WL, Hablitz JJ. Involvement of non-NMDA receptors in picrotoxin-induced epileptiform activity in the hippocampus. Neurosci Lett 1989; 107: 129–134.

Lemke JR, Lal D, Reinthaler EM, Steiner I, Nothnagel M, Alber M, et al. Mutations in GRIN2A cause idiopathic focal epilepsy with rolandic spikes. Nat. Genet. 2013; 45: 1067–1072.

Lesca G, Rudolf G, Bruneau N, Lozovaya N, Labalme A, Boutry-Kryza N, et al. GRIN2A mutations in acquired epileptic aphasia and related childhood focal epilepsies and encephalopathies with speech and language dysfunction. Nat. Genet. 2013; 45: 1061–1066.

Lesné S, Ali C, Gabriel C, Croci N, MacKenzie ET, Glabe CG, et al. NMDA receptor activation inhibits alpha-secretase and promotes neuronal amyloid-beta production. J. Neurosci. 2005; 25: 9367–9377.

Leypoldt F, Buchert R, Kleiter I, Marienhagen J, Gelderblom M, Magnus T, et al. Fluorodeoxyglucose positron emission tomography in anti-N-methyl-D-aspartate receptor encephalitis: distinct pattern of disease. J Neurol Neurosurg Psychiatr 2012; 83: 681–686.

Li S, Jin M, Koeglsperger T, Shepardson NE, Shankar GM, Selkoe DJ. Soluble Aβ oligomers inhibit long-term potentiation through a mechanism involving excessive activation of extrasynaptic NR2B-containing NMDA receptors. J. Neurosci. 2011; 31: 6627–6638.

Lim J-A, Lee S-T, Moon J, Jun J-S, Kim T-J, Shin Y-W, et al. Development of the clinical assessment scale in autoimmune encephalitis. Ann. Neurol. 2019; 85: 352–358.

Lipton SA. Paradigm shift in neuroprotection by NMDA receptor blockade: memantine and beyond. Nat Rev Drug Discov 2006; 5: 160–170.

Lisman JE, Fellous JM, Wang XJ. A role for NMDA-receptor channels in working memory. Nat. Neurosci. 1998; 1: 273–275.

Lissin DV, Gomperts SN, Carroll RC, Christine CW, Kalman D, Kitamura M, et al. Activity differentially regulates the surface expression of synaptic AMPA and NMDA glutamate receptors. Proc Natl Acad Sci USA 1998; 95: 7097–7102.

Liu L, Wong TP, Pozza MF, Lingenhoehl K, Wang Y, Sheng M, et al. Role of NMDA receptor subtypes in governing the direction of hippocampal synaptic plasticity. Science 2004; 304: 1021–1024.

Liu S, Ruenes GL, Yezierski RP. NMDA and non-NMDA receptor antagonists protect against excitotoxic injury in the rat spinal cord. Brain Res. 1997; 756: 160–167.

Liu S-J, Zheng P, Wright DK, Dezsi G, Braine E, Nguyen T, et al. Sodium selenate retards epileptogenesis in acquired epilepsy models reversing changes in protein phosphatase 2A and hyperphosphorylated tau. Brain 2016; 139: 1919–1938.

Liu Y, Wong TP, Aarts M, Rooyakkers A, Liu L, Lai TW, et al. NMDA receptor subunits have differential roles in mediating excitotoxic neuronal death both in vitro and in vivo. J. Neurosci. 2007; 27: 2846–2857.

Logan J, Fowler JS, Volkow ND, Wolf AP, Dewey SL, Schlyer DJ, et al. Graphical analysis of reversible radioligand binding from time-activity measurements applied to [N-11C-methyl]-(-)-cocaine PET studies in human subjects. J. Cereb. Blood Flow Metab. 1990; 10: 740–747.

Loup F, Wieser HG, Yonekawa Y, Aguzzi A, Fritschy JM. Selective alterations in GABAA receptor subtypes in human temporal lobe epilepsy. Journal of Neuroscience 2000; 20: 5401–5419.

Löscher W, Hirsch LJ, Schmidt D. The enigma of the latent period in the development of symptomatic acquired epilepsy - Traditional view versus new concepts. Epilepsy Behav 2015; 52: 78–92.

Magnusson KR, Brim BL, Das SR. Selective Vulnerabilities of N-methyl-D-aspartate (NMDA) Receptors During Brain Aging. Front Aging Neurosci 2010; 2: 11.

Magnusson KR, Cotman CW. Effects of aging on NMDA and MK801 binding sites in mice. Brain Res. 1993; 604: 334–337.

Magnusson KR, Kresge D, Supon J. Differential effects of aging on NMDA receptors in the intermediate versus the dorsal hippocampus. Neurobiol. Aging 2006; 27: 324–333.

Magnusson KR, Nelson SE, Young AB. Age-related changes in the protein expression of subunits of the NMDA receptor. Brain Res. Mol. Brain Res. 2002; 99: 40–45.

Magnusson KR, Scruggs B, Zhao X, Hammersmark R. Age-related declines in a two-day reference memory task are associated with changes in NMDA receptor subunits in mice. BMC Neurosci 2007; 8: 43.

Magnusson KR. Declines in mRNA expression of different subunits may account for differential effects of aging on agonist and antagonist binding to the NMDA receptor. J. Neurosci. 2000; 20: 1666–1674.

Manzoni OJ, Manabe T, Nicoll RA. Release of adenosine by activation of NMDA receptors in the hippocampus. Science 1994; 265: 2098–2101.

Mariotto S, Andreetta F, Farinazzo A, Monaco S, Ferrari S. Persistence of anti-NMDAR antibodies in CSF after recovery from autoimmune encephalitis. Neurol Sci 2017; 38: 1523–1524.

Martinussen R, Hayden J, Hogg-Johnson S, Tannock R. A meta-analysis of working memory impairments in children with attention-deficit/hyperactivity disorder. J Am Acad Child Adolesc Psychiatry 2005; 44: 377–384.

Maschio M, Pauletto G, Zarabla A, Maialetti A, Ius T, Villani V, et al. Perampanel in patients with brain tumor-related epilepsy in real-life clinical practice: a retrospective analysis. Int. J. Neurosci. 2019; 129: 593–597.

Maschio M, Zarabla A, Maialetti A, Giannarelli D, Koudriavtseva T, Villani V, et al. Perampanel in brain tumor-related epilepsy: Observational pilot study. Brain Behav 2020: e01612.

Massey PV, Johnson BE, Moult PR, Auberson YP, Brown MW, Molnar E, et al. Differential roles of NR2A and NR2B-containing NMDA receptors in cortical long-term potentiation and long-term depression. J. Neurosci. 2004; 24: 7821–7828.

Masters CL, Simms G, Weinman NA, Multhaup G, McDonald BL, Beyreuther K. Amyloid plaque core protein in Alzheimer disease and Down syndrome. Proc. Natl. Acad. Sci. U.S.A. 1985; 82: 4245–4249.

Mathern GW, Pretorius JK, Kornblum HI, Mendoza D, Lozada A, Leite JP, et al. Human hippocampal AMPA and NMDA mRNA levels in temporal lobe epilepsy patients. Brain 1997; 120 (Pt 11): 1937–1959.

Mathern GW, Pretorius JK, Leite JP, Kornblum HI, Mendoza D, Lozada A, et al. Hippocampal AMPA and NMDA mRNA levels and subunit immunoreactivity in human temporal lobe epilepsy patients and a rodent model of chronic mesial limbic epilepsy. Epilepsy Res 1998; 32: 154–171.

McDonald JW, Garofalo EA, Hood T, Sackellares JC, Gilman S, McKeever PE, et al. Altered excitatory and inhibitory amino acid receptor binding in hippocampus of patients with temporal lobe epilepsy. Ann. Neurol. 1991; 29: 529–541.

McGinnity CJ, Årstad E, Beck K, Brooks DJ, Coles JP, Duncan JS, et al. Comment on " In Vivo [18F]GE-179 Brain Signal Does Not Show NMDA-Specific Modulation with Drug Challenges in Rodents and Nonhuman Primates". ACS Chem Neurosci 2019; 10: 768–772.

McGinnity CJ, Hammers A, Riaño Barros DA, Luthra SK, Jones PA, Trigg W, et al. Initial evaluation of 18F-GE-179, a putative PET Tracer for activated N-methyl D-aspartate receptors. J Nucl Med 2014; 55: 423–430.

McGinnity CJ, Koepp MJ, Hammers A, Riaño Barros DA, Pressler RM, Luthra S, et al. NMDA receptor binding in focal epilepsies. J Neurol Neurosurg Psychiatr 2015; 86: 1150–1157.

McGinnity CJ, Riaño Barros DA, Trigg W, Brooks DJ, Hinz R, Duncan JS, et al. Simplifying [18F]GE-179 PET: are both arterial blood sampling and 90-min acquisitions essential? EJNMMI Res 2018; 8: 46.

McMillan R, Forsyth A, Campbell D, Malpas G, Maxwell E, Dukart J, et al. Temporal dynamics of the pharmacological MRI response to subanaesthetic ketamine in healthy volunteers: A simultaneous EEG/fMRI study. J. Psychopharmacol. (Oxford) 2019; 33: 219–229.

McNamara JO, Russell RD, Rigsbee L, Bonhaus DW. Anticonvulsant and antiepileptogenic actions of MK-801 in the kindling and electroshock models. Neuropharmacology 1988; 27: 563–568.

Meldrum BS. Excitotoxicity and selective neuronal loss in epilepsy. Brain Pathol. 1993; 3: 405–412.

Meyer PT, Elmenhorst D, Zilles K, Bauer A. Simplified quantification of cerebral A1 adenosine receptors using [18F]CPFPX and PET: analyses based on venous blood sampling. Synapse 2005; 55: 212–223.

Miyazaki T, Nakajima W, Hatano M, Shibata Y, Kuroki Y, Arisawa T, et al. Visualization of AMPA receptors in living human brain with positron emission tomography. Nat. Med. 2020; 25: 103.

Modica PA, Tempelhoff R, White PF. Pro- and anticonvulsant effects of anesthetics (Part I). Anesth. Analg. 1990; 70: 303–315.

Mody I, Heinemann U. NMDA receptors of dentate gyrus granule cells participate in synaptic transmission following kindling. Nature 1987; 326: 701–704.

Moghaddam B, Adams B, Verma A, Daly D. Activation of glutamatergic neurotransmission by ketamine: a novel step in the pathway from NMDA receptor blockade to dopaminergic and cognitive disruptions associated with the prefrontal cortex. Journal of Neuroscience 1997; 17: 2921–2927.

Moghaddam B, Adams BW. Reversal of phencyclidine effects by a group II metabotropic glutamate receptor agonist in rats. Science 1998; 281: 1349–1352.

Monyer H, Burnashev N, Laurie DJ, Sakmann B, Seeburg PH. Developmental and regional expression in the rat brain and functional properties of four NMDA receptors. Neuron 1994; 12: 529–540.

Mori H, Mishina M. Structure and function of the NMDA receptor channel. Neuropharmacology 1995; 34: 1219–1237.

Moscato EH, Peng X, Jain A, Parsons TD, Dalmau J, Balice-Gordon RJ. Acute mechanisms underlying antibody effects in anti-N-methyl-D-aspartate receptor encephalitis. Ann. Neurol. 2014; 76: 108–119.

Murrough JW, Iosifescu DV, Chang LC, Jurdi Al RK, Green CE, Perez AM, et al. Antidepressant efficacy of ketamine in treatment-resistant major depression: a two-site randomized controlled trial. Am J Psychiatry 2013; 170: 1134–1142.

Nakazawa K, McHugh TJ, Wilson MA, Tonegawa S. NMDA receptors, place cells and hippocampal spatial memory. Nat. Rev. Neurosci. 2004; 5: 361–372.

Naylor DE, Liu H, Niquet J, Wasterlain CG. Rapid surface accumulation of NMDA receptors increases glutamatergic excitation during status epilepticus. Neurobiol. Dis. 2013; 54: 225–238.

Naylor DE, Liu H, Wasterlain CG. Trafficking of GABA(A) receptors, loss of inhibition, and a mechanism for pharmacoresistance in status epilepticus. J. Neurosci. 2005; 25: 7724–7733.

Neuman R, Cherubini E, Ben-Ari Y. Epileptiform bursts elicited in CA3 hippocampal neurons by a variety of convulsants are not blocked by N-methyl-D-aspartate antagonists. Brain Res. 1988; 459: 265–274.

Ngugi AK, Bottomley C, Kleinschmidt I, Sander JW, Newton CR. Estimation of the burden of active and life-time epilepsy: a meta-analytic approach. Epilepsia 2010; 51: 883–890.

Nickell J, Salvatore MF, Pomerleau F, Apparsundaram S, Gerhardt GA. Reduced plasma membrane surface expression of GLAST mediates decreased glutamate regulation in the aged striatum. Neurobiol. Aging 2007; 28: 1737–1748.

Niswender CM, Conn PJ. Metabotropic glutamate receptors: physiology, pharmacology, and disease. Annu. Rev. Pharmacol. Toxicol. 2010; 50: 295–322.

Northoff G, Richter A, Bermpohl F, Grimm S, Martin E, Marcar VL, et al. NMDA hypofunction in the posterior cingulate as a model for schizophrenia: an exploratory ketamine administration study in fMRI. Schizophr. Res. 2005; 72: 235–248.

Nyberg L, McIntosh AR, Houle S, Nilsson LG, Tulving E. Activation of medial temporal structures during episodic memory retrieval. Nature 1996; 380: 715–717.

Okamura N, Harada R, Furumoto S, Arai H, Yanai K, Kudo Y. Tau PET imaging in Alzheimer's disease. Curr Neurol Neurosci Rep 2014; 14: 500.

Olney JW, Newcomer JW, Farber NB. NMDA receptor hypofunction model of schizophrenia. J Psychiatr Res 1999; 33: 523–533.

Olney JW, Wozniak DF, Farber NB. Excitotoxic neurodegeneration in Alzheimer disease. New hypothesis and new therapeutic strategies. Arch Neurol 1997; 54: 1234–1240.

Olney JW. Brain lesions, obesity, and other disturbances in mice treated with monosodium glutamate. Science 1969; 164: 719–721.

Ontl T, Xing Y, Bai L, Kennedy E, Nelson S, Wakeman M, et al. Development and aging of N-methyl-D-aspartate receptor expression in the prefrontal/frontal cortex of mice. Neuroscience 2004; 123: 467–479.

Ormandy GC, Jope RS, Snead OC. Anticonvulsant actions of MK-801 on the lithium-pilocarpine model of status epilepticus in rats. Experimental Neurology 1989; 106: 172–180.

Owen AM, McMillan KM, Laird AR, Bullmore E. N-back working memory paradigm: a meta-analysis of normative functional neuroimaging studies. Hum Brain Mapp 2005; 25: 46–59.

Palmada M, Centelles JJ. Excitatory amino acid neurotransmission. Pathways for metabolism, storage and reuptake of glutamate in brain. Front. Biosci. 1998; 3: d701–18.

Palop JJ, Chin J, Roberson ED, Wang J, Thwin MT, Bien-Ly N, et al. Aberrant excitatory neuronal activity and compensatory remodeling of inhibitory hippocampal circuits in mouse models of Alzheimer's disease. Neuron 2007; 55: 697–711.

Papouin T, Ladépêche L, Ruel J, Sacchi S, Labasque M, Hanini M, et al. Synaptic and extrasynaptic NMDA receptors are gated by different endogenous coagonists. Cell 2012; 150: 633–646.

Paradiso B, Marconi P, Zucchini S, Berto E, Binaschi A, Bozac A, et al. Localized delivery of fibroblast growth factor-2 and brain-derived neurotrophic factor reduces spontaneous seizures in an epilepsy model. Proc. Natl. Acad. Sci. U.S.A. 2009; 106: 7191–7196.

Park DC, Lautenschlager G, Hedden T, Davidson NS, Smith AD, Smith PK. Models of visuospatial and verbal memory across the adult life span. Psychol Aging 2002; 17: 299–320.

Pellock JM, Faught E, Leppik IE, Shinnar S, Zupanc ML. Felbamate: consensus of current clinical experience. Epilepsy Res 2006; 71: 89–101.

Pellock JM. Felbamate in epilepsy therapy: evaluating the risks. Drug Saf 1999; 21: 225–239.

Peltz G, Pacific DM, Noviasky JA, Shatla A, Mehalic T. Seizures associated with memantine use. Am J Health Syst Pharm 2005; 62: 420–421.

Pereira AC, Lambert HK, Grossman YS, Dumitriu D, Waldman R, Jannetty SK, et al. Glutamatergic regulation prevents hippocampal-dependent age-related cognitive decline through dendritic spine clustering. Proc. Natl. Acad. Sci. U.S.A. 2014; 111: 18733–18738.

Piggott MA, Perry EK, Perry RH, Court JA. [3H]MK-801 binding to the NMDA receptor complex, and its modulation in human frontal cortex during development and aging. Brain Res. 1992; 588: 277–286.

Pilowsky LS, Bressan RA, Stone JM, Erlandsson K, Mulligan RS, Krystal JH, et al. First in vivo evidence of an NMDA receptor deficit in medication-free schizophrenic patients. Mol. Psychiatry 2006; 11: 118–119.

Pitkänen A, Engel J. Past and present definitions of epileptogenesis and its biomarkers. Neurotherapeutics 2014; 11: 231–241.

Pitkänen A, Nehlig A, Brooks-Kayal AR, Dudek FE, Friedman D, Galanopoulou AS, et al. Issues related to development of antiepileptogenic therapies. Epilepsia 2013; 54 Suppl 4: 35–43.

Polascheck N, Bankstahl M, Löscher W. The COX-2 inhibitor parecoxib is neuroprotective but not antiepileptogenic in the pilocarpine model of temporal lobe epilepsy. Experimental Neurology 2010; 224: 219–233.

Potier B, Billard J-M, Rivière S, Sinet P-M, Denis I, Champeil-Potokar G, et al. Reduction in glutamate uptake is associated with extrasynaptic NMDA and metabotropic glutamate receptor activation at the hippocampal CA1 synapse of aged rats. Aging Cell 2010; 9: 722–735.

Prince M, Albanese E, Guerchet M, Prina M. World Alzheimer Report 2014 Dementia and Risk Reduction an Analysis of Protective and Modifiable Factors. London: Alzheimers Disease; 2014.

Probasco JC, Solnes L, Nalluri A, Cohen J, Jones KM, Zan E, et al. Decreased occipital lobe metabolism by FDG-PET/CT: An anti-NMDA receptor encephalitis biomarker. Neurol Neuroimmunol Neuroinflamm 2018; 5: e413.

Provost J-S, Hanganu A, Monchi O. Neuroimaging studies of the striatum in cognition Part I: healthy individuals. Front Syst Neurosci 2015; 9: 140.

Prüss H, Holtkamp M. Ketamine successfully terminates malignant status epilepticus. Epilepsy Res 2008; 82: 219–222.

Ramadan E, Basselin M, Rao JS, Chang L, Chen M, Ma K, et al. Lamotrigine blocks NMDA receptor-initiated arachidonic acid signalling in rat brain: implications for its efficacy in bipolar disorder. Int. J. Neuropsychopharmacol. 2012; 15: 931–943.

Ramaswamy P, Aditi Devi N, Hurmath Fathima K, Dalavaikodihalli Nanjaiah N. Activation of NMDA receptor of glutamate influences MMP-2 activity and proliferation of glioma cells. Neurol Sci 2014; 35: 823–829.

Rauner C, Köhr G. Triheteromeric NR1/NR2A/NR2B receptors constitute the major N-methyl-D-aspartate receptor population in adult hippocampal synapses. J. Biol. Chem. 2011; 286: 7558–7566.

Raza M, Blair RE, Sombati S, Carter DS, Deshpande LS, DeLorenzo RJ. Evidence that injury-induced changes in hippocampal neuronal calcium dynamics during epileptogenesis cause acquired epilepsy. Proc Natl Acad Sci USA 2004; 101: 17522–17527.

Ribak CE, Bradburne RM, Harris AB. A preferential loss of GABAergic, symmetric synapses in epileptic foci: a quantitative ultrastructural analysis of monkey neocortex. Journal of Neuroscience 1982; 2: 1725–1735.

Rice AC, DeLorenzo RJ. NMDA receptor activation during status epilepticus is required for the development of epilepsy. Brain Res. 1998; 782: 240–247.

Rice AC, DeLorenzo RJ. N-methyl-D-aspartate receptor activation regulates refractoriness of status epilepticus to diazepam. Neuroscience 1999; 93: 117–123.

Rice AC, Floyd CL, Lyeth BG, Hamm RJ, DeLorenzo RJ. Status epilepticus causes long-term NMDA receptor-dependent behavioral changes and cognitive deficits. Epilepsia 1998; 39: 1148–1157.

Roberts BM, Shaffer CL, Seymour PA, Schmidt CJ, Williams GV, Castner SA. Glycine transporter inhibition reverses ketamine-induced working memory deficits. Neuroreport 2010; 21: 390–394.

Roberts DS, Hu Y, Lund IV, Brooks-Kayal AR, Russek SJ. Brain-derived neurotrophic factor (BDNF)-induced synthesis of early growth response factor 3 (Egr3) controls the levels of type A GABA receptor alpha 4 subunits in hippocampal neurons. J. Biol. Chem. 2006; 281: 29431–29435.

Robins EG, Zhao Y, Khan I, Wilson A, Luthra SK, Rstad E. Synthesis and in vitro evaluation of (18)F-labelled S-fluoroalkyl diarylguanidines: Novel high-affinity NMDA receptor antagonists for imaging with PET. Bioorg. Med. Chem. Lett. 2010; 20: 1749–1751.

Rogawski MA. Revisiting AMPA receptors as an antiepileptic drug target. Epilepsy Curr 2011; 11: 56–63.

Rothman S. Synaptic release of excitatory amino acid neurotransmitter mediates anoxic neuronal death. J. Neurosci. 1984; 4: 1884–1891.

Rothman SM, Olney JW. Excitotoxicity and the NMDA receptor--still lethal after eight years. Trends Neurosci. 1995; 18: 57–58.

Salmon E, Van der Linden M, Collette F, Delfiore G, Maquet P, Degueldre C, et al. Regional brain activity during working memory tasks. Brain 1996; 119 (Pt 5): 1617–1625.

Sambataro F, Murty VP, Callicott JH, Tan H-Y, Das S, Weinberger DR, et al. Age-related alterations in default mode network: impact on working memory performance. Neurobiol. Aging 2010; 31: 839–852.

Sari H, Erlandsson K, Law I, Larsson HB, Ourselin S, Arridge S, et al. Estimation of an image derived input function with MR-defined carotid arteries in FDG-PET human studies using a novel partial volume correction method. J. Cereb. Blood Flow Metab. 2016

Sari H, Erlandsson K, Marner L, Law I, Larsson HBW, Thielemans K, et al. Non-invasive kinetic modelling of PET tracers with radiometabolites using a constrained simultaneous estimation method: evaluation with 11C-SB201745. EJNMMI Res 2018; 8: 58.

Sattler R, Xiong Z, Lu WY, MacDonald JF, Tymianski M. Distinct roles of synaptic and extrasynaptic NMDA receptors in excitotoxicity. J. Neurosci. 2000; 20: 22–33.

Sayyah M, Javad-Pour M, Ghazi-Khansari M. The bacterial endotoxin lipopolysaccharide enhances seizure susceptibility in mice: involvement of proinflammatory factors: nitric oxide and prostaglandins. Neuroscience 2003; 122: 1073–1080.

Schoenberger M, Schroeder FA, Placzek MS, Carter RL, Rosen BR, Hooker JM, et al. In Vivo [18F]GE-179 Brain Signal Does Not Show NMDA-Specific Modulation with Drug Challenges in Rodents and Nonhuman Primates. ACS Chem Neurosci 2017

Seghier ML, Ramlackhansingh A, Crinion J, Leff AP, Price CJ. Lesion identification using unified segmentation-normalisation models and fuzzy clustering. Neuroimage 2008; 41: 1253–1266.

Senatorov VV, Friedman AR, Milikovsky DZ, Ofer J, Saar-Ashkenazy R, Charbash A, et al. Blood-brain barrier dysfunction in aging induces hyperactivation of TGFβ signaling and chronic yet reversible neural dysfunction. Sci Transl Med 2019; 11: eaaw8283.

Sepulcre J, Schultz AP, Sabuncu M, Gomez-Isla T, Chhatwal J, Becker A, et al. In Vivo Tau, Amyloid, and Gray Matter Profiles in the Aging Brain. J. Neurosci. 2016; 36: 7364–7374.

Serra M, Ghiani CA, Foddi MC, Motzo C, Biggio G. NMDA receptor function is enhanced in the hippocampus of aged rats. Neurochem Res 1994; 19: 483–487.

Shankar GM, Bloodgood BL, Townsend M, Walsh DM, Selkoe DJ, Sabatini BL. Natural oligomers of the Alzheimer amyloid-beta protein induce reversible synapse loss by modulating an NMDA-type glutamate receptor-dependent signaling pathway. J. Neurosci. 2007; 27: 2866–2875.

Shaw PJ, Ince PG. Glutamate, excitotoxicity and amyotrophic lateral sclerosis. J Neurol 1997; 244 Suppl 2: S3–14.

Shipton OA, Paulsen O. GluN2A and GluN2B subunit-containing NMDA receptors in hippocampal plasticity. Philos. Trans. R. Soc. Lond., B, Biol. Sci. 2014; 369: 20130163.

Silver H, Feldman P, Bilker W, Gur RC. Working memory deficit as a core neuropsychological dysfunction in schizophrenia. Am J Psychiatry 2003; 160: 1809–1816.

Simister RJ, McLean MA, Barker GJ, Duncan JS. A proton magnetic resonance spectroscopy study of metabolites in the occipital lobes in epilepsy. Epilepsia 2003a; 44: 550–558.

Simister RJ, McLean MA, Barker GJ, Duncan JS. Proton MRS reveals frontal lobe metabolite abnormalities in idiopathic generalized epilepsy. Neurology 2003b; 61: 897–902.

Simister RJ, McLean MA, Barker GJ, Duncan JS. Proton magnetic resonance spectroscopy of malformations of cortical development causing epilepsy. Epilepsy Res 2007; 74: 107–115.

Simister RJ, Woermann FG, McLean MA, Bartlett PA, Barker GJ, Duncan JS. A short-echo-time proton magnetic resonance spectroscopic imaging study of temporal lobe epilepsy. Epilepsia 2002; 43: 1021–1031.

Simon RP, Swan JH, Griffiths T, Meldrum BS. Blockade of N-methyl-D-aspartate receptors may protect against ischemic damage in the brain. 1984; 226: 850–852.

Sloviter RS. Decreased hippocampal inhibition and a selective loss of interneurons in experimental epilepsy. Science 1987; 235: 73–76.

Snyder EM, Nong Y, Almeida CG, Paul S, Moran T, Choi EY, et al. Regulation of NMDA receptor trafficking by amyloid-beta. Nat. Neurosci. 2005; 8: 1051–1058.

Sobrio F, Gilbert G, Perrio C, Barré L, Debruyne D. PET and SPECT imaging of the NMDA receptor system: an overview of radiotracer development. Mini Rev Med Chem 2010; 10: 870–886.

Spinks TJ, Jones T, Bloomfield PM, Bailey DL, Miller M, Hogg D, et al. Physical characteristics of the ECAT EXACT3D positron tomograph. Phys Med Biol 2000; 45: 2601–2618.

Spreafico R, Battaglia G, Arcelli P, Andermann F, Dubeau F, Palmini A, et al. Cortical dysplasia: an immunocytochemical study of three patients. Neurology 1998; 50: 27–36.

Stasheff SF, Anderson WW, Clark S, Wilson WA. NMDA antagonists differentiate epileptogenesis from seizure expression in an in vitro model. Science 1989; 245: 648–651.

Stone JM, Erlandsson K, Årstad E, Squassante L, Teneggi V, Bressan RA, et al. Relationship between ketamine-induced psychotic symptoms and NMDA receptor occupancy: a [(123)I]CNS-1261 SPET study. Psychopharmacology (Berl.) 2008; 197: 401–408.

Stopford CL, Thompson JC, Neary D, Richardson AMT, Snowden JS. Working memory, attention, and executive function in Alzheimer's disease and frontotemporal dementia. Cortex 2012; 48: 429–446.

Stöhr T, Kupferberg HJ, Stables JP, Choi D, Harris RH, Kohn H, et al. Lacosamide, a novel anti-convulsant drug, shows efficacy with a wide safety margin in rodent models for epilepsy. Epilepsy Res 2007; 74: 147–154.

Strehlow V, Heyne HO, Vlaskamp DRM, Marwick KFM, Rudolf G, De Bellescize J, et al. GRIN2A-related disorders: genotype and functional consequence predict phenotype. Brain 2019; 142: 80–92.

Stretton J, Thompson PJ. Frontal lobe function in temporal lobe epilepsy. Epilepsy Res 2012; 98: 1–13.

Stretton J, Winston G, Sidhu M, Centeno M, Vollmar C, Bonelli S, et al. Neural correlates of working memory in Temporal Lobe Epilepsy--an fMRI study. Neuroimage 2012; 60: 1696–1703.

Strittmatter WJ, Saunders AM, Schmechel D, Pericak-Vance M, Enghild J, Salvesen GS, et al. Apolipoprotein E: high-avidity binding to beta-amyloid and increased frequency of type 4 allele in late-onset familial Alzheimer disease. Proc. Natl. Acad. Sci. U.S.A. 1993; 90: 1977–1981.

Sun X-Y, Tuo Q-Z, Liuyang Z-Y, Xie A-J, Feng X-L, Yan X, et al. Extrasynaptic NMDA receptor-induced tau overexpression mediates neuronal death through suppressing survival signaling ERK phosphorylation. Cell Death Dis 2016; 7: e2449–e2449.

Sutula T, Cascino G, Cavazos J, Parada I, Ramirez L. Mossy fiber synaptic reorganization in the epileptic human temporal lobe. Ann. Neurol. 1989; 26: 321–330.

Sutula TP, Hagen J, Pitkänen A. Do epileptic seizures damage the brain? Curr. Opin. Neurol. 2003; 16: 189–195.

Suzuki Y, Jodo E, Takeuchi S, Niwa S, Kayama Y. Acute administration of phencyclidine induces tonic activation of medial prefrontal cortex neurons in freely moving rats. Neuroscience 2002; 114: 769–779.

Sveinbjornsdottir S, Sander JW, Upton D, Thompson PJ, Patsalos PN, Hirt D, et al. The excitatory amino acid antagonist D-CPP-ene (SDZ EAA-494) in patients with epilepsy. Epilepsy Res 1993; 16: 165–174.

Takagi S, Takahashi W, Shinohara Y, Yasuda S, Ide M, Shohtsu A, et al. Quantitative PET cerebral glucose metabolism estimates using a single non-arterialized venous-blood sample. Ann Nucl Med 2004; 18: 297–302.

Takano T, Lin JH, Arcuino G, Gao Q, Yang J, Nedergaard M. Glutamate release promotes growth of malignant gliomas. Nat. Med. 2001; 7: 1010–1015.

Talantova M, Sanz-Blasco S, Zhang X, Xia P, Akhtar MW, Okamoto S-I, et al. Aβ induces astrocytic glutamate release, extrasynaptic NMDA receptor activation, and synaptic loss. Proc. Natl. Acad. Sci. U.S.A. 2013; 110: E2518–27.

Tanaka K, Watase K, Manabe T, Yamada K, Watanabe M, Takahashi K, et al. Epilepsy and exacerbation of brain injury in mice lacking the glutamate transporter GLT-1. Science 1997; 276: 1699–1702.

Tekin S, Aykut-Bingöl C, Tanridağ T, Aktan S. Antiglutamatergic therapy in Alzheimer's disease--effects of lamotrigine. J Neural Transm (Vienna) 1998; 105: 295–303.

Thomas BA, Cuplov V, Bousse A, Mendes A, Thielemans K, Hutton BF, et al. PETPVC: a toolbox for performing partial volume correction techniques in positron emission tomography. Phys Med Biol 2016; 61: 7975–7993.

Titulaer MJ, McCracken L, Gabilondo I, Armangué T, Glaser C, Iizuka T, et al. Treatment and prognostic factors for long-term outcome in patients with anti-NMDA receptor encephalitis: an observational cohort study. The Lancet Neurology 2013; 12: 157–165.

Tovar KR, Westbrook GL. Mobile NMDA receptors at hippocampal synapses. Neuron 2002; 34: 255–264.

Trinka E, Brigo F. Antiepileptogenesis in humans: disappointing clinical evidence and ways to move forward. Curr. Opin. Neurol. 2014; 27: 227–235.

United Nations Department of Economic and Social Population Affairs. World Population Prospects 2019: Highlights (ST/ESA/SER. A/423). 2019.

van der Aart J, Golla SSV, van der Pluijm M, Schwarte LA, Schuit RC, Klein PJ, et al. First in human evaluation of [18F]PK-209, a PET ligand for the ion channel binding site of NMDA receptors. EJNMMI Res 2018; 8: 69.

van der Aart J, Yaqub M, Kooijman EJM, Bakker J, Langermans JAM, Schuit RC, et al. Evaluation of the Novel PET Tracer [11C]HACH242 for Imaging the GluN2B NMDA Receptor in Non-Human Primates. Mol Imaging Biol 2019; 21: 676–685.

van der Doef TF, Golla SS, Klein PJ, Oropeza-Seguias GM, Schuit RC, Metaxas A, et al. Quantification of the novel N-methyl-d-aspartate receptor ligand [11C]GMOM in man. J. Cereb. Blood Flow Metab. 2016; 36: 1111–1121.

Vatassery GT, Lai JC, Smith WE, Quach HT. Aging is associated with a decrease in synaptosomal glutamate uptake and an increase in the susceptibility of synaptosomal vitamin E to oxidative stress. Neurochem Res 1998; 23: 121–125.

Venkataramani V, Tanev DI, Strahle C, Studier-Fischer A, Fankhauser L, Kessler T, et al. Glutamatergic synaptic input to glioma cells drives brain tumour progression. Nature 2019; 573: 532–538.

Venkatesh HS, Morishita W, Geraghty AC, Silverbush D, Gillespie SM, Arzt M, et al. Electrical and synaptic integration of glioma into neural circuits. Nature 2019; 573: 539–545.

Vezzani A, French J, Bartfai T, Baram TZ. The role of inflammation in epilepsy. Nat Rev Neurol 2011; 7: 31–40.

Vezzani A, Wu HQ, Moneta E, Samanin R. Role of the N-methyl-D-aspartate-type receptors in the development and maintenance of hippocampal kindling in rats. Neurosci Lett 1988; 87: 63–68.

Vibholm A, Christensen J, Beniczky S, Landau A, Dietz M, Møller A, et al. In-vivo imaging of activated NMDA receptor ion channels with the radioligand 18F-GE179. Epilepsia 2017; 58: S22.

Vibholm AK, Landau AM, Alstrup AKO, Jacobsen J, Vang K, Munk OL, et al. Activation of NMDA receptor ION channels by deep brain stimulation in the PIG visualised with [18F]GE-179 PET. Brain Stimulation 2020: 1–32.

Vibholm AK, Landau AM, Møller A, Jacobsen J, Vang K, Munk OL, et al. NMDA receptor ion channel activation detected in vivo with [18F]GE-179 PET after electrical stimulation of rat hippocampus. J. Cereb. Blood Flow Metab. 2020: 271678X20954928.

Vlachos A, Helias M, Becker D, Diesmann M, Deller T. NMDA-receptor inhibition increases spine stability of denervated mouse dentate granule cells and accelerates spine density recovery following entorhinal denervation in vitro. Neurobiol. Dis. 2013; 59: 267–276.

Vollenweider FX, Leenders KL, Oye I, Hell D, Angst J. Differential psychopathology and patterns of cerebral glucose utilisation produced by (S)- and (R)-ketamine in healthy volunteers using positron emission tomography (PET). Eur Neuropsychopharmacol 1997; 7: 25–38.

Wakita K, Imahori Y, Ido T, Fujii R, Horii H, Shimizu M, et al. Simplification for measuring input function of FDG PET: investigation of 1-point blood sampling method. J Nucl Med 2000; 41: 1484–1490.

Walsh DM, Klyubin I, Fadeeva JV, Cullen WK, Anwyl R, Wolfe MS, et al. Naturally secreted oligomers of amyloid beta protein potently inhibit hippocampal long-term potentiation in vivo. Nature 2002; 416: 535–539.

Walters MR, Bradford APJ, Fischer J, Lees KR. Early clinical experience with the novel NMDA receptor antagonist CNS 5161. Br J Clin Pharmacol 2002; 53: 305–311.

Wang M, Yang Y, Wang C-J, Gamo NJ, Jin LE, Mazer JA, Morrison JH, Wang X-J, Arnsten AFT. NMDA receptors subserve persistent neuronal firing during working memory in dorsolateral prefrontal cortex. Neuron 2013a; 77: 736–749.

Wang M, Yang Y, Wang C-J, Gamo NJ, Jin LE, Mazer JA, Morrison JH, Wang X-J, Arnsten AFT. NMDA receptors subserve persistent neuronal firing during working memory in dorsolateral prefrontal cortex. Neuron 2013b; 77: 736–749.

Wang SJ, Huang CC, Hsu KS, Tsai JJ, Gean PW. Presynaptic inhibition of excitatory neurotransmission by lamotrigine in the rat amygdalar neurons. Synapse 1996; 24: 248–255.

Wang XJ. Synaptic basis of cortical persistent activity: the importance of NMDA receptors to working memory. J. Neurosci. 1999; 19: 9587–9603.

Waterhouse RN. Imaging the PCP site of the NMDA ion channel. Nucl. Med. Biol. 2003; 30: 869–878.

Watkins JC, Evans RH. Excitatory amino acid transmitters. Annu. Rev. Pharmacol. Toxicol. 1981; 21: 165–204.

Weiner AL, Vieira L, McKay CA, Bayer MJ. Ketamine abusers presenting to the emergency department: a case series. J Emerg Med 2000; 18: 447–451.

Weiss JH, Hartley DM, Koh J, Choi DW. The calcium channel blocker nifedipine attenuates slow excitatory amino acid neurotoxicity. Science 1990; 247: 1474–1477.

Whelan CD, Altmann A, Botía JA, Jahanshad N, Hibar DP, Absil J, et al. Structural brain abnormalities in the common epilepsies assessed in a worldwide ENIGMA study. Brain 2018; 141: 391–408.

Williams PA, White AM, Clark S, Ferraro DJ, Swiercz W, Staley KJ, et al. Development of spontaneous recurrent seizures after kainate-induced status epilepticus. J. Neurosci. 2009; 29: 2103–2112.

Williams S, Johnston D. Long-term potentiation of hippocampal mossy fiber synapses is blocked by postsynaptic injection of calcium chelators. Neuron 1989; 3: 583–588.

Willmann O, Wennberg R, May T, Woermann FG, Pohlmann-Eden B. The contribution of 18F-FDG PET in preoperative epilepsy surgery evaluation for patients with temporal lobe epilepsy A meta-analysis. Seizure 2007; 16: 509–520.

Wollmuth LP, Sobolevsky AI. Structure and gating of the glutamate receptor ion channel. Trends Neurosci. 2004; 27: 321–328.

Wolosker H. D-serine regulation of NMDA receptor activity. Sci. STKE 2006; 2006: pe41.

World Health Organization. The global campaign against epilepsy: out of the shadows. Geneva: WHO; 2000.

Wright S, Hashemi K, Stasiak L, Bartram J, Lang B, Vincent A, et al. Epileptogenic effects of NMDAR antibodies in a passive transfer mouse model. Brain 2015; 138: 3159–3167.

Wroge CM, Hogins J, Eisenman L, Mennerick S. Synaptic NMDA receptors mediate hypoxic excitotoxic death. J. Neurosci. 2012; 32: 6732–6742.

Xu X-X, Luo J-H. Mutations of N-Methyl-D-Aspartate Receptor Subunits in Epilepsy. Neurosci Bull 2018; 34: 549–565.

Yassa MA, Stark SM, Bakker A, Albert MS, Gallagher M, Stark CEL. High-resolution structural and functional MRI of hippocampal CA3 and dentate gyrus in patients with amnestic Mild Cognitive Impairment. Neuroimage 2010; 51: 1242–1252.

Ye ZC, Sontheimer H. Glioma cells release excitotoxic concentrations of glutamate. Cancer Res. 1999; 59: 4383–4391.

Yeh GC, Bonhaus DW, Nadler JV, McNamara JO. N-methyl-D-aspartate receptor plasticity in kindling: quantitative and qualitative alterations in the N-methyl-D-aspartate receptor-channel complex. Proc Natl Acad Sci USA 1989; 86: 8157–8160.

Yildiz M, Borgwardt SJ, Berger GE. Parietal lobes in schizophrenia: do they matter? Schizophr Res Treatment 2011; 2011: 581686.

Young AB. Cortical amino acidergic pathways in Alzheimer's disease. J. Neural Transm. Suppl. 1987; 24: 147–152.

Yuen TI, Morokoff AP, Bjorksten A, D'Abaco G, Paradiso L, Finch S, et al. Glutamate is associated with a higher risk of seizures in patients with gliomas. Neurology 2012; 79: 883–889.

Zahr NM, Mayer D, Rohlfing T, Chanraud S, Gu M, Sullivan EV, et al. In vivo glutamate measured with magnetic resonance spectroscopy: behavioral correlates in aging. Neurobiol. Aging 2013; 34: 1265–1276.

Zamzow DR, Elias V, Shumaker M, Larson C, Magnusson KR. An increase in the association of GluN2B containing NMDA receptors with membrane scaffolding proteins was related to memory declines during aging. J. Neurosci. 2013; 33: 12300–12305.

Zanotti-Fregonara P, Chen K, Liow J-S, Fujita M, Innis RB. Image-derived input function for brain PET studies: many challenges and few opportunities. J. Cereb. Blood Flow Metab. 2011; 31: 1986–1998.

Zanotti-Fregonara P, Liow J-S, Fujita M, Dusch E, Zoghbi SS, Luong E, et al. Image-derived input function for human brain using high resolution PET imaging with [C](R)-rolipram and [C]PBR28. PLoS ONE 2011; 6: e17056.

Zanotti-Fregonara P, Maroy R, Peyronneau M-A, Trébossen R, Bottlaender M. Minimally invasive input function for 2-18F-fluoro-A-85380 brain PET studies. Eur. J. Nucl. Med. Mol. Imaging 2012; 39: 651–659.

Zeng L-H, Rensing NR, Wong M. The mammalian target of rapamycin signaling pathway mediates epileptogenesis in a model of temporal lobe epilepsy. J. Neurosci. 2009; 29: 6964–6972.

Zeng L-H, Xu L, Gutmann DH, Wong M. Rapamycin prevents epilepsy in a mouse model of tuberous sclerosis complex. Ann. Neurol. 2008; 63: 444–453.

Zhang J, Li Y, Xu J, Yang Z. The role of N-methyl-D-aspartate receptor in Alzheimer's disease. Journal of the Neurological Sciences 2014; 339: 123–129.

Zhang Y, Li P, Feng J, Wu M. Dysfunction of NMDA receptors in Alzheimer's disease. Neurol Sci 2016; 37: 1039–1047.

Zhou X, Hollern D, Liao J, Andrechek E, Wang H. NMDA receptor-mediated excitotoxicity depends on the coactivation of synaptic and extrasynaptic receptors. Cell Death Dis 2013; 4: e560.